

Copyright
by
Bridget Eva Hawkins
2008

**The Dissertation Committee for Bridget Eva Hawkins Certifies that this is the
approved version of the following dissertation:**

**ZINC-MEDIATED CELL DEATH IN THE HIPPOCAMPUS
FOLLOWING EXPERIMENTAL TRAUMATIC BRAIN INJURY**

Committee:

Donald S. Prough, M.D., Supervisor

Giulio Taglialatela, Ph.D., Chair

Kelly Dineley, Ph.D.

Wolfgang Maret, Ph.D.

Helen Hellmich, Ph.D.

Claudia Robertson, M.D.

Dean, Graduate School

**ZINC-MEDIATED CELL DEATH IN THE HIPPOCAMPUS
FOLLOWING EXPERIMENTAL TRAUMATIC BRAIN INJURY**

by

Bridget Eva Hawkins, B.S.

Dissertation

Presented to the Faculty of the Graduate School of
The University of Texas Medical Branch
in Partial Fulfillment
of the Requirements
for the Degree of

Doctor of Philosophy

**The University of Texas Medical Branch
December, 2008**

Dedication

Dedicated to my wonderful friends and loving family without which this would not have been possible.

Acknowledgements

I would first like to express gratitude to my mentor, Dr. Donald S. Prough, who accepted me as his first graduate student, despite his tremendously busy schedule. He has remained supportive and enthusiastic about our research throughout the four years I have spent in his lab, even when my enthusiasm waned. I thank Dr. Giulio Taglialatela for accepting the responsibility of chairperson of my dissertation committee and providing invaluable guidance. I would also like to thank the rest of my committee members, Drs. Helen Hellmich, Kelly Dineley, and Claudia Robertson for their constant encouragement and advice and especially Dr. Wolfgang Maret for wonderful conversations about life, research and zinc. Special thanks to Drs. Golda and Robert Leonard who have helped with the silver autometallography experiments and have been greatly supportive to me during my time as a graduate student. I would also like to express my gratitude to Drs. Cheryl Watson and Mary Moslen who have been supportive before I even applied to Graduate School. Drs. V.R.S. Ramanujam, Olivera Nesic and Shakeel Ansari provided help with GF-AAS, analysis of gene array data and technical issues with nitric oxide donor compounds, respectively. I would like to acknowledge the members of our lab group for providing an entertaining and educational work environment. I am also very grateful for the help of Brenda Silverstein and Cynthia Cheatham for scheduling and administrative assistance and Jeffrey Meserve and Andrew Hall for excellent editorial assistance with poster presentations, this dissertation and future manuscripts. This work was supported by NS042849-01A1 from NINDS and an NIEHS Predoctoral Fellowship (T32 ES007254) “Molecular Mechanisms for Environmental Injury” at The University of Texas Medical Branch.

ZINC-MEDIATED CELL DEATH IN THE HIPPOCAMPUS FOLLOWING EXPERIMENTAL TRAUMATIC BRAIN INJURY

Publication No. _____

Bridget Eva Hawkins, Ph.D.

The University of Texas Medical Branch, 2008

Supervisor: Donald S. Prough

Traumatic brain injury (TBI) is a leading cause of morbidity and mortality of Americans both in the 15-25 age range and in the elderly population. Hippocampal neuronal damage is a key feature of experimental fluid percussion traumatic brain injury in rodents. However, the mechanisms contributing to the susceptibility to neuronal injury in this region are largely unknown. Since free ionic zinc (Zn^{2+}) was shown to be toxic to neurons *in vitro*, I sought to examine the effects of Zn^{2+} on neuronal injury following TBI. To study this problem, I characterized a model of Zn^{2+} -induced injury in an attempt to isolate zinc's effect on cell death, *in vivo*. I also adapted a fluorimetric method to measure the amount of extracellular Zn^{2+} present following TBI, using microdialysis techniques. To date, the measurement of free ionic Zn^{2+} release *in vivo* after trauma has not been shown. I demonstrate that the amount of Zn^{2+} found in the extracellular fluid of TBI rats was below the range that causes neuronal injury and was not different than the

amount of Zn^{2+} found in sham operated rats. Results of my experiments do not support the idea that presynaptic release of Zn^{2+} causes injury to surrounding neurons.

Table of Contents

List of Figures	x
List of Abbreviations	xii
INTRODUCTION	1
Chapter 1: Background and Significance	1
Clinical Traumatic Brain Injury	2
Experimental Traumatic Brain Injury	4
Hippocampal Injury Resulting From Traumatic Brain Injury	5
Mechanisms of Cell Death Following Experimental Traumatic Brain Injury	7
Zinc Signaling in the Brain: Cytotoxic or Neuroprotective?	8
Evidence Supporting Extracellular Zn ²⁺ Release	9
Evidence Supporting Intracellular Zn ²⁺ Release	11
Evidence Supporting Neuroprotective Effects of Zn ²⁺ Release	12
Overall Significance	15
METHODS	17
Chapter 2: Materials and Methods	17
Reagents	17
Animals	17
Animal Surgical Preparation	17
Parasagittal Fluid Percussion Injury	18
Histochemical Staining	19
Zinc Chelation Experiments	19
Neuronal Counting	20
Channel Blocker Experiments	20
Laser Capture Microdissection	21
Ribonuclease Protection Assay	21
Statistical Analysis of RPA Gene Expression Levels	22
Zinc Chloride Injection	23

Silver Autometallography	23
Morris Water Maze	24
Barnes Maze.....	25
Statistical Analysis of Behavior Tests	25
Rat Toxicology Gene Array.....	25
Array Analysis	26
Microdialysis Preparation	26
Graphite Furnace Atomic Absorption Spectrophotometry	27
apo-CA/ABDN	28
RESULTS	31
Chapter 3: Traumatic Brain Injury Causes Increased Intracellular Zn ²⁺	31
Zinc Indicator Time Course Experiments.....	31
Zinc Accumulation Following Traumatic Brain Injury is Partially Prevented in the Rat Hippocampus by Lamotrigine and Nicardipine Pretreatment .	33
Summary and Conclusions	36
Chapter 4: Increased Extracellular Zn ²⁺ Causes Injury to Hippocampal Neurons	52
Characterization of Zinc Chloride Injection Model.....	52
Summary and Conclusions	58
Chapter 5: Traumatic Brain Injury Does Not Contribute to Increased Extracellular Zn ²⁺	83
Summary and Conclusions	86
DISCUSSION	91
Chapter 6: Summary and Conclusions.....	91
Appendices.....	96
Reference List	105
VITA	121

List of Figures

Figure 1. Representation of Zn ²⁺ translocation and intracellular Zn ²⁺ release hypotheses	16
Figure 2. Comparison of hippocampal sections stained with zinc indicator dyes.	39
Figure 3. FluoroJade-positive hippocampal neurons in sham and traumatic brain injury (TBI) rats.	40
Figure 4. Newport Green-positive hippocampal neurons in sham and traumatic brain injury (TBI) rats.	41
Figure 5. FluoZin-3-positive hippocampal neurons in sham and traumatic brain injury (TBI) rats.	42
Figure 6. RhodZin-3-positive hippocampal neurons in sham and traumatic brain injury (TBI) rats.	43
Figure 7. TSQ-positive hippocampal neurons in sham and traumatic brain injury (TBI) rats.	44
Figure 8. Prevention of neuronal degeneration in rat hippocampus CA1 and CA3.	45
Figure 9. Fluoro-Jade- and Newport Green-positive neurons after lamotrigine or nicardipine pretreatment.	46
Figure 10. Zinc accumulation in rat hippocampus CA1 and CA3 following lamotrigine or nicardipine pretreatment.	47
Figure 11. Ribonuclease protection assay of traumatic brain injured rats pretreated with lamotrigine.	48
Figure 12. Gene expression of surviving neurons after saline or lamotrigine (Lam) treatment followed by traumatic brain injury (TBI).	49
Figure 13. Ribonuclease protection assay for traumatic brain injury rats pretreated with nicardipine.	50
Figure 14. Gene expression of surviving neurons after saline or nicardipine (Nicard) treatment followed by traumatic brain injury (TBI).	51
Figure 15. Morris water maze testing at days 11-15 post-injection.	60
Figure 16. Timeline of behavior experiments for ZnCl ₂ and vehicle injected rats.	61
Figure 17A. Latency measurement: Morris water maze testing at days 1-10 post-injection.	62
Figure 17B. Total latency values for all 4 trials per day for all 10 days of Morris water maze testing.	63
Figure 18A. Path length measurement: Morris water maze testing at days 1-10 post-injection.	64
Figure 18B. Total path length values for all 4 trials per day for all 10 days of Morris water maze testing.	65
Figure 19. Total number of <i>no platform</i> measurements: Morris water maze testing at days 1-10 post-injection.	66
Figure 20A. Time to target hole: Barnes Maze performance at days 16-20 post-injection.	67
Figure 20B. Cumulative time to target hole in Barnes maze behavior test at days 16-20 post-injection.	68

Figure 21A. Time to first hole: Barnes maze locomotor behavior at days 16-20 post-injection.....	69
Figure 21B. Cumulative time to first hole in Barnes maze behavior test at days 16-20 post-injection.....	70
Figure 22. Survival time course of ZnCl ₂ injection injury.....	72
Figure 23. Dose response of ZnCl ₂ injection injury.	74
Figure 24. Zn ²⁺ detection in brain sections using silver autometallography.	75
Figure 25. Densitometry measurements of hippocampal Zn ²⁺ using silver autometallography.....	76
Figure 26. Densitometry measurements of Zn ²⁺ in the cortex using silver autometallography.....	77
Figure 27. N-(6-methoxy-8-quinoly)-p-toluenesulfonamide-stained silver AMG sections.	79
Figure 28. Hippocampal gene expression of vehicle and ZnCl ₂ injection rats 24 hours post injection using an Atlas Rat Toxicology 1.2 gene array.	80
Figure 29. Hippocampal gene expression of sham and TBI rats 24 hours post injury using an Atlas Rat Toxicology 1.2 gene array.....	81
Figure 30. Pie chart of gene expression.	82
Figure 31. Illustration of microdialysis probe placement.	88
Figure 32. Total zinc measured in microdialysate from rats receiving sham injury or moderate traumatic brain injury, using Graphite Furnace Atomic Absorption Spectrophotometry.....	89
Figure 33. Free Zn ²⁺ standard curve that was fit using the Hill equation.	90

List of Abbreviations

ABDF	4-(Aminosulfonyl)-7-fluorobenzofurazane
ABDN	7-(<i>N</i> -amino ethane-2-ol)benz-2-oxa-1,3-diazole-4-sulfonamide
aCSF	artificial cerebrospinal fluid
AMG	autometallography
AMPA	alpha-amino-3-hydroxy-5-methyl-4-isoxazolepropionic acid
ANOVA	analysis of variance
apo-CA	apo-carbonic anhydrase
ASIC	acid-sensing ion channel
BM	Barnes Maze
CA	cornu ammonis
Ca ²⁺	calcium ion
Ca-A/K	calcium permeant AMPA/KA channels
CaCl ₂	calcium chloride
CV	cresyl violet
dH ₂ O	deionized water
DMF	dimethylformamide
DNA	deoxyribonucleic acid
DPA	dipicolinate (pyridine-2,6-dicarboxylate)
FJ	Fluoro-Jade

FPI	fluid percussion injury
FZ3	FluoZin-3
GAPDH	glyceraldehyde-3-phosphate dehydrogenase
GF-AAS	graphite furnace atomic absorption spectrophotometry
GPX-1	glutathione peroxidase-1
HEPES	N-2-hydroxyethylpiperazine-N-2-ethanesulfonic acid
holo-CA	holo-carbonic anhydrase
KA	kainic acid
KCl	potassium chloride
LCM	laser capture microdissection
LTP	long term potentiation
MAP	mean arterial pressure
MD	microdialysis
MgCl ₂	magnesium chloride
Milli-Q	Millipore quality water
mRNA	messenger ribonucleic acid
MT	metallothionein
MWM	Morris water maze
NaCl	sodium chloride
NG	Newport Green
NMDA	N-methyl-D-aspartate
nNOS	neuronal nitric oxide synthase

NO	nitric oxide
ONOO-	peroxynitrite
PCR	polymerase chain reaction
ppb	parts per billion
ppm	parts per million
RNA	ribonucleic acid
ROS	reactive oxygen species
RPA	ribonuclease protection assay
RT-PCR	reverse transcription polymerase chain reaction
RZ3	RhodZin-3
SEM	standard error of the mean
SOD-2	superoxide dismutase-2
TBI	traumatic brain injury
TPEN	N,N,N,N-tetrakis(2-pyridylmethyl)ethylenediamine
TSQ	N-(6-methoxy-8-quinolyl)-p-toluenesulfonamide
VGCC	voltage-gated calcium channels
WDIA	weight drop impact-acceleration
Zn ²⁺	zinc ion
ZnCl ₂	zinc chloride
ZnSO ₄	zinc sulfate
ZnT3	zinc transporter 3

INTRODUCTION

Chapter 1: Background and Significance

Every 21 seconds, one person in the United States sustains a traumatic brain injury (TBI) (Brain Injury Association, 2008). Twenty-eight percent of hospitalizations for TBI from 1995-2001 resulted from falls and 20% were from motor vehicle-related accidents (Center for Disease Control and Prevention, 2006). The 1.5 million U.S. residents who incur a TBI each year (Thurman et al., 1999) far exceed the yearly cases reported for breast cancer, HIV/AIDS, spinal cord injury and multiple sclerosis combined. Survivors of TBI are often left with significant cognitive, behavioral, and communicative disabilities, and some patients develop long-term medical complications, such as epilepsy (NINDS, 2002). In cases of severe TBI, these cognitive (thinking, reasoning, problem solving, information processing, and memory) impairments often render the survivor incapable of performing basic tasks necessary for independent living. Even patients with mild to moderate head injuries suffer long-term disability as they may become easily confused and have problems with concentration (Sosin et al., 1996). Many TBI survivors have problems with executive functions, such as planning, organizing, abstract reasoning, problem-solving, and making judgments, which may make it difficult to resume pre-injury work-related activities (NINDS, 2002). In 2000, the total costs (direct and indirect) of TBI to the U.S. were over \$60 billion (Finkelstein et al., 2006). Currently, no pharmacologic interventions improve outcome following TBI in humans

(Marklund et al., 2006). More research is necessary in order to gain more insight into the mechanisms behind neuronal cell death resulting from TBI.

Despite substantial gains in understanding the pathophysiology following neurotrauma, little has been determined regarding the actual mechanisms that contribute to neuronal death. Lack of knowledge in this area has contributed to the plethora of ineffective treatments for survivors of TBI. This may be due to innate differences between rodents and humans in response to TBI or to differences in injury levels, as animals receiving experimental TBI under anesthesia generally experience a lower level of injury, which must be compatible with post-injury ambulation and feeding, than a severely injured human, in whom intensive care may be required for days or weeks (NIH Consensus Statement, 1998).

CLINICAL TRAUMATIC BRAIN INJURY

The Center for Disease Control and Prevention has defined TBI as a blow to the head that results in disruption of the brain's normal functions (Center for Disease Control and Prevention, 2006). TBI is dissimilar to *congenital* (Cerebral palsy, Down's syndrome, autism, and epilepsy) and *acquired* (stroke or transient ischemic attacks) *brain injury* classifications which also cause brain damage but have different mechanisms of action. Clinical TBI can produce a focal (localized to one particular brain region) or a diffuse (damage that affects multiple brain regions) injury and can be the result of either an open or closed skull injury. Mild TBI is defined as a trauma to the head that results in a loss of consciousness of 30 minutes or less and can be associated with minor disruptions in

cognitive functioning (Alexander, 1995). Concussions may be thought of as a mild TBI and most often occur from sports-related injuries or from whiplash injuries. Moderate TBI is typically defined as a loss of consciousness of between 30 minutes and 24 hours accompanied by moderate changes in cognitive functions while severe TBI results in major impairments and a loss of consciousness lasting longer than 24 hours (Hellowell et al., 1999). Most survivors of severe TBI require rehabilitation therapy to recover either their physical, occupational or mental functions after being in a coma. Age and TBI severity are the two biggest predictors of outcome (Giza et al., 2002; Marquez de la Plata et al., 2008). Systemic complications may also be present that can affect outcome following TBI (Chesnut et al., 1993; Lim and Smith, 2007) and could result in long-term dysfunction of the neuroendocrine system (Popovic et al., 2004; Popovic, 2005; Behan and Agha, 2007; Rothman et al., 2007) and disruption of circadian rhythms (Ayalon et al., 2007) and sleep patterns (Baumann et al., 2007; Parcell et al., 2008) of the survivor. Long-term changes in behavior and emotional state may affect the survivor's quality of life and ability to reintegrate into society (Ashman et al., 2006).

The primary mechanical injury associated with TBI occurs at the moment of impact usually results in damage resulting from when the brain and blood vessels are stretched, torn and compressed (Povlishock, 1986; Werner and Engelhard, 2007). Since the primary mechanical injury happens at the moment of trauma, it is nearly impossible to repair. Secondary injury which occurs from minutes to days after the TBI causes the neuronal deterioration and includes brain swelling, oxidative stress (Raghupathi, 2004), acidosis (Inao et al., 1988; Hovda et al., 1992) and excitotoxicity (Arundine and

Tymianski, 2004). Most pharmacologic interventions are targeted to prevent further damage caused by the secondary injury phase (McIntosh et al., 1998).

EXPERIMENTAL TRAUMATIC BRAIN INJURY

Several models of experimental TBI are currently used, but none of them completely replicates every feature of clinical TBI. Part of the difficulty in studying TBI results from the heterogenic nature of TBI as no two brain injuries are identical (Saatman et al., 2008). Most models share certain features of clinical TBI and hence may be used to understand the pathophysiology behind TBI (Morales et al., 2005). The impact acceleration model (Marmarou et al., 1994) of experimental TBI adequately mimics diffuse axonal injury and some cognitive deficits found in human TBI, but only selective regions of the hippocampus are affected by this model.

The midline fluid percussion injury (FPI) model of experimental TBI was originally developed for use in cats and rabbits (Hayes et al., 1987), and was subsequently adapted for use in rats (Dixon et al., 1987). Lateral or parasagittal injury sites were later developed (McIntosh et al., 1989) in order to use the animal's own contralateral (uninjured) hemisphere as a control for the injured hemisphere. FPI has been shown to induce brain edema, progressive gray matter necrosis and intracranial hemorrhage in a similar manner to human TBI (Graham et al., 2000).

In one study that compared the behavioral outcome and neuronal degeneration in rats resulting from either lateral FPI or weight drop impact-acceleration (WDIA) models of experimental TBI, it was determined that the lateral FPI model delivered injury to the hippocampus (evidenced by Fluoro-Jade staining and poor outcome on the Morris water

maze and the radial arm maze), whereas the rats receiving WDIA did not experience injury to the hippocampus (Hallam et al., 2004). Mild FPI has been shown to induce cognitive impairment with selective subfield damage to the hippocampus (Hicks et al., 1993). The position of the craniotomy site both anteroposterior and lateral to the midline also determines the location of injury to the brain and which hippocampal subfields are affected (Floyd et al., 2002).

Our laboratory uses parasagittal FPI as our experimental TBI model. It is one of the most widely used models of experimental TBI in rodents because it can replicate certain clinical features such as diffuse axonal injury and vulnerability to ischemic and mediator-related secondary injury. In a study that examined necrosis for up to one year post TBI in rats, the amount of injury surrounding the hippocampus is quite striking (Smith et al., 1997) and FPI also yields persistent cognitive dysfunction and neurological motor function up to one year post-injury, similar to that in clinical TBI.

HIPPOCAMPAL INJURY RESULTING FROM TRAUMATIC BRAIN INJURY

Neuronal damage can be detected within the first few hours following clinical and experimental TBI (Adams et al., 1989; Dietrich et al., 1994). The hippocampus is a region that is selectively vulnerable to injury following TBI (Lowenstein et al., 1992). Likewise, injury to the hippocampal neurons located ipsilateral to the injury site is a common effect of parasagittal FPI in rodents (Hicks et al., 1993). This is particularly relevant because in human TBI cases, cognitive deficits, learning and memory dysfunction, and memory loss are the most common long-lasting effects suffered. Our

previous studies indicated that the survival of rat hippocampal neurons following FPI correlates with expression of genes that promote survival such as heme oxygenase-1, heat shock protein 70 and superoxide dismutase (Shimamura et al., 2004; Hellmich et al., 2005b; Shimamura et al., 2005). The hippocampus has long been known to play a role in the processing of memories (Scoville and Milner, 1957) and is involved with spatial discrimination (Olton et al., 1978), which makes impairment in rodents detectable using learning and memory behavior testing based on spatial cues such as 3-dimensional objects in the room, lighting cues and symbols painted on the wall.

The structure of the hippocampus is elegantly organized into anatomically defined multiple layers and various subfields; which facilitates histological evaluation of FPI damage. For the following experiments, I focused on CA1/2 and CA3 pyramidal neurons, because they demonstrate a selective vulnerability to excitotoxic cell death following FPI (Cortez et al., 1989; Kotapka et al., 1991; Lowenstein et al., 1992; Hicks et al., 1996; Royo et al., 2006).

Fluoro-Jade (FJ) is a histological dye that stains injured or dead neurons. Fluoro-Jade-positive (FJ+) neurons have been detected in the CA1, CA2 and CA3 regions in as early as 2 hours following FPI, but maximal staining occurs at 24 hours post injury (Sato et al., 2001; Hellmich et al., 2005a). FJ (Schmued et al., 1997), an anionic fluorescein-derivative dye, was originally thought to be specific for detecting degenerating neurons. However, recent studies have shown FJ+ astroglia and blood vessels in the primate cerebral cortex (Colombo and Puissant, 2002) and FJ+ astrocytes (but not FJ+ neurons) following spinal cord injury in rats and mice (Anderson et al., 2003). In my dissertation

experiments, FJ is used as an indicator for degenerating neurons along with a cresyl violet counterstain, making the pyramidal cells easily visible in our sections.

MECHANISMS OF CELL DEATH FOLLOWING EXPERIMENTAL TRAUMATIC BRAIN INJURY

Experimental TBI can cause alterations in regional cerebral blood flow at early time points following FPI (Yuan et al., 1988). These early decreases in blood flow that cause ischemia are followed by reperfusion to the injured area that then causes an increase of reactive species (Kirsch et al., 1992) that then go on to cause damage to the cell membranes (Hall, 1993; Hall et al., 1993). Cells are also exposed to increased glutamate release followed by ionic flux which eventually results in fatigue of ATP-dependent Na^+/K^+ pumps trying to rebalance the electrochemical gradients. When the cell runs out of energy, it begins to operate in an anaerobic state which leads to accumulation of lactate (Kawamata et al., 1995), maximal at 2 hours post TBI (Inao et al., 1988), and a decrease in pH (Yuan and Wade, 1993). Decreased extracellular pH activates acid-sensing ion channels (ASICs) which induce a strong Na^+ current followed by a sustained non-selective cation current (Baron et al., 2002). Activation of ASIC1a receptors, which are Ca^{2+} permeable, have been shown to contribute to acidosis-related neuronal injury (Xiong et al., 2004; Yermolaieva et al., 2004). Zinc ions may gain entry via these ASIC1a receptors as they have been previously shown to gain entry into the cell via Ca^{2+} permeable channels (Sensi et al., 1997; Weiss and Sensi, 2000; Kwak and Weiss, 2006). Zinc has also been shown to stimulate the production of ROS and inhibit the antioxidant effects of glutathione reductase in astrocytes (Bishop et al., 2007).

Elevated intracellular free calcium has been linked to neuronal cell death after TBI and is associated with cognitive impairment in a study that correlated the Ca^{2+} fluctuations with the MWM performance (Deshpande et al., 2008). An increase in intracellular Ca^{2+} either from the extracellular space, or released from mitochondrial or endoplasmic reticulum stores can mediate cell death by activating calpains and caspases (Bano and Nicotera, 2007). Zinc ions may be cytotoxic through a variety of mechanisms; however there are also instances where zinc ions have been shown to be neuroprotective.

ZINC SIGNALING IN THE BRAIN: CYTOTOXIC OR NEUROPROTECTIVE?

Zinc is the most abundant trace metal in the human body after iron. A 70-kg human is said to contain 2.3 g of total zinc (McCance and Widdowson, 1942). Over 300 enzymes require zinc to be functional as it performs catalytic and structural tasks (Vallee and Auld, 1990, 1992, 1993). Zinc is also important to the processes of DNA replication (Vallee et al., 1991; Vallee and Falchuk, 1993) and protein synthesis and plays a role in cell cycle control (Beyersmann and Haase, 2001). Zinc was first detected in the brain by a histochemical stain (Maske, 1955) and confirmed using Timm's silver stain (Frederickson and Danscher, 1990).

Roughly 90-98% of zinc in the brain is bound, mostly to proteins, and the remaining 2-10% is thought to be unbound (free) ionic zinc (Zn^{2+}) sequestered in vesicles near the presynaptic membrane. The concentration of available free Zn^{2+} is tightly controlled by the cell and has been estimated to be in the femtomolar range in the cytosol during resting phase (Outten and O'Halloran, 2001) and has been detected in glial cell

lines (Haase and Beyersmann, 2002). Vesicular Zn^{2+} was first detected by electron microscopy (Haug, 1967) and has been found in both glutamatergic (Frederickson et al., 1983; Perez-Clausell and Danscher, 1985) and spinal cord GABAergic (Wang et al., 2001) neurons. Zn^{2+} , whether bound to metalloproteins such as metallothionein (MT) or enclosed in synaptic vesicles, is important in many cellular processes.

Neural circuits of zinc and glutamate containing neurons are important in behavior (Takeda et al., 2000), episodic memory formation and emotional expression (Frederickson and Danscher, 1990). Zinc acts as a modulator of synaptic function in the hippocampus and has been linked to neuronal cell death following brain injury (Choi and Koh, 1998; Lee et al., 1999; Frederickson and Bush, 2001). Glutamate release has been shown to increase during mossy fiber-CA3 long-term potentiation (LTP, a mechanism linked to increased learning and synaptic function), but not during Schaffer Collateral-CA1 LTP (Kawamura et al., 2004). The chelation of zinc has been shown to prevent LTP in mossy fibers (Li et al., 2001a) and to induce overexcitation in CA3 of the rat hippocampus (Blasco-Ibanez et al., 2004) resulting in neuronal death in the mouse hippocampus (Dominguez et al., 2003). Two theories of how zinc causes neuronal death have been proposed; one supports Zn^{2+} being released into the synapse and the other supports Zn^{2+} that is released from intracellular proteins.

Evidence Supporting Extracellular Zn^{2+} Release

Vesicular Zn^{2+} is thought to be co-released with glutamate because there have been interventions that inhibit release of both glutamate and zinc. One group developed a

method for the visualization of synaptic release dynamics with a zinc-imaging photodiode in mouse hippocampal slice preparations and claims that zinc is co-released with glutamate (Qian and Noebels, 2005). Synaptic activity or depolarization of the neuron can cause release of vesicular zinc, initially calculated to reach concentrations of 300 μM in the synaptic cleft (Assaf and Chung, 1984). More recent studies have estimated 10-100 μM Zn^{2+} present following stimulation (Vogt et al., 2000), while others believe it is closer to low nM range Zn^{2+} (Frederickson et al., 2006).

In an *in vitro* study, there was a rise in intracellular Zn^{2+} and widespread neuronal injury, when neuronal cells were incubated for 15 minutes with 300-1000 μM Zn^{2+} and excited by glutamate (Koh and Choi, 1994), which initially was attributed to extracellular zinc gaining entry into the postsynaptic neuron via voltage-gated calcium channels (VGCC) or ligand-gated receptor channels (Sensi et al., 1997). According to the translocation theory, vesicular Zn^{2+} is released in the presence of sodium-dependent action potentials and is calcium-dependent (Li et al., 2001b) and then translocates across the synaptic cleft to enter the postsynaptic neuron (Li et al., 2001b) via NMDA channels, VGCC and calcium permeable AMPA/kainate (Ca-A/K) channels (Yin et al., 2002). Once the Zn^{2+} has entered the postsynaptic cell, it may act as a secondary signaling messenger or it may interact negatively with the mitochondria, thereby contributing to the cell's death (Sensi et al., 2003). Figure 1 models two possible mechanisms of Zn^{2+} toxicity; i. translocation of synaptically released Zn^{2+} which then gains entry into the postsynaptic neuron, thereby overwhelming the neuron's buffering capacity that results in a lethal accumulation of free Zn^{2+} and ii. Calcium ions cause neuronal nitric oxide

synthase to be activated which causes an increase in reactive species which then release the Zn^{2+} ions from metallothionein proteins, thereby causing a similar lethal accumulation of free Zn^{2+} . It has proven difficult to provide evidence for Zn^{2+} translocation, especially *in vivo*. The current studies have attempted to address this controversy.

Evidence Supporting Intracellular Zn^{2+} Release

While the zinc translocation theory (Suh et al., 2000; Li et al., 2001b) may apply under certain circumstances, it is possible that the increase in intracellular zinc is due to release from MT proteins (Aizenman et al., 2000). Researchers in the MT biochemistry field discovered the release of metals from MT proteins by reactive oxygen species (ROS), specifically NO and peroxynitrite (ONOO^-) (Berendji et al., 1997; Cuajungco and Lees, 1998; Maret and Vallee, 1998). Excessive stimulation of NMDA receptors causes an activation of neuronal nitric oxide synthase (nNOS) (by the influx of Ca^{2+}), which then produces NO and indirectly ONOO^- . Bossy-Wetzel and colleagues provided evidence that NO/ ONOO^- could release zinc ions from the MT proteins in cortical neuronal culture cells, implicating both ROS and zinc ions in neurodegenerative pathologies (Bossy-Wetzel et al., 2004).

Mechanisms of Zinc Toxicity

There is mounting evidence to support the existence of zinc toxicity in neurons, both *in vitro* and *in vivo* (Weiss et al., 1993; Cuajungco and Lees, 1998). It is not clear as to whether the injury to neurons following TBI is due to a programmed cell death response or necrosis during the primary insult or secondary damage. Zinc toxicity may also involve uptake of zinc (possibly attached to MT proteins) into mitochondria, interfering with cellular energy production (Dineley et al., 2003). Some possible mechanisms include zinc inhibition of glycolysis, TCA cycle and electron transport chain, opening of the permeability transition pore (for review, see (Jiang et al., 2001)), and zinc-induced generation of ROS (Dineley et al., 2003). Mitochondrial energy depletion is a mechanism of a caspase-independent neuronal death which may occur secondary to cytochrome c release and non-functioning (respiratory chain) complexes III and IV (Lang-Rollin et al., 2003). Cytochrome C may be released and could activate a caspase-dependent apoptosis pathway which causes death to CA1 hippocampal neurons after ischemia (Zhan et al., 2001). There are many possible mechanisms of zinc neurotoxicity that require further exploration.

Evidence Supporting Neuroprotective Effects of Zn^{2+} Release

In addition to the evidence that increased intracellular Zn^{2+} causes neuronal injury and that exogenously applied Zn^{2+} also leads to cell death in high concentrations, reports of neuroprotective effects of Zn^{2+} can be found in the literature. Evidence exist that shows zinc supplementation through various routes leads to increased neuronal survival. Zinc supplementation in the diet appeared to improve neurologic recovery in patients

with severe brain injury when compared with a control group that received standard zinc therapy (Young et al., 1996). In an animal model of neurotrauma, unilateral cortical stab wounds were performed on adult rats that afterwards received either adequate zinc (30 mg/kg), supplemental zinc (180 mg/kg) or moderately deficient zinc (5 mg/kg) diets for four weeks and the authors found a statistically significant increase in terminal deoxynucleotidyl transferase-mediated biotinylated dUTP nick-end labeling (TUNEL) stained cells that expressed both ED-1 and OX-42 microglial markers (Yeiser et al., 2002) in the zinc deficient group. Levenson's group suggests neuroimmune cell death is prevented by maintaining adequate zinc levels in the brain (Yeiser et al., 2002). Generally speaking, certain levels of zinc are necessary to perform functions in the brain and when a deficiency exists, it may hinder repair processes.

An *in vitro* model found that exogenously applied zinc (100 and 500 μM , but not 25 μM ZnCl_2) given as a pretreatment prior to anoxia provided protection against apoptotic cell death in organotypic rat hippocampal cultures (Naganska and Matyja, 2002). In another study, the addition of 500 or 700 μM , but not 100 μM Zn^{2+} prevented nuclear translocation of the tumor suppressor protein p53 and protected cultured neurons from copper-induced neurotoxicity (Vanlandingham et al., 2002). Micromolar zinc was also applied to organotypic rat hippocampal slice cultures during a quick period of induced anoxic-hypoglycemia and prevented neuronal injury in contrast to increased cell injury when endogenous zinc was chelated using calcium ethylenediaminetetraacetic acid (Ca-EDTA) and demonstrated this protective effect of zinc was mediated through ATP-sensitive K^+ channels (Bancila et al., 2004).

Perhaps the most interesting evidence of zinc neuroprotection comes from *in vivo* studies in mice in which the zinc transporter 3 (ZnT3) gene was knocked out (Cole et al., 1999). Mice lacking the ZnT3 protein are phenotypically similar to wildtype mice despite their lack of vesicular Zn^{2+} stores (Cole et al., 1999). The only difference documented thus far is ZnT3 knockouts have a greater susceptibility to kainic acid (KA) induced seizures (Cole et al., 2000). ZnT3 knockout mice did not display impaired spatial learning and memory based on behavioral tests and they exhibited normal sensorimotor functions implying synaptic vesicle Zn^{2+} is not necessary for these tasks (Cole et al., 2001). Therefore, synaptically released Zn^{2+} may play a role in preventing seizure activity or provide neuroprotection from excitotoxicity under normal conditions.

When extracellular zinc was chelated after TBI in rats, we found a correlation between the uninjured neurons and an upregulation of neuroprotective genes (Hellmich et al., 2004). Zinc neurotoxicity has also been prevented *in vivo* by the co-injection of a zinc chelator and zinc chloride (ZnCl_2) (Cuajungco and Lees, 1996). Moreover, extracellular Zn^{2+} chelation using CaEDTA causes significant impairment learning and memory as evidenced by poor Morris water maze (MWM) performance (Hellmich et al., 2008). Recently Zn^{2+} has been shown to inhibit ASIC currents at nanomolar concentrations (Chu et al., 2004) and that extracellular Zn^{2+} protects against acidosis-induced injury (Hey et al., 2007). Needless to say, zinc ion homeostasis is complex (Takeda, 2000) especially in pathologic conditions (Choi and Koh, 1998).

OVERALL SIGNIFICANCE

The overall goal of my research was to examine the role of Zn^{2+} in neuronal cell death following TBI *in vivo*. I chose to study zinc and TBI because of compelling evidence of Zn^{2+} excitotoxicity in ischemia and seizure models and thought the same mechanism of cell death may apply to the injury found following TBI. I hypothesized that Zn^{2+} is an important pathogenic component of TBI and I predicted the following: 1) TBI causes accumulation of intracellular Zn^{2+} , 2) Injections of exogenous Zn^{2+} produce hippocampal damage similar to TBI, and 3) Zn^{2+} levels present in the extracellular fluid following TBI are toxic. My project was part of a long-term effort to increase our understanding of the role Zn^{2+} plays in the events following TBI. To this end, my studies present evidence that presynaptic Zn^{2+} release following TBI is not, by itself, sufficient to cause neuronal injury. I also present data that show spatial learning and memory deficits occur following hippocampal injections of ZnCl_2 . These findings contribute to the ever-expanding pool of knowledge in the field of zinc and neuronal injury, which may one day lead to effective treatments for TBI survivors.

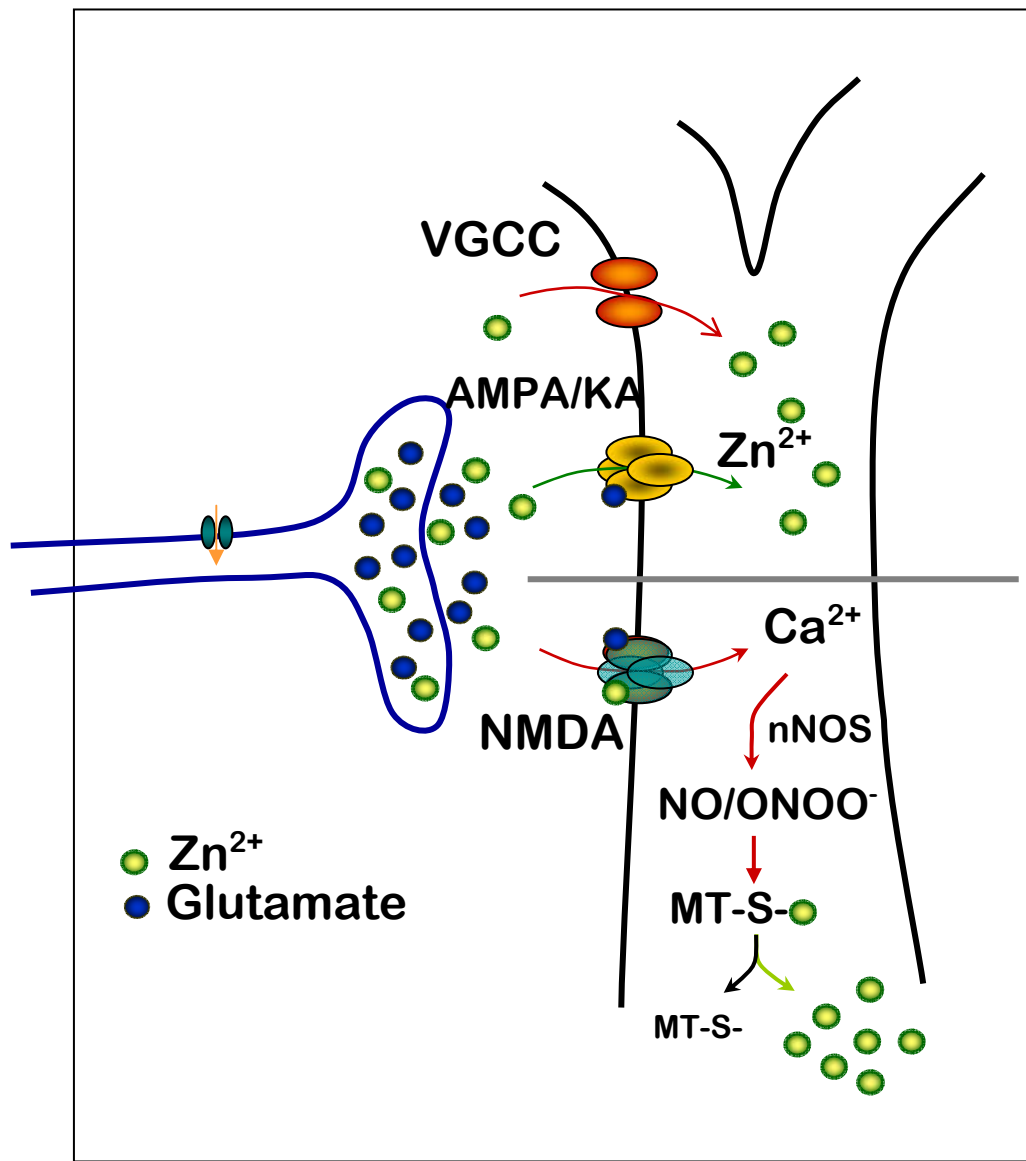


Figure 1. Representation of Zn²⁺ translocation and intracellular Zn²⁺ release hypotheses

Translocation hypothesis: presynaptic release of Zn²⁺ may gain entry into the postsynaptic neuron via voltage-gated calcium channels (VGCC) or calcium permeable alpha-amino-3-hydroxy-5-methyl-4-isoxazolepropionic acid/kainite receptors (AMPA/KA) causing a lethal accumulation of free Zn²⁺ in the postsynaptic neuron. Intracellular Zn²⁺ release hypothesis: presynaptically released glutamate activates N-methyl-D-aspartate (NMDA) receptors which allow calcium entry into the postsynaptic neuron. Calcium ions (Ca²⁺) may activate neuronal nitric oxide synthase (nNOS) which could produce reactive oxygen species such as nitric oxide (NO) and peroxynitrite (ONOO⁻) which then could react with the sulfide bond that binds Zn²⁺ to metallothionein (MT) proteins, causing a lethal accumulation of free Zn²⁺.

METHODS

Chapter 2: Materials and Methods

REAGENTS

All reagents used were purchased either from Sigma-Aldrich (St. Louis, MO) or Invitrogen Corporation (Carlsbad, CA) unless otherwise stated.

ANIMALS

The Institutional Animal Care and Use Committee of the University of Texas Medical Branch approved all experimental protocols and all experiments conformed to their guidelines on the ethical use of animals. All experiments were performed on male Sprague Dawley rats (400-500g, 4-6 months of age) that were provided with food and water *ad libitum* and were exposed to 12 hour light and dark cycles.

ANIMAL SURGICAL PREPARATION

Male Sprague-Dawley (Charles Rivers Laboratories, Inc.,Wilmington, MA) rats were anesthetized (4% isoflurane), intubated, mechanically ventilated (1.5% isoflurane in O₂:air (30:70) using a volume ventilator (NEMI Scientific: New England Medical Instruments, Medway, MA)), prepared for moderate or severe or sham parasagittal fluid percussion injury (Dixon et al., 1987; McIntosh et al., 1989). Rectal and temporalis muscle temperatures were monitored using telethermometers (Physitemp Instruments, Clifton, NJ) and temperatures were maintained within a range of 37.5 ± 0.5 °C using an overhead lamp and a thermostatically controlled water blanket (Gaymar, Orchard Park,

NY). Rats were placed in a stereotaxic head holder and a midline incision of the skin was performed and the skull exposed. With the use of a Michele trephine, a craniotomy was performed 1 mm lateral to the sagittal suture, midway between lambda and bregma sutures, over the right hemisphere. The bone chip was removed, leaving the dura intact. A modified 20-gauge needle hub was secured in place over the exposed dura with cyanoacrylic adhesive and cemented into place with hygienic dental acrylic. An arterial line was placed in some animals to monitor the mean arterial pressure. Blood gas measurements were made by removing up to 0.5 cc of blood from the arterial line. Hematocrit and blood glucose were also determined using the same blood sample. Drug treatments (if applicable) were given to rats via a jugular vein catheter, which is typically implanted just prior to the arterial line.

PARASAGITTAL FLUID PERCUSSION INJURY

Trauma was administered by means of a fluid percussion injury (FPI) device (Dixon et al., 1987; Hayes et al., 1987) consisting of a Plexiglas cylinder 60 cm long and 4.5 cm in diameter filled with isotonic saline, one end of which was connected to a hollow metal cylinder housing a pressure transducer (Statham PA856-100, Data Instruments, Acton, MA) and the other end of which was closed by a Plexiglas piston mounted on O rings. The transducer housing was connected to the rat by a plenum tube at the craniotomy site. Traumatic brain injury (TBI) was induced when a 4.8 kg steel pendulum struck the piston after being dropped from a variable height that determined the intensity of the injury. The fluid pressure pulse was then recorded on an oscilloscope triggered photoelectrically by the descent of the pendulum.

HISTOCHEMICAL STAINING

Rats were prepared as stated above. Frozen coronal sections (10 μm thick) were cut on a cryostat (Leica Microsystems, Inc., Bannockburn, IL) and mounted onto pre-cleaned uncoated glass slides (Fisher Scientific, Pittsburgh, PA). Slides were kept at -20°C until sectioning was completed. Briefly, the sections were fixed in 75% (v/v) ethanol for 1 minute, rinsed with Milli-Q water for 1 minute, counterstained with cresyl violet for 15 seconds (if applicable) and rinsed with Milli-Q water, stained with appropriate fluorescent dye for 4 minutes, rinsed with Milli-Q water for 3 minutes, 95% ethanol for 30 seconds, 100% ethanol for 30 seconds and 3 minutes in xylene to dehydrate the sections, as previously published (Hellmich et al., 2005a; Hellmich et al., 2007). Serial adjacent sections were collected (every 15th section allotted for the same indicator) and stained with either: Fluoro-Jade (FJ; an indicator of lethal cell injury), FluoZin-3 (FZ3; $K_d = 15\text{ nM}$; the highest affinity dye), RhodZin-3 (RZ3; $K_d = 65\text{ nM}$; intermediate affinity), Newport Green (NG; $K_d = 1\text{ }\mu\text{M}$; lowest affinity), N-(6-methoxy-8-quinolyl)-p-toluenesulfonamide (TSQ; $K_d = 14\text{ nM}$). All indicators were purchased from Invitrogen/Molecular Probes except Fluoro-Jade (Histo-Chem, Inc., Jefferson, AR).

ZINC CHELATION EXPERIMENTS

A subset of brain sections taken from rats survived 24 hours post-injury was used in zinc chelation experiments. These brain sections were either fixed with 75% (v/v) ethanol and stained for 4 minutes with TSQ either before or after chelation with 2 mM N,N,N,N-tetrakis(2-pyridylmethyl)ethylenediamine (TPEN) or they were stained and chelated in the absence of fixation.

NEURONAL COUNTING

Numbers of FJ-, FZ3-, RZ3-, TSQ-, and NG-positive neurons in CA1 and CA3 in each of the ten slides per rat brain were counted blindly using a PixCell Iie imaging system (Arcturus-Molecular Devices, Sunnyvale, CA). For each hippocampal subfield, the numbers of positive neurons were averaged to get a total average number of positive neurons per rat which were then averaged within treatment groups (Hellmich et al., 2005a). We performed one-way analyses of variance (ANOVA) and Fisher's post hoc tests using Statview 5.0 (SAS Institute, Inc., Cary, NC). Since under normal conditions, sham injured rats display very few, if any, positive neurons in comparison to rats that have undergone severe FPI, stereologic counting techniques were unnecessary to obtain accurate estimates of cell death in the injured region of the hippocampus.

CHANNEL BLOCKER EXPERIMENTS

Animals were prepared as described above with tail artery and jugular vein catheters. Thirty minutes prior to fluid percussion traumatic brain injury (or sham injury), the animals were given a slow infusion (over a period of 15 minutes) of a randomly selected drug intervention (lamotrigine: 20 mg/kg, nicardipine: 5 mg/kg, or saline vehicle) via the jugular vein catheter, followed by a 2 cc flush of saline. After blood gases and physiologic measurements were maintained at appropriate levels, the fluid percussion injury device was then connected to the adapter and a quick bolus of water was propelled towards the dura, causing displacement and injury of the underlying brain tissue. After waking from anesthesia, the rats were survived for 24 hours and then decapitated and their brains were kept in -80°C freezer until sectioned. Using separate slides, both injured (FJ-positive) and adjacent uninjured neurons were collected from the

hippocampus (from the CA1/2 and CA3 subregions) using laser capture microdissection (LCM) and RNA was isolated from them for a ribonuclease protection assay (RPA).

LASER CAPTURE MICRODISSECTION

I fixed 10- μ m frozen hippocampal sections in 75% (v/v) ethanol (1 min), stained with FJ, counterstained with 1% (w/v) cresyl violet (15 sec) and dehydrated in graded alcohols and xylene as previously described (Hellmich et al., 2005b). I performed LCM with a PixCell IIe LCM system (Arcturus). Twenty-five FJ-positive were captured from each rat hippocampus on separate Capsure HS LCM Caps (Arcturus). I isolated total RNA with the RNAAqueous Micro kit (Ambion, Austin, TX) and linearly amplified the mRNA with T7 polymerase (MessageAmp II kit, Ambion) as previously described (Hellmich et al., 2005b).

RIBONUCLEASE PROTECTION ASSAY

To quantitatively compare mRNA expression in FJ stained and LCM captured neurons between the drug intervention and injury groups, we used the ribonuclease protection assay (RPA), a simple and linear assay that is sufficiently sensitive to detect even low abundance transcripts (i.e., less than 14 copies of mRNA per cell). Probes for the RPA were cloned using reverse transcription-polymerase chain reaction (RT-PCR) as previously described (Shimamura et al., 2004). Using RT-PCR, we have cloned four genes that have been shown to be involved in either the progression or prevention of oxidative stress and cell death processes (caspase 9, nNOS, glutathione peroxidase-1 (GPX-1), Mn-superoxide dismutase-2 (SOD-2)). The housekeeping gene glyceraldehyde-3-phosphate dehydrogenase (GAPDH) was used for normalization. To prepare DNA

templates for RPA probes, consensus promoter sequences for T3 (sense strand) and T7 (antisense strand) RNA polymerase were incorporated into the 5' ends of gene-specific oligonucleotides used to PCR amplify the nested DNA templates from the RT-PCR cloned gene fragments. Sequences of cloned genes were verified by manual sequencing using a *fmol* DNA Cycle Sequencing System (Promega, Madison, WI). Sequences of PCR primers for initial RT-PCR cloning of the genes and for subsequent PCR amplification of RPA template DNA are shown in Appendix Table 1. RPA analyses were performed with 100 ng (equivalent to approximately 5 µg of total RNA) of linearly amplified mRNA samples according to manufacturer's protocols using the HybSpeed RPA kit (Ambion) as previously described (Shimamura et al., 2004). RPA gels were dried on 3M paper and exposed to phosphorimaging screens for 72 hours, scanned on a Cyclone PhosphorImager (Perkin-Elmer Life Sciences, Downers Grove, IL), analyzed with the associated OptiQuant software (Perkin-Elmer Life Sciences) and the data imported into an Excel spreadsheet for further analysis. Digitized data were normalized to the housekeeping gene GAPDH (Shimamura et al., 2004).

STATISTICAL ANALYSIS OF RPA GENE EXPRESSION LEVELS

We analyzed the levels of mRNA separately for each gene (nNOS, GPX-1, SOD2, caspase 9 and GAPDH) using a two-way mixed model. The two factors were rat (random effect) and drug treatment (Lamotrigine, Nicardipine or Saline). To account for multiple testing, differences in gene expression of the four genes between the different drug treatments were considered significant at the 0.025 level. We conducted data analysis using SAS® 9.1.

ZINC CHLORIDE INJECTION

Animals were prepared with a tail artery cannula and a trepaned craniotomy, similar to the rats undergoing a fluid percussion injury, but instead of receiving a TBI, they received a hippocampal injection of zinc chloride (ZnCl_2) or vehicle (chelexed artificial cerebrospinal fluid). ZnCl_2 (60 pM-1 mM) was injected into the CA2/CA3 region of the dorsal hippocampus using the stereotaxic coordinates of -3.6 A-P, -3.6 L-R, -3.6 dura (Paxinos and Watson, 1986). Animals were sacrificed at designated survival time (30 minutes-20 days) and their brains were harvested, frozen using dry ice and kept at -80°C until sectioned. Rats that were survived for 20 days underwent behavior testing and all rats survived for longer than 24 hours underwent sterile operations using autoclaved instruments and drapes and their heads were shaved and coated in betadine solution prior to incision.

SILVER AUTOMETALLOGRAPHY

Rats were prepared as described above. In all but naïve controls, a 3 mm-diameter skull piece was removed from the right side of the skull halfway in between lambda and bregma, leaving the dura intact. Rats received either moderate or sham TBI or either (125 μM) ZnCl_2 , (aCSF) vehicle or 5 mM TPEN injection and were survived 6 hours prior to perfusion. All rats were re-anesthetized using pentobarbital and were transcardially perfused with 0.1% sodium sulfide and phosphate-buffered 3% glutaraldehyde (the NeoTimm method). Rats were then decapitated, brains harvested and post-fixed overnight and then switched to 30% (w/v) sucrose solution until the brain sank to bottom of the jar. At least 10 coronal sections (30 μm thickness) were cut using a cryostat and mounted onto glass slides.

Silver autometallography (AMG) techniques were used (Danscher et al., 2004). Briefly, sections were rinsed with Farmers solution, rinsed with dH₂O and then developed for 60 minutes in a temperature-controlled darkroom. AMG development was halted by removing sections from the silver lactate (AMG development solution) and rinsed for 10 min with 5% thiosulfate solution. The sections were dipped into 2 dH₂O dishes and then immersed for 30 seconds in 2% Farmers solution and then sections were immediately dehydrated and either mounted without counterstain or counterstained with toluidine blue.

MORRIS WATER MAZE

Animals were assessed either on days 1-10 or 11-15 post-injury. Four trials were completed each day. The water maze is a 1.8 m diameter tank, filled to 2 cm above an invisible platform that is 10 cm in diameter and 26 cm high (Morris, 1984; Hamm et al., 1996; Hamm, 2001). The water temperature was held at 26-27 °C. The platform was stationary throughout the experiment. Our tank is divided into four quadrants marked on the wall in each quadrant by shapes of different colors (stationary cues). The animals' starting point was randomly chosen each day based on these quadrants, one trial is started from each quadrant. The SMART computer system (San Diego Instruments, San Diego, CA) was used to track and monitor the animal during each trial. After placing the animal in the water facing the wall of the tank, the handler stepped behind a curtain to monitor the rat being tracked on a computer monitor. The animal was allowed two minutes to find and climb the platform and escape the water, he must remain on the platform for 30 seconds. If the animal does not find the platform, the handler placed him on it for 30

seconds before removing him from the maze. The animals were given a four-minute rest period in a warming chamber between each trial.

BARNES MAZE

ZnCl₂ injection animals were assessed on days 16-20 post-injection. Two trials were completed each day. The Barnes maze is a 48" diameter circular platform, 36" high, brightly lit with 20 holes (4" d) around the periphery (Barnes, 1979). The target hole has an escape box underneath and the same target hole was used for each animal for all 5 testing days. Rats were given a maximum of 4 minutes to locate the target box and the rats were left in the target box for 30 seconds to remember where the target hole is located. A 1-2 minute resting period in the home cage was used in between trials while the platform was cleaned.

STATISTICAL ANALYSIS OF BEHAVIOR TESTS

Repeated Measures analyses of variance (RM-ANOVA) followed by Fisher's posthoc tests were used to assess the statistical significance (Statview 5.0). P values of less than or equal to 5% ($p \leq 0.05$) were considered significant.

RAT TOXICOLOGY GENE ARRAY

Total RNA was extracted from each hippocampus using Ultraspec RNA isolation kit (Biotechx, Houston, TX) according to the manufacturer's instructions. The ³³P-labelled cDNA probes were separated from unincorporated nucleotides and small cDNA fragments by using a spin column (microspin S-200 HR columns kit, GE Healthcare UK, Buckinghamshire, UK). We used the Atlas Rat Toxicology Array II (Clontech

Laboratories, Mountain View, CA), which includes 450 rat cDNAs immobilized in duplicate dots on a nylon membrane. The cDNA microarray analysis was performed according to the instruction manual (Clontech). The radioactivity on the membrane was analyzed and quantified by using a phosphoimager. Expression levels of the housekeeping genes were used as standards for normalizing the expression levels of the genes of interest.

ARRAY ANALYSIS

Expression levels of genes correspond to the radioactivity on the membrane's "spots" which were digitized by the OptiQuant 4.0 program quantified by using a densitometry function and normalized to internal housekeeping genes using Atlas Image 2.7 (Clontech). Differences in gene expression between the treatment groups were examined using both GeneSpring GX 7.3 Expression Analysis (Agilent Technologies, Santa Clara, CA) and SAM 3.02 (Stanford tools for Excel) programs. A pair-wise comparison was used to further exclude the possibility of false positive genes.

MICRODIALYSIS PREPARATION

Tail artery cannulation was used in all animals to monitor mean arterial pressure (MAP) throughout the experiment and record baseline blood gasses. Rats were prepared as described above except the adapter and acrylic resin steps were omitted in order to insert the microdialysis (MD) probes without interference. Artificial cerebrospinal fluid (aCSF) was made (147.0 mM NaCl, 2.3 mM CaCl₂, 4.0 mM KCl, and 0.9 mM MgCl₂ in Milli-Q purified deionized water, addition of CaCl₂ and MgCl₂ after chelation) and chelexed (Chelex-100 resin, BioRad, to remove free zinc that may have been in the Milli-

Q water) ahead of time and stored in a Teflon bottle at 4°C until used. All tubing (PE 50), probes (4mm membrane, MD-2204 BR-4, Bioanalytical, West Lafayette, Indiana) and syringes (Hamilton glass syringe) used were flushed multiple times with aCSF prior to each usage in order to dislodge any zinc embedded in the plastic or glass material. Only eppendorff tubes, conical tubes, bottles and beakers made of either Teflon or polypropylene were used to limit chelation and absorption of zinc. *In vitro* recovery rate determination: MD probe was inserted into a polypropylene beaker filled with a known concentration of zinc (diluted in aCSF sitting on a hotplate set at 37°C during entire recovery), syringe was filled with aCSF and infused through tubing at a pump rate of 1 µl per minute for 20 minutes, dialysate was collected into eppendorff tubes covered with parafilm. *In vivo* MD: MD probe was inserted stereotactically (coordinates: -3.6 A-P, -3.6 L-R, and -3.6 dura), aCSF was infused at a pump rate of 1 µl per minute for at least 1 hour, microdialysate was collected into eppendorff tubes covered with parafilm. Once collected, all samples were kept at -80°C until taken for GF-AAS analysis of total zinc or free Zn²⁺ measurement using the apo-CA/ABDN technique. Zinc standards used for *in vitro* recovery rate determination were diluted from primary zinc standard (AAS verified, Sigma). Animals were sacrificed either by KCl injection, 100% Nitrogen induced ischemia or decapitation immediately following collection.

GRAPHITE FURNACE ATOMIC ABSORPTION SPECTROPHOTOMETRY

Concentrations of zinc in the microdialysis samples were determined by graphite furnace atomic absorption spectrophotometry (GF-AAS). A Perkin-Elmer model 5100 atomic absorption spectrophotometer with Zeeman-5100 deuterium arc correction, equipped with a Perkin-Elmer HGA-600 graphite furnace, a Perkin-Elmer electrodeless discharge lamp (EDL System-2) and a Perkin-Elmer-60 autosampler was used for all GF-

AAS analyses. Argon gas was used to protect and purge the graphite tubes. The data acquisition was routinely carried out using Perkin-Elmer AA WinLab Analyst software version 3.0. The zinc standards were prepared by diluting the stock solution [1000 mg/L (ppm) Aldrich high purity standard] using Chelexed Milli-Q water. The calibration standards were 0.00, 0.5, 1.0, 2.0, and 4.0 microgram/L (ppb). Calibration standards were run in between each set of six samples to check accuracy.

To avoid zinc contamination from external sources, all solutions were stored in Teflon or polypropylene containers and solutions were transferred using either metal-certified pipette tips or individually wrapped plastic transfer pipettes rinsed with 0.25 M double-distilled Ultra-pure nitric acid (GFS Chemicals, Powell, OH) and rinsed thoroughly with Milli-Q deionized water followed by chelexed water prior to loading each standard or sample. The disposable autosampler cups were rinsed in this manner prior to the transfer of samples.

APO-CA/ABDN

Removal of metal from carbonic anhydrase

Metal was removed from carbonic anhydrase using methods described in Thompson et al., 2000 (Thompson et al., 2000). Dipycolinate (50 mM pyridine-2,6-dicarboxylate; DPA) diluted in chelexed HEPES (pH 7.4) was added to holo-bovine carbonic anhydrase II (holo-CA) and stored overnight at 4°C and then transferred to an Amicon Centricon 10 concentrator tube (Millipore Corporation, Bedford, MA). Centricon tubes were centrifuged for 60 minutes at 6000 rpm and filtrate was removed and saved in polypropylene microcentrifuge tubes to measure the amount of DPA contamination. After each spin (up to 10), initial volume was maintained at 2 mL by

adding chelexed HEPES without DPA. Each spin removed approximately 10-fold DPA and was verified by lack of DPA intrinsic absorbance at A_{271} in last flow-through sample. Approximate concentration of apo-CA (metal-free CA) was determined by measuring absorbance at 280 nm using a UV spectrophotometer and dividing that value by the extinction coefficient of bovine carbonic anhydrase II ($\epsilon = 57057$).

Synthesis of ABD-N from ABD-F

ABD-N was synthesized using methods described in Thompson et al., 2000 (Thompson et al., 2000). Anhydrous dimethylformamide (DMF) and a 5X molar excess of ethanolamine were added to ABD-F and left at room temperature for 1 hour, until the solution turned from yellow to orange. Confirmation of complete synthesis was verified by comparing non-overlapping absorbance spectra from both ABD-F and ABD-N. ABD-N was also evaluated for zinc contamination with GF-AAS prior to use.

Measurement of Zn^{2+} in samples

Prior to determination of Zn^{2+} in samples, pM- μ M $ZnSO_4$ samples were measured and then plotted in log scale against calculated free zinc values and fit the data using a Hill equation and a logistic sigmoidal function using Origin 7.5 software (Origin Lab Corporation, Northampton, MA). Sample or Zn standard, apo-CA (3.2 μ M), ABD-N (2.5 μ M) and chelexed HEPES were added to each microcuvette covered with Parafilm and fluorescence was measured with an SLM 8000 spectro-fluorimeter with ISS data acquisition and Vinci Multidimensional Fluorescence Spectroscopy software (25 °C, 415 nm excitation, 560 nm emission). Fluorescence intensity values from each sample were compared to the values obtained from the Zn standard curve to estimate the Zn^{2+}

concentration. Temperature measurements were taken hourly to gauge changes in fluorescence intensity.

RESULTS

Chapter 3: Traumatic Brain Injury Causes Increased Intracellular Zn^{2+}

ZINC INDICATOR TIME COURSE EXPERIMENTS

Since there is a high correlation between the number of FJ+ neurons and NG+ neurons appearing in brain sections following FPI, we thought FJ could also stain zinc, similar to NG (Hellmich et al., 2007). As NG has a K_d of 1 μM for Zn^{2+} , it is also possible that it would take a few hours to accumulate that concentration of Zn^{2+} in the cell, which would explain why no positive neurons are detected prior to 2-4 hours post-injury. To evaluate the time course of ionic zinc staining as a reflection of ionic zinc accumulation in hippocampal neurons associated with commercially available zinc indicator dyes with markedly different affinities for zinc after 30 minute or 2, 8, or 24 hour survival following fluid percussion TBI. I hypothesized that dyes with greater affinities for Zn^{2+} would detect intraneuronal zinc accumulation at earlier time points than lower affinity dyes.

FJ, an anionic fluorescein derivative stain, detects injured neurons but the precise entity that it binds to remains unknown. Consecutive sections were stained with dyes of varying affinities for Zn^{2+} because many of them are excited at the same wavelength. The animals were prepared as described in Animal Surgery and FPI sections of the methods chapter and the indicators used included Fluoro-Jade (FJ; an indicator of lethal

cell injury), FluoZin-3 (FZ3; $K_d = 15$ nM; the highest affinity dye), RhodZin-3 (RZ3; $K_d = 65$ nM; intermediate affinity), Newport Green (NG; $K_d = 1$ μ M; lowest affinity), N-(6-methoxy-8-quinolyl)-p-toluenesulfonamide (TSQ; $K_d = 14$ nM). Despite differences in zinc ion detection limits, the indicator dyes stained approximately identical neurons found in similar locations as shown in Figure 2. Interestingly, the most sensitive indicators tested revealed zinc staining around the edge of the cell as well as staining of vasculature and astrocytes. There were very few, if any, positive neurons in the animals surviving less than 8 hours post-TBI. None of the sham-injured animals displayed positive neurons.

Figure 3A shows the number of FJ+ neurons counted in both sham and TBI animals in the CA1/2 subregions of the hippocampus at 30 minutes, 2 hours, 8 hours and 24 hours survival times. Both 8 and 24 hours time points showed an average of 30 positive neurons. In the CA3 region, there were approximately 15 FJ+ neurons (Figure 3B). Average positive neurons in the CA1/2 regions were 27 in NG stained sections (Figure 4A), 26 in FZ3 (Figure 5A), 26 in RZ3 (Figure 6A) and 27 in TSQ (Figure 7A) stained sections. For the CA3 region, average numbers of positive neurons were 15 for NG (Figure 4B), 14 for FZ3 (Figure 5B), 12 for RZ3 (Figure 6B) and 11 for TSQ (Figure 7B) stained sections. Overall, there were no statistically significant differences between the different indicator dyes at any of the survival time points.

Results of this study suggest that zinc accumulation, as evidenced by detection by indicator dyes, is a rapidly occurring event that occurs prior to death, rather than a gradual accumulation. This zinc accumulation is associated with a cell death process that

occurs in between 2 and 8 hours post trauma. This may be the effect of the cell releasing large quantities of Zn^{2+} that is normally bound to proteins and may be the result of the cell irreversibly committing itself to die. It is unclear at this time whether the intracellular Zn^{2+} *causes* the cell to die or if it is being detected after the cell has committed to die.

ZINC ACCUMULATION FOLLOWING TRAUMATIC BRAIN INJURY IS PARTIALLY PREVENTED IN THE RAT HIPPOCAMPUS BY LAMOTRIGINE AND NICARDIPINE PRETREATMENT

After a traumatic brain injury, hippocampal injury contributes to cognitive disability, yet little is known about the molecular mechanisms responsible for hippocampal neuronal degeneration. Zn^{2+} accumulation via voltage-operated calcium channels may contribute to excitotoxicity (Frederickson et al., 2004; Kwak and Weiss, 2006). Nicardipine, an L-type calcium channel antagonist, inhibits Zn^{2+} accumulation and lamotrigine, a sodium channel blocker, inhibits glutamate release (Bacher and Zornow, 1997) and protects hippocampal (CA1) neurons from ischemic injury (Crumrine et al., 1997). To examine the role of sodium or L-type calcium channels in Zn^{2+} accumulation and neuronal injury (Sensi et al., 1997), we counted the numbers of NG and FJ positive neurons in rats treated with nicardipine or lamotrigine 30 minutes prior to fluid percussion TBI (Hellmich et al., 2007).

The following experiments were designed to test the hypothesis that presynaptically-released Zn^{2+} translocates and gains entry into the cell via voltage-gated calcium channels (VGCC). Nicardipine, a selective L-type VGCC inhibitor, was selected

to block this particular route of entry. Lamotrigine, a sodium channel inhibitor, was used to prevent the initial glutamate and zinc vesicle release from the presynaptic neuron.

Animals for this set of experiments were prepared as described in the Channel Blockers section of the Methods chapter. The hippocampal sections were counterstained with cresyl violet (CV, Nissl stain) to visualize the pyramidal cells using a light microscope. After 24 hour survival post moderate parasagittal FPI, the animals that were pretreated with lamotrigine or nicardipine had fewer FJ+ (injured) neurons compared to saline vehicle treatment animals (Figure 8). None of the animals receiving sham injury in combination with any drug treatment displayed FJ+ neurons (Figure 8). The total numbers of FJ+ neurons were counted in a total of 10 sections per rat and a total of six rats were averaged per treatment group, as shown in Figure 9, which was published with permission from Elsevier (Hellmich et al., 2007). The sham injured rats were excluded from this graph due to their negligible amount of FJ+ neurons. The numbers of FJ+ neurons were significantly reduced by lamotrigine treatment in CA1 and CA3 ($p < 0.05$, compared to TBI + saline). The numbers of FJ+ neurons were significantly reduced in CA1 by nicardipine treatment ($p < 0.05$, compared to TBI + saline). Nicardipine also reduced FJ+ neuron counts, but not significantly ($p = 0.069$) with this number of rats (Hellmich et al., 2007).

Adjacent sections were taken from each rat to be stained for zinc with NG in order to be stained and counted on the same day as FJ-stained sections. After 24 hour survival post moderate parasagittal FPI, the animals that had been pretreated with lamotrigine or nicardipine had fewer NG+ neurons compared to saline vehicle treatment

animals (Figure 10). None of the animals receiving sham injury in combination with any drug treatment displayed NG+ neurons (Figure 10). Following a similar staining protocol to FJ, the NG+ (zinc positive) neurons were counted in a total of 10 sections per rat and a total of six rats were averaged per treatment group, as shown in Figure 9 (Hellmich et al., 2007). The sham injured rats were also excluded from this graph due to their negligible amount of NG+ neurons. The numbers of NG+ neurons were significantly reduced by lamotrigine treatment in CA1 and CA3 ($p < 0.05$, compared to TBI + saline). The numbers of NG+ neurons were significantly reduced in CA1 by nicardipine treatment ($p < 0.05$, compared to TBI + saline). Nicardipine also reduced NG+ neuron counts, but not significantly ($p = 0.074$) with this number of rats. The amount of chelatable zinc that accumulates increases in neurons dying as a result of cerebral ischemia and epilepsy (Frederickson et al., 1989). This being said, it was not surprising that the number of FJ+ neurons closely correlated with the number of NG+ neurons from the same rats (Hellmich et al., 2005a).

To address the molecular mechanisms of zinc neurotoxicity following moderate parasagittal FPI, we isolated the mRNA from individual neurons that were removed from the hippocampal section using laser capture microdissection (LCM) and then examined the expression of neuroprotective and oxidative stress related genes using a ribonuclease protection assay (RPA). Both FJ+ (injured, data not shown) and adjacent FJ- (uninjured) neurons were captured in both the CA1/2 and CA3 regions from each rat ($n = 6$ per treatment group). Collected neuronal mRNA from each treatment group was isolated and amplified and used in two RPAs, one comparing lamotrigine pretreatment (Figures 11

and 12) to saline group and the other comparing nicardipine pretreatment (Figures 13 and 14) to the same saline vehicle control. Genes that have been shown to be involved in either the progression or prevention of oxidative stress and cell death processes (caspase 9, neuronal nitric oxide synthase (nNOS), glutathione peroxidase-1 (GPX-1), Mn-superoxide dismutase-2 (SOD-2)) were examined and the housekeeping gene glyceraldehyde-3-phosphate dehydrogenase (GAPDH) was used for normalization. Lamotrigine upregulated both nNOS and caspase 9 in CA3 FJ- neurons compared to saline vehicle treated controls (Figure 12) while changes in gene expression were not statistically significant in the nicardipine-treated animals (Figure 14).

Both nNOS and caspase 9 are traditionally thought of as genes that contribute to injury, but in this case they were both upregulated as a neuroprotective mechanism in surviving cells. Neuronal NOS has been shown to demonstrate neuroprotective effects in estrogen-mediated neuroprotection (Wen et al., 2004) while caspase 9 has been cited as having a neuroprotective effect in adult rats that were pretreated with erythropoietin in a model of retinal injury (Ranchon et al., 2007). The results suggest that at 24 hours post injury, both nicardipine and lamotrigine prevented neuronal death in the hippocampus and the surrounding uninjured (FJ-) neurons may be upregulating neuroprotective genes that allow them to survive.

SUMMARY AND CONCLUSIONS

Lamotrigine significantly reduced both Zn^{2+} accumulation and neuronal injury in hippocampal neurons after TBI. The effects of lamotrigine may be due to inhibition of presynaptic glutamate or to effects on post-synaptic sodium channels. Nicardipine

treatment also reduced Zn^{2+} accumulation in CA1 but was less effective than lamotrigine at reducing neuronal injury as assessed by FJ staining. This difference between the two channel blockers may be due to differences in gene expression, specifically upregulation of neuroprotective genes that increase their chances of survival.

Zinc accumulation in injured neurons seems to occur as a pre-terminal, rather than a gradual, event and appears to happen in between 2 and 8 hours post trauma. This may be an effect of the cell releasing large quantities of Zn^{2+} that is normally bound to proteins and may be the result of the cell irreversibly committing itself to die. It is unclear at this time whether the intracellular Zn^{2+} contributes to the cell death process or if itself is the principle cause of death.

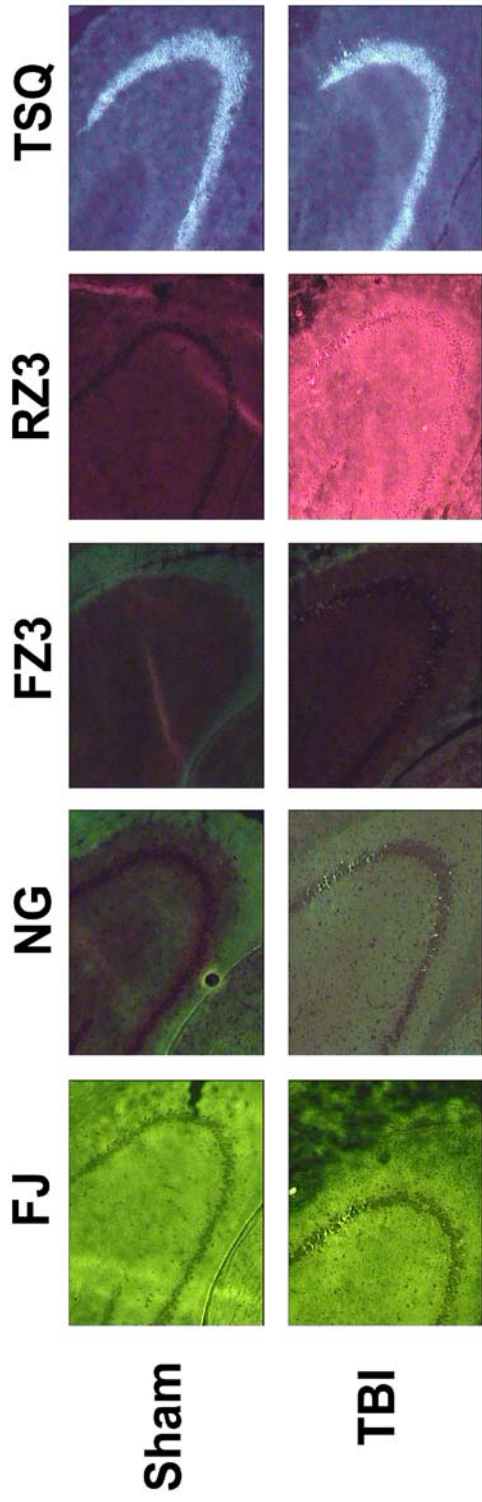
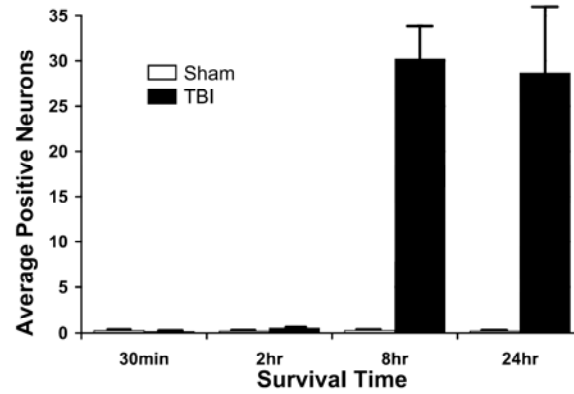


Figure 2. Comparison of hippocampal sections stained with zinc indicator dyes.

Adjacent sections of rat hippocampus stained with either Fluoro-Jade (FJ), Newport Green (NG), FluoZin-3 (FZ3), RhodZin-3 (RZ3) or TSQ following sham (top row) or traumatic brain injury (TBI). Animals were survived for 24 hours and counterstained with Nissl stain (cresyl violet). Slides were examined using a PixCell2E Olympus microscope and photos were taken under 4X magnification.

A. FJ CA1



B. FJ CA3

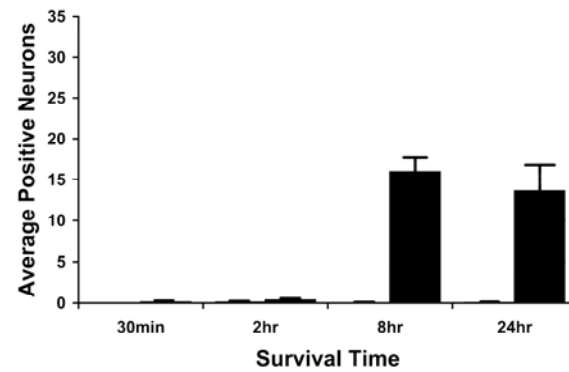
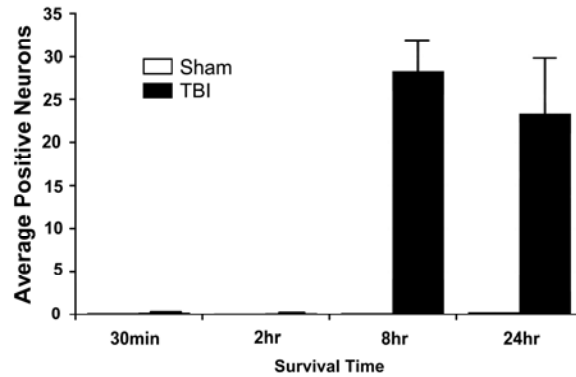


Figure 3. FluoroJade-positive hippocampal neurons in sham and traumatic brain injury (TBI) rats.

Neurons were counted in the CA1 (A) and CA3 (B) regions of the dorsal hippocampus in animals that survived 30 minutes, 2 hours, 8 hours or 24 hours post sham or TBI. Bars represent the mean number of positive neurons counted from 10 sections per animal per survival time (n = 6). Error bars represent SEM.

A. NG CA1



B. NG CA3

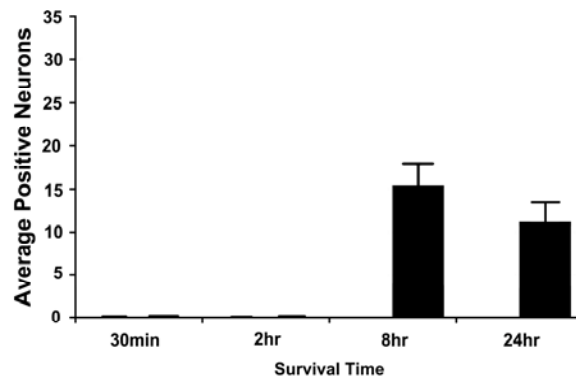
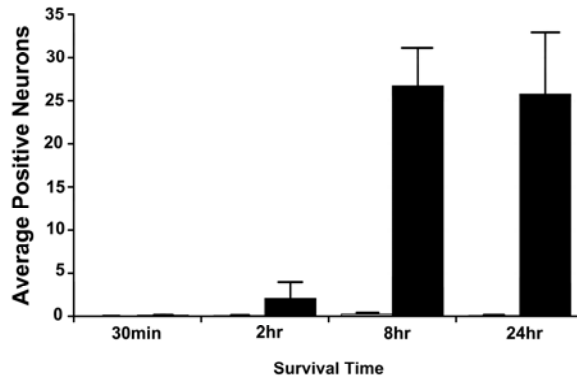


Figure 4. Newport Green-positive hippocampal neurons in sham and traumatic brain injury (TBI) rats.

Neurons were counted in the CA1 (A) and CA3 (B) regions of the dorsal hippocampus in animals that survived 30 minutes, 2 hours, 8 hours or 24 hours post sham or TBI. Bars represent the mean number of positive neurons counted from 10 sections per animal per survival time (n = 6). Error bars represent SEM.

A. FZ3 CA1



B. FZ3 CA3

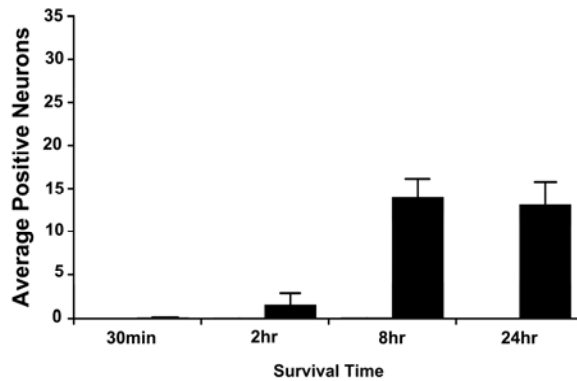
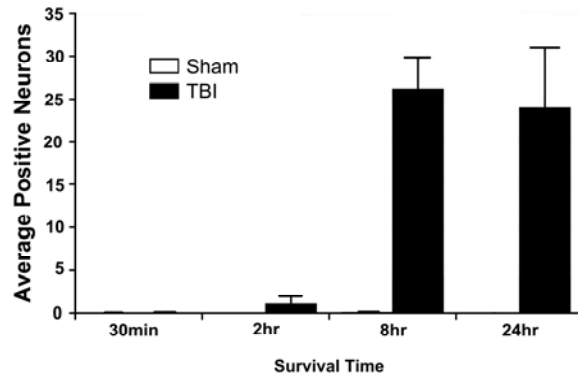


Figure 5. FluoZin-3-positive hippocampal neurons in sham and traumatic brain injury (TBI) rats.

Neurons were counted in the CA1 (A) and CA3 (B) regions of the dorsal hippocampus in animals that survived 30 minutes, 2 hours, 8 hours or 24 hours post sham or TBI. Bars represent the mean number of positive neurons counted from 10 sections per animal per survival time ($n = 6$). Error bars represent SEM.

A. RZ3 CA1



B. RZ3 CA3

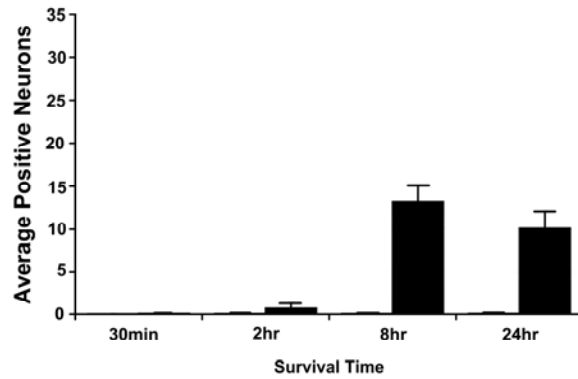
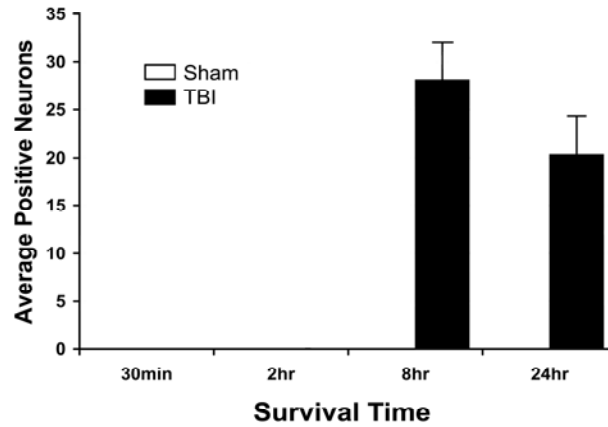


Figure 6. RhodZin-3-positive hippocampal neurons in sham and traumatic brain injury (TBI) rats.

Neurons were counted in the CA1 (A) and CA3 (B) regions of the dorsal hippocampus in animals that survived 30 minutes, 2 hours, 8 hours or 24 hours post sham or TBI. Bars represent the mean number of positive neurons counted from 10 sections per animal per survival time ($n = 6$). Error bars represent SEM.

A. TSQ CA1



B. TSQ CA3

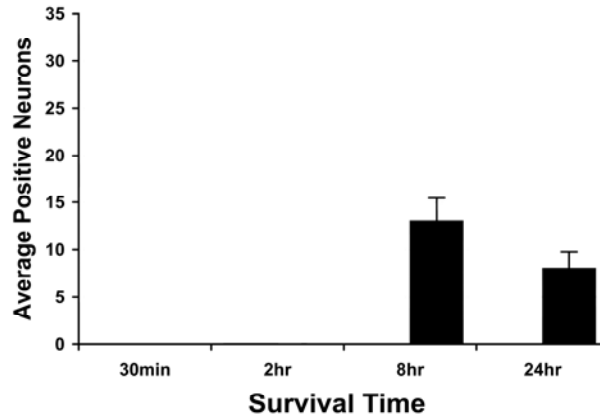


Figure 7. TSQ-positive hippocampal neurons in sham and traumatic brain injury (TBI) rats.

Neurons were counted in the CA1 (A) and CA3 (B) regions of the dorsal hippocampus in animals that survived 30 minutes, 2 hours, 8 hours or 24 hours post sham or TBI. Bars represent the mean number of positive neurons counted from 10 sections per animal per survival time (n = 6). Error bars represent SEM.

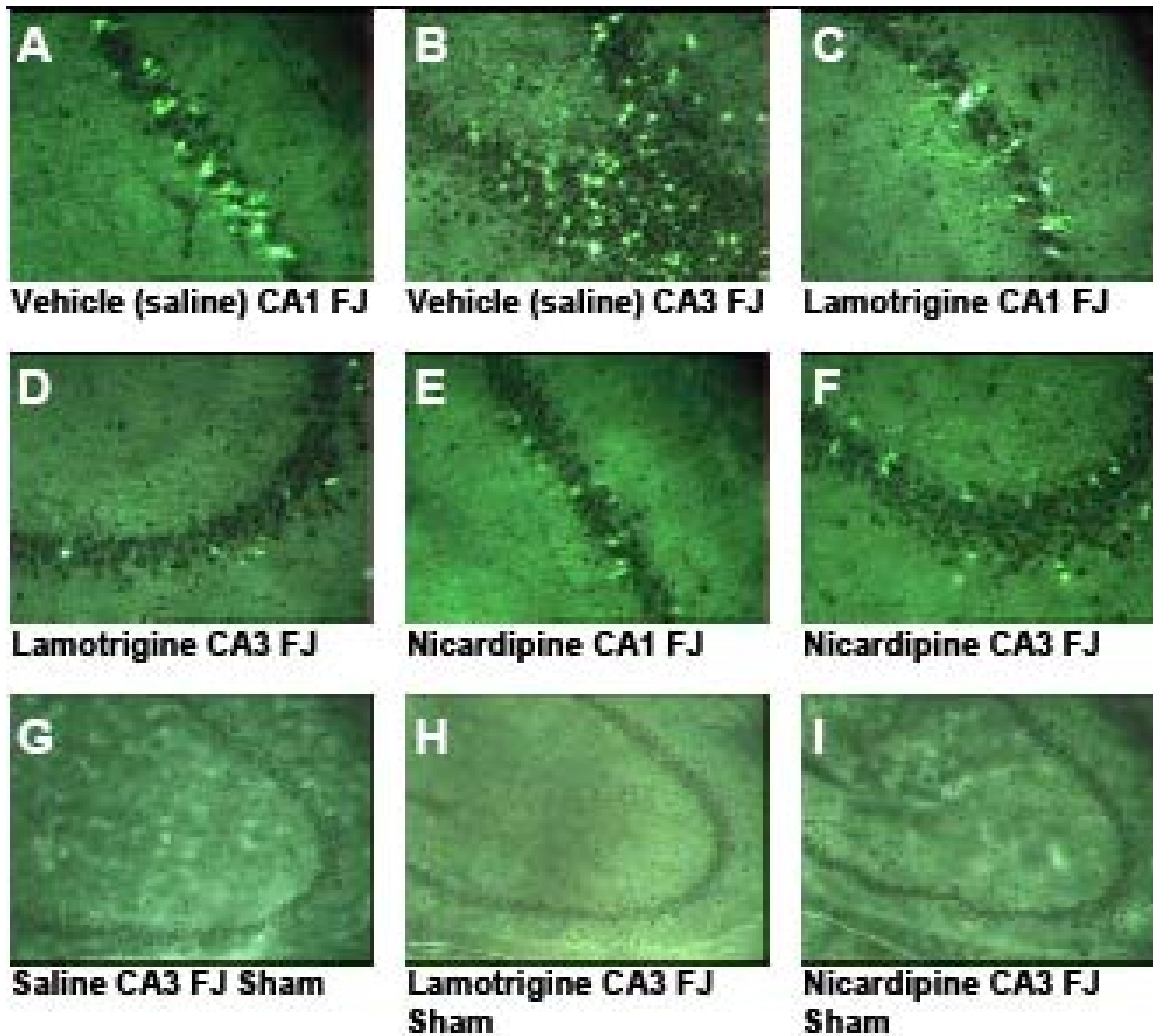


Figure 8. Prevention of neuronal degeneration in rat hippocampus CA1 and CA3.

Fluoro-Jade positive (FJ+) neurons in CA1 (A) and CA3 (B) from vehicle-treated traumatic brain injured (TBI), lamotrigine (C,D) and nicardipine (E,F) treated TBI rats. No FJ+ neurons were seen in sham-injured saline vehicle (G), lamotrigine (H), and nicardipine (I). Slides were examined using a PixCell2E Olympus microscope and photos were taken under 10X (A-F) or 4X (G-I) magnification.

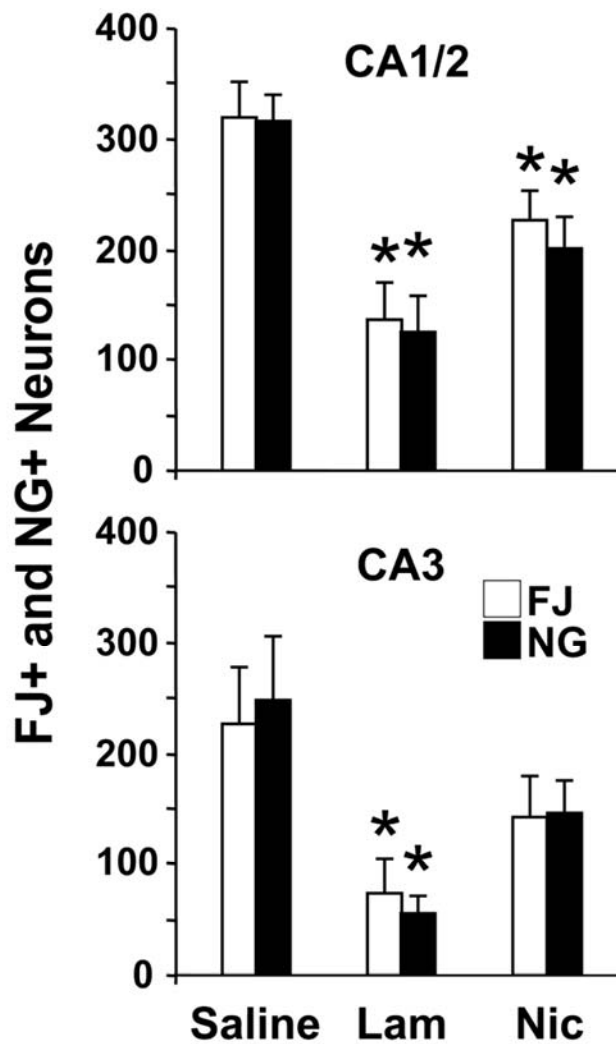


Figure 9. Fluoro-Jade- and Newport Green-positive neurons after lamotrigine or nicardipine pretreatment.

Pretreatment with lamotrigine (lam) or nicardipine (nic) 30 min before traumatic brain injury (TBI) significantly reduced numbers of Fluoro-Jade-positive and Newport Green-positive neurons in both the CA1 (for both lam and nic) and CA3 (lam only) when compared to saline injected TBI rats. * $p < 0.05$. Reprinted from Brain Research, Vol. 1127, Hellmich et al. Injured Fluoro-Jade-positive hippocampal neurons contain high levels of zinc after traumatic brain injury, 119-126, 2008, with permission from Elsevier.

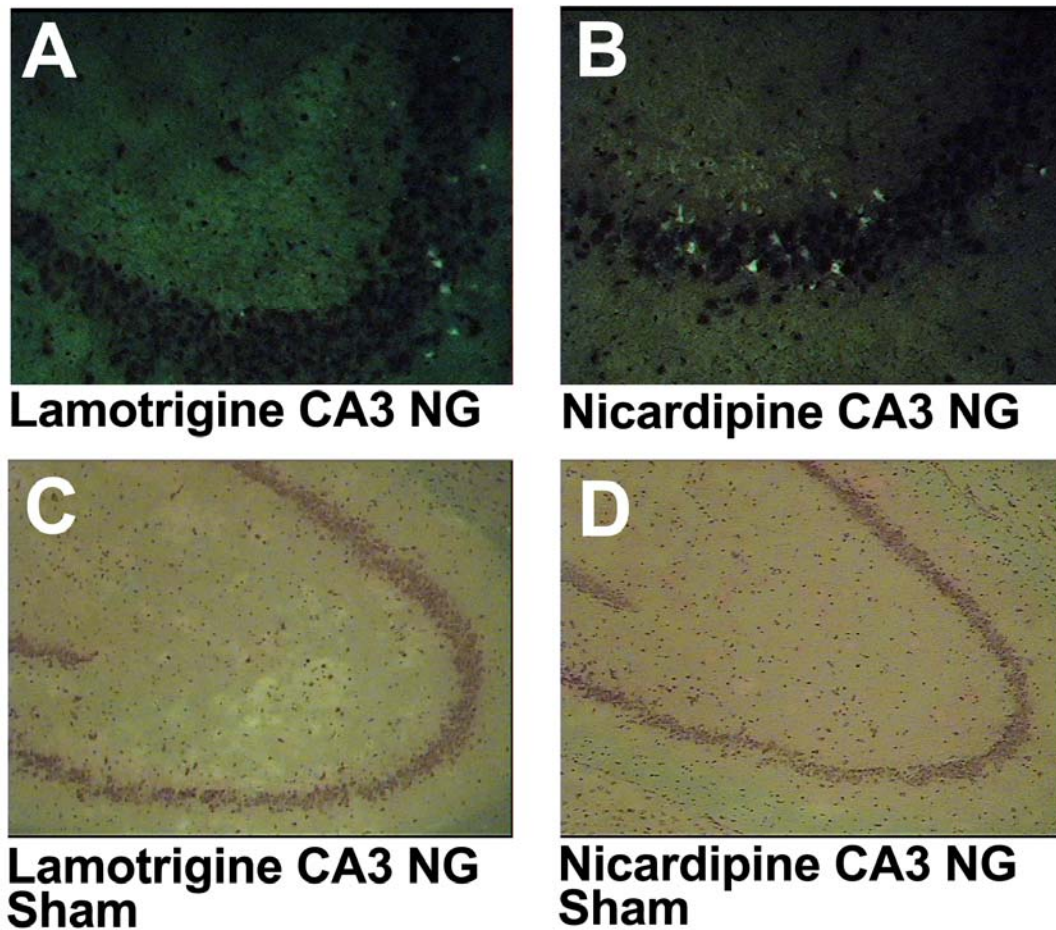


Figure 10. Zinc accumulation in rat hippocampus CA1 and CA3 following lamotrigine or nicardipine pretreatment.

Newport green positive (NG+) neurons from lamotrigine (A) and nicardipine (B) pretreated moderate traumatic brain injury (TBI) rats. No NG+ neurons were noticed in sham-injured lamotrigine (C) and nicardipine (D) treated rats. Slides were examined using a PixCell2E Olympus microscope and photos were taken under 10X (A-B) or 4X (C-D) magnification.

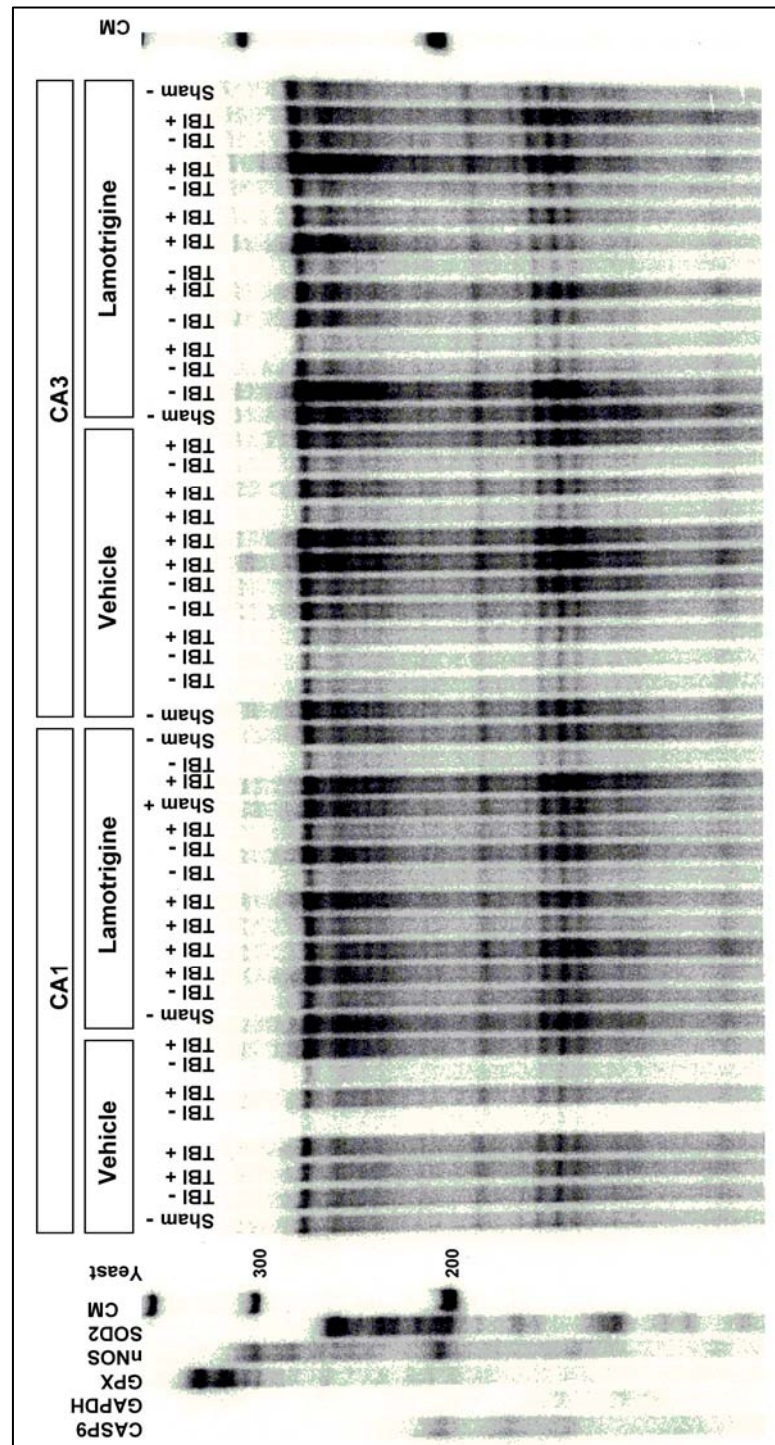


Figure 11. Ribonuclease protection assay of traumatic brain injured rats pretreated with lamotrigine.

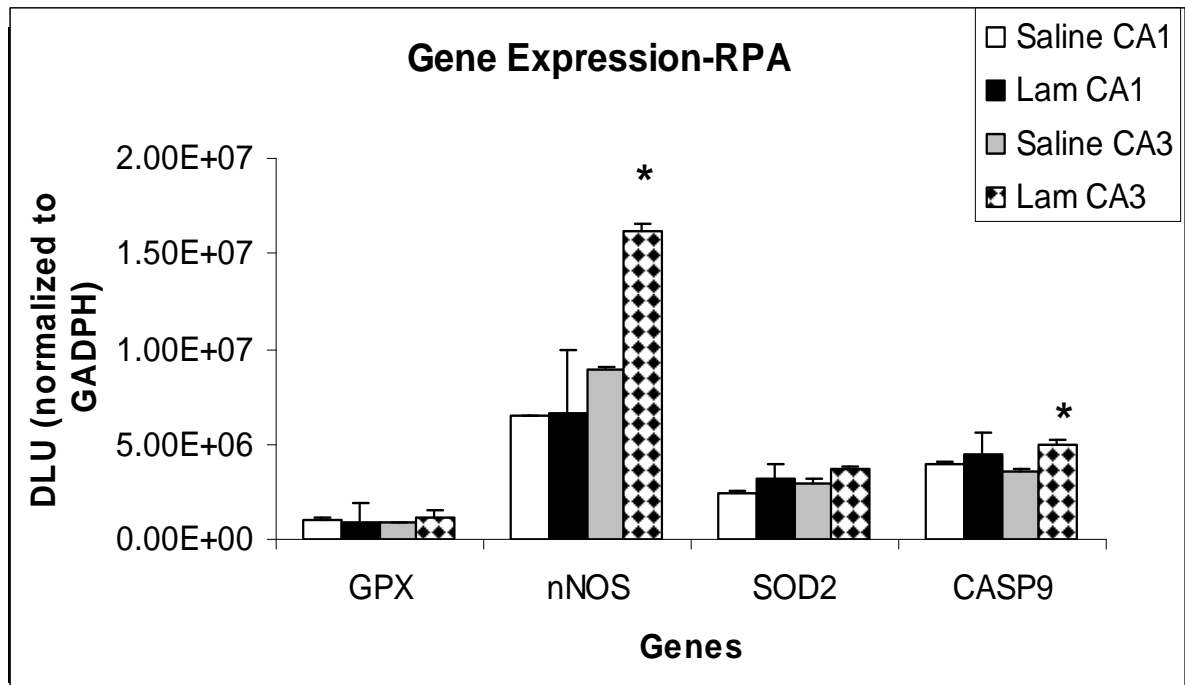


Figure 12. Gene expression of surviving neurons after saline or lamotrigine (Lam) treatment followed by traumatic brain injury (TBI).

There were no significant differences between groups in expression of glutathione peroxidase (GPX) and Mn-superoxide dismutase (SOD2). There were statistically significant increases in gene expression of both neuronal nitric oxide synthase (nNOS) and caspase 9 (CASP9) in CA3, but not CA1 neurons collected from lamotrigine treated rats. Error bars represent SEM values, n = 6 animals per group.

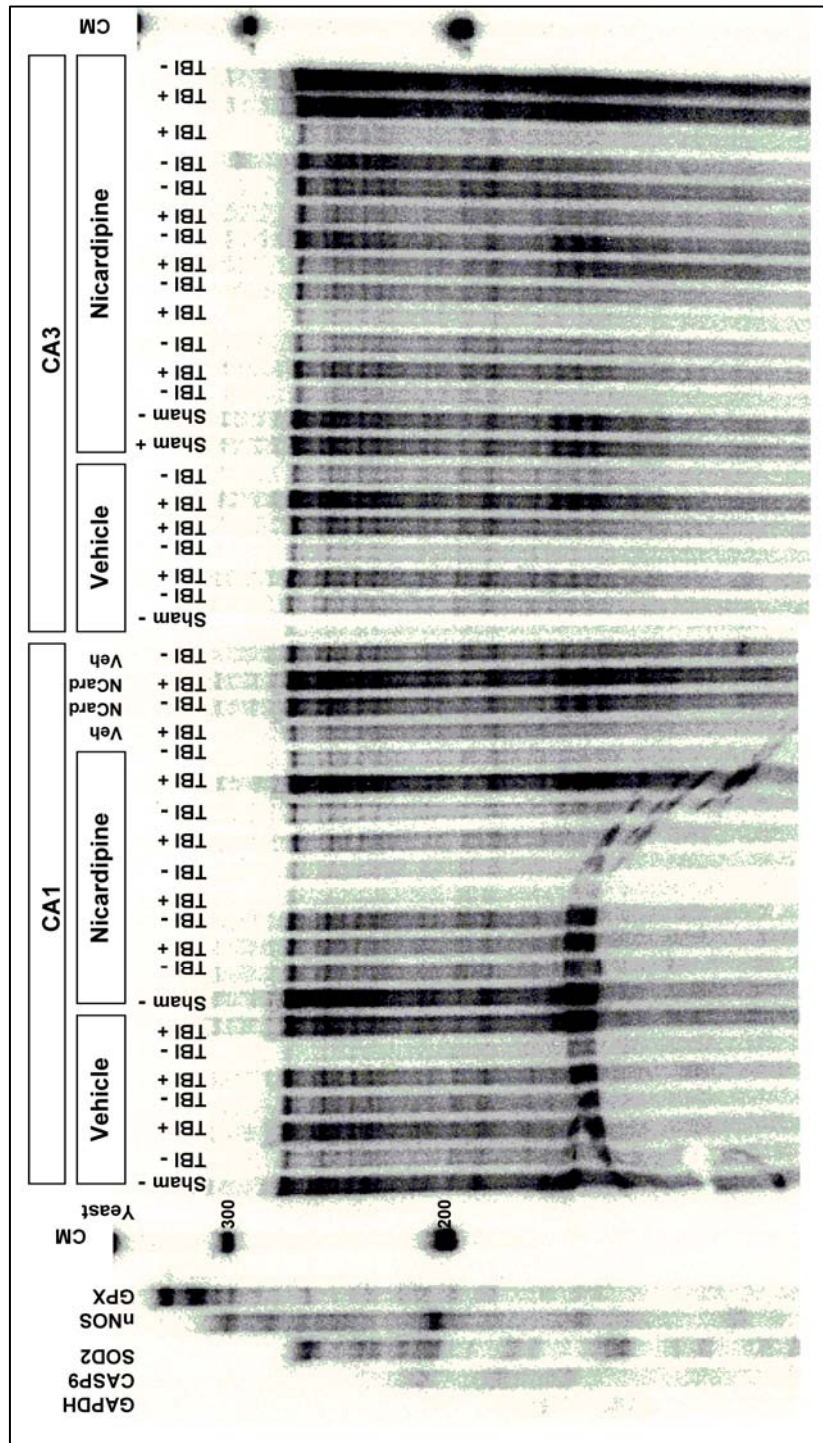


Figure 13. Ribonuclease protection assay for traumatic brain injury rats pretreated with nicardipine

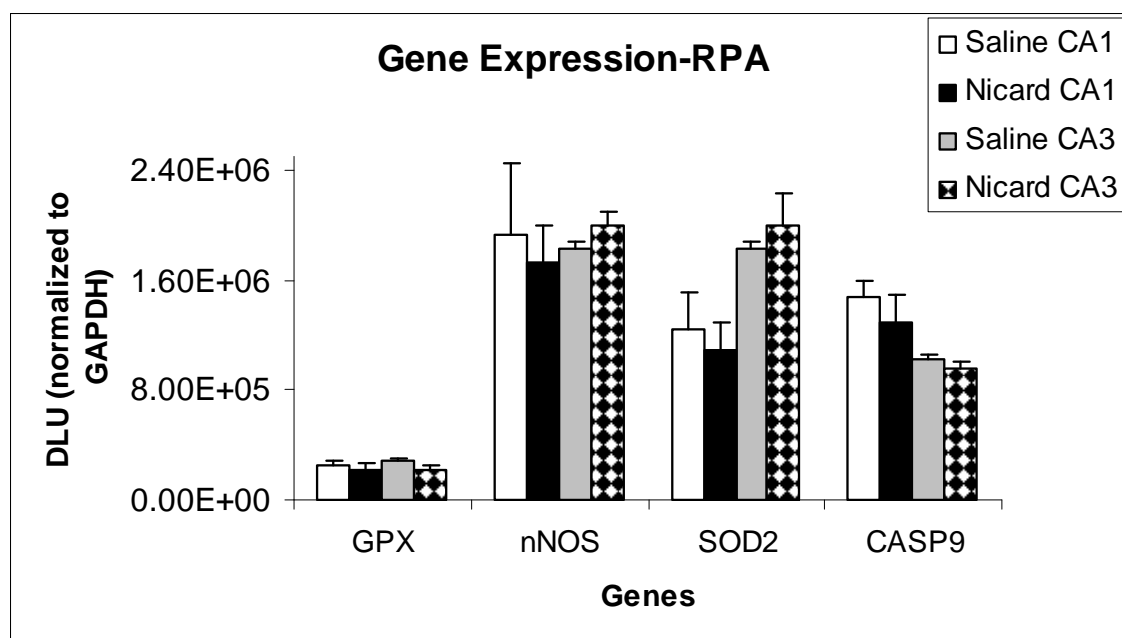


Figure 14. Gene expression of surviving neurons after saline or nicardipine (Nicard) treatment followed by traumatic brain injury (TBI).

There were no significant differences between groups in expression of any of the genes listed. Error bars represent SEM values, n = 6 animals per group.

Chapter 4: Increased Extracellular Zn²⁺ Causes Injury to Hippocampal Neurons

CHARACTERIZATION OF ZINC CHLORIDE INJECTION MODEL

Post-synaptic hippocampal neurons appear to accumulate zinc after TBI. Zinc acts as a modulator of synaptic function in the hippocampus and has been linked to neuronal cell death following TBI. Lees et al. (1990) have shown this to occur *in vivo* using an intrahippocampal injection of ZnCl₂ (5-10 nmoles) which caused neuronal loss (CA1, CA3 and DG) detected at 8 hours-3 weeks using a Nissl stain (Lees et al., 1990; Cuajungco and Lees, 1996). I used this model of ZnCl₂ injection to isolate the Zn²⁺ neurotoxicity mechanism of FPI.

Animals for this study were prepared as described in the ZnCl₂ Injection section of the Methods chapter. *In vitro* studies have shown that 15 minute exposures to 1 mM ZnCl₂ effectively kills neurons grown in a neuronal and glia co-culture, while 100 µM ZnCl₂ killed neurons and glia only after a 24 hour incubation (Choi et al., 1988). I began using 3 µl of 1 mM ZnCl₂ intrahippocampal injection and the animal died upon emergence from anesthesia. Next, I tried 3 µl of 500 µM and the animal died within the first 24 hours. The animal survived the 250 µM (3 µl) dose but exhibited erratic behavior upon waking and when exposed to stimuli such as bright light. ZnCl₂ injection of 125 µM was the highest concentration in which the animal behaved normally but still produced massive neuronal injury to the hippocampus within 24 hours.

To determine the behavioral deficits in rats that sustained a unilateral ZnCl₂ injection, I tested their ability to learn and remember the location of a submerged invisible platform using spatial cues by employing a behavior test called the Morris water

maze (MWM) (Morris, 1984). None of the rats underwent training prior to the injection. Two main outcomes from the MWM test are latency (the amount of time it takes the animal to swim from its starting point to the platform) and path length (the distance measured from the animal's starting point to the platform). My preliminary studies of the effects of zinc toxicity revealed no significant differences in MWM performance between zinc and vehicle injection groups at days 11-15 post-injection (Figure 15), despite massive neuronal injury (FJ staining of hippocampal neurons, 24 hrs post-TBI). However, since delayed MWM testing may miss early cognitive deficits, we assessed MWM performance 1–10 days and Barnes maze performance 16-20 days after an injection of 3 μ l of 125 μ M ZnCl₂ into the right hippocampus of male Sprague-Dawley rats. Removal of zinc by CaEDTA does not cause a significant improvement of MWM performance (Hellmich et al., 2008). The timeline of the behavior experiments is shown in Figure 16. Zinc (TSQ) and morphological (CV) staining were also performed on sections of brains from these rats.

Behavior

MWM latency ($p < 0.001$) was significantly different between the ZnCl₂ and vehicle injection rats (Figure 17A & B), while the path length (Figure 18A) was not significant ($p = 0.078$) on each day, however when the total distances from all trials were combined, there was a large difference between ZnCl₂ and vehicle-injected rats (Figure 18B). When comparing the number of failures (as demonstrated by the number of no platforms recorded for each day of testing), a clear difference in performance can be seen (Figure 19). ZnCl₂-injected rats clearly exhibit an impairment of spatial learning and memory compared with vehicle injected controls during the first 6 days of MWM testing.

After 5 days of rest, during which time the animals were being handled for approximately 5-10 minutes each, the Barnes Maze, a different spatial learning and memory test, was performed. Barnes maze (days 16-20) performance was much more variable in the ZnCl_2 group compared to the vehicle group and, while the ZnCl_2 injection rats were slower to learn the location of the target box, there was no significant difference for average time to target between the two groups across all 5 days (Figure 20A), despite differences in the total amount of time it took all of the rats in each group to reach their target holes (Figure 20B). The average time it took for the rats to explore the first hole was not different across all 5 days of testing (Figure 21A), despite a difference in the total amount of time it took all of the rats in each group to explore the first hole (Figure 21B).

Histology

Cresyl Violet (CV) staining demonstrates the loss of neuronal cells in the right hippocampus following intrahippocampal injection of ZnCl_2 . In order to examine the progression of hippocampal damage following ZnCl_2 (125 μM) injection, I sacrificed rats at different time points and then stained the brain sections with CV. Panels of individual brain sections of rats were injected with an aCSF vehicle (24 hour survival) or a ZnCl_2 injection and sacrificed at 30 minutes, 1, 2, 4, 6, 12, 24, 48 and 72 hours, 7 and 20 days post-injection (Figure 22). There was no apparent damage 30 minutes following ZnCl_2 injection, while maximal damage occurred at 2 hour survival. By 20 days post injection, the entire dorsal hippocampus on the side injected with ZnCl_2 is missing, presumably removed by microglia.

To estimate the minimum ZnCl_2 concentration needed to cause neuronal damage when injected into the hippocampus, I injected half doses of ZnCl_2 into multiple rats and

then sacrificed them at either 2 or 24 hours and then stained their brains with CV (Figure 23). The 62.5 μM dose showed destruction similar to that of the rat that survived 1 hour after receiving an injection of 125 μM ZnCl_2 (Figure 22). The next dose, 15.6 μM ZnCl_2 , showed minimal neuronal damage and the 156 nM and 156 pM doses showed no detectable neuronal damage. Accordingly, the minimum injected amount of ZnCl_2 to cause injury is near 15.6 μM .

Silver Autometallography

The current gold-standard in the field to detect chelatable Zn^{2+} is the silver autometallography (AMG) method by which the animal is perfused with sodium sulphide and glutaraldehyde which precipitates Zn^{2+} and crosslinks proteins to fix structures in place (Danscher et al., 2004; Perez-Clausell and Danscher, 1985). The precipitated Zn^{2+} is then exposed to silver lactate that forms Zn-S-Ag crystals that are seen as black dots in the section. A weight-drop model of TBI was shown to decrease the amount of silver-AMG Zn^{2+} in the cortex and hippocampus of the injured side 6 hours post-TBI (Suh et al., 2000). In an effort to replicate these results, I also used rats that were survived for 6 hours. Animals were prepared as described in the silver autometallography section of the Methods chapter. Sections from moderate or sham TBI, ZnCl_2 or TPEN injection and naïve (receiving no isoflurane) rats underwent the AMG procedure and the processed brains on the slides were scanned using a normal photo scanner (Figure 24). Naïve rats exhibited very little Zn^{2+} compared to the sham operated animals, suggesting this may be a stress response or a reaction to anesthesia. Rats injected with TPEN displayed a disappearance of Zn^{2+} around the injection site whereas the ZnCl_2 injection site showed an enhancement of staining. Upon visual inspection there is very little difference between the sham and TBI AMG sections. Densitometry was used to quantify the

amount of Zn^{2+} shown in the hippocampus (Figure 25) and cortex (Figure 26) of these animals. There was an obvious increase in the amount of Zn^{2+} in the hippocampus (Figure 25), but not cortex (Figure 26) of the ZnCl_2 animals compared to the TPEN injected rats. No statistically significant difference was found between the sham and TBI rats for Zn^{2+} in the hippocampus (Figure 25) but a slight difference was found in the cortex (Figure 26).

To ensure that all of the chelatable zinc was precipitated from the tissue, alternate sections were saved for TSQ staining (Figure 27). If the sections still held Zn^{2+} , the neuropil would stain brightly with TSQ. This occurred in one of our naïve rats (not shown) that received an incomplete transcardial perfusion where the right side was TSQ stained.

Gene Expression

To better characterize the ZnCl_2 injection model, I decided to look at the molecular mechanisms associated with ZnCl_2 induced cell death and compare them with that of TBI. Changes in gene expression 24 hours following either a unilateral hippocampal ZnCl_2 injection or TBI were examined using a rat toxicology gene array. Animals were prepared as described in the Parasagittal Fluid Percussion Injury, ZnCl_2 Injection, Rat Toxicology Gene Array and Array Analysis sections of the Methods chapter. Twenty-four animals ($n = 6$ per group) underwent either ZnCl_2 (125 μM) or aCSF vehicle injection or sham or TBI without cannulations during the animal preparation. Right hippocampuses from 2 rats were used per array, for a total of 3 arrays per treatment group.

After completing array analyses using multiple software programs, I further excluded the possibility of false positive results by running a pair-wise comparison of the genes that exhibited a 2-fold (or higher) change in gene expression. The list of genes that

were either up or down regulated following ZnCl₂ injection compared to vehicle injection are listed in Appendix Table 2. Only 15 genes were significantly up or down regulated following the pair-wise comparison test. Prior to the pair-wise comparison test, there were 279 genes that exhibited at least a 2-fold change depicted in a condition gene tree comparing vehicle to ZnCl₂ animals (Figure 28). Genes that were affected by TBI (compared to sham injury) are listed in Appendix Table 3. There were 126 genes affected by TBI following the pair-wise comparison test compared to the 428 genes affected prior the test as shown in the condition gene tree (Figure 29). Many of the significant genes that were affected 24 hours following TBI were also found to be significant by other groups in the field (Marciano et al., 2004; Dash et al., 2004). Signal transduction, cell cycle, metabolism and inflammation related genes were among the groups of genes most affected by early responses (<24 hours) following TBI (Dash et al., 2004).

Only one of the genes that were down regulated in the ZnCl₂ animals was also affected by the TBI animals in the hippocampus as shown in the pie chart comparing the two treatment groups (Figure 30). This common gene is listed as collagen, type III, alpha 1 and is not known to play a significant role in either Zn²⁺ neurotoxicity or TBI. The lack of genes in common may be due to the fact that we used a mini-array instead of a more costly entire genome array and also the time course of injury is more accelerated in the ZnCl₂ injection model compared with the TBI model and may have left less surviving neuronal tissue with which to study changes in gene expression. To be valid, these data would need to be confirmed using another method of gene expression such as realtime PCR and protein confirmation using either immunocytochemistry or Western blotting techniques.

SUMMARY AND CONCLUSIONS

Injecting ZnCl_2 ($>15.6 \mu\text{M}$) directly into the hippocampus results in neuronal damage after 1 hour survival. Results that intrahippocampal injections of zinc were associated with significantly impaired MWM performance within the first 10 days after injection suggest that zinc accumulation may contribute to early cognitive deficits after TBI. This is particularly relevant because in human TBI cases, cognitive deficits and learning and memory dysfunction and loss are the most common long-lasting effects suffered. There may have been some compensation from the unaffected hippocampus located in the contralateral hemisphere when rats were tested at later time points (Figure 15). To test this theory, I administered bilateral ZnCl_2 injections and tested the rats on day 10 post-injection (data not shown). These bilaterally injured rats not only lost 1/3 of their body weight and shed their fur, but they also just spun in circles when placed in the MWM pool. When placed onto the platform, they did not recognize it and would jump off and start spinning in circles again. After the one day of testing, these rats were sacrificed because it would have been inhumane to continue with those experiments.

The differences in silver AMG grains that exist between my data and that of Suh et al., 2000 can be explained by differences in animal preparation, including anesthesia, and that they used a weight-drop model of TBI whereas our lab uses a fluid percussion model of injury. In a cortical stab wound model of brain trauma, Doering et al. could not replicate the silver AMG patterns shown in Suh et al., 2000 (Doering et al., 2007). In wildtype mice, they saw an increase of Zn^{2+} staining adjacent to the lesion site, but not in individual soma, whereas the zinc transporter 3 (ZnT3) knockout mice displayed silver-enhanced ZnSe crystals in the neuronal somata near the lesion. The authors concluded that vesicular zinc may not contribute to neuronal damage following neurotrauma (Doering et al., 2007).

Differences in gene expression changes between the ZnCl₂ and TBI animals were difficult to ascertain using a mini-array and may best be served by looking at a time course of survival (instead of one survival time point) from 30 minutes to 24 hours and by using a gene array that looks at not only toxicology-related genes but the entire genome. Overall, on a molecular level, FPI and ZnCl₂ injection are distinctly different.

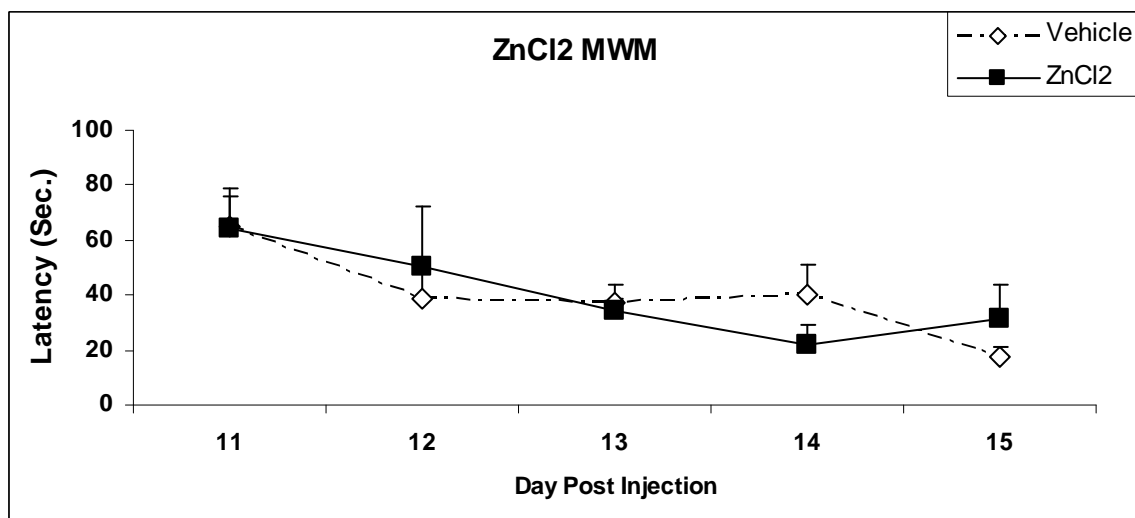


Figure 15. Morris water maze testing at days 11-15 post-injection.

Rats were given either 125 μ M ZnCl₂ (n = 3) or aCSF vehicle (n = 3) injection into right hippocampus. Repeated measures ANOVA revealed no statistically significant ($p < 0.05$) differences in latency between the two treatments over times tested. Error bars represent SEM.

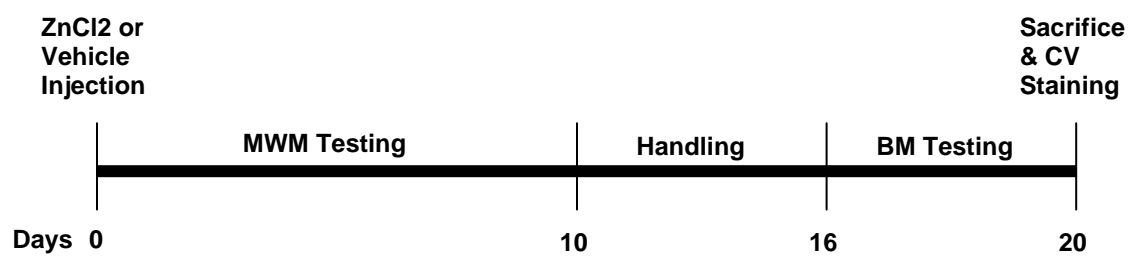


Figure 16. Timeline of behavior experiments for ZnCl_2 and vehicle injected rats.

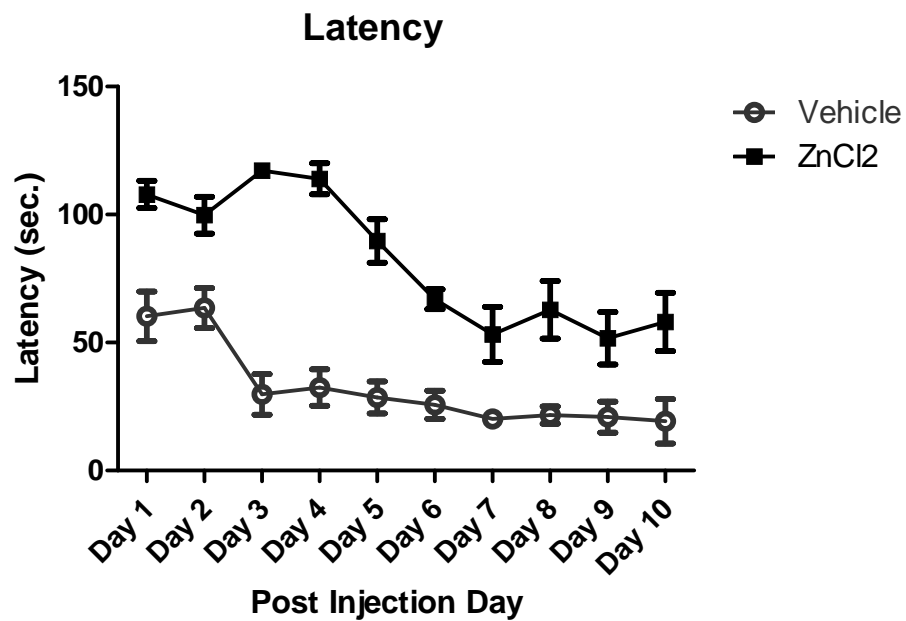


Figure 17A. Latency measurement: Morris water maze testing at days 1-10 post-injection.

Rats were given either 125 μ M ZnCl₂ (n = 5) or aCSF vehicle (n = 5) injection into right hippocampus. Repeated measures ANOVA revealed a statistically significant ($p < 0.001$) difference between the two treatments over times tested when looking at latency (time to find hidden platform). Error bars represent SEM.

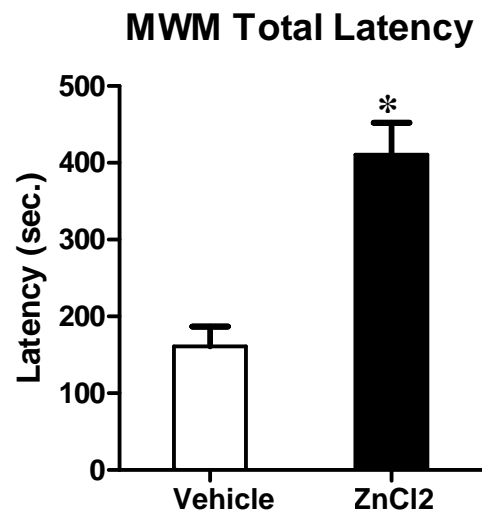


Figure 17B. Total latency values for all 4 trials per day for all 10 days of Morris water maze testing.

Student's t-test revealed a statistically significant difference in latency overall between the two groups ($p < 0.001$). Error bars represent SEM, $n = 5$ animals per group.

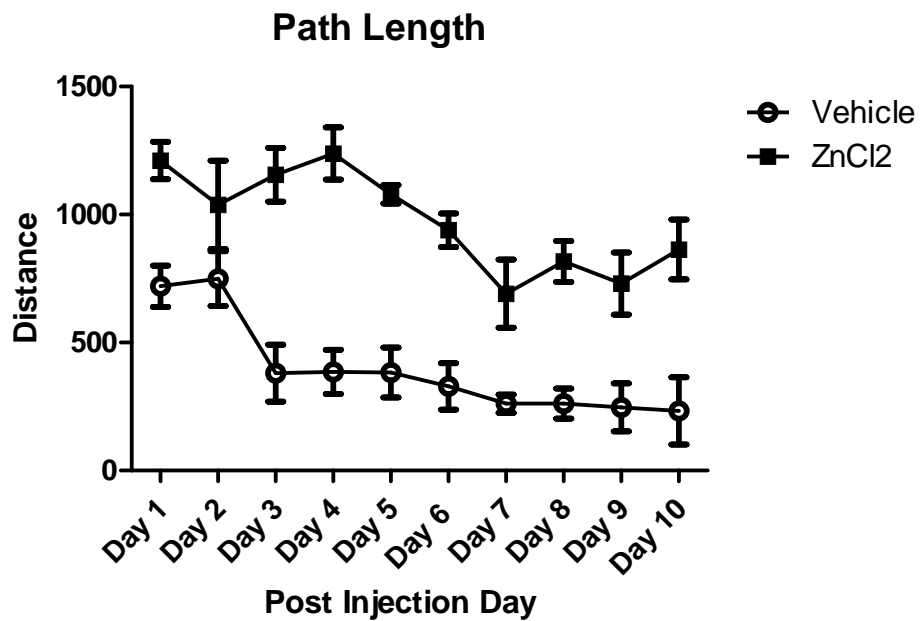


Figure 18A. Path length measurement: Morris water maze testing at days 1-10 post-injection.

Rats were given either 125 μ M ZnCl₂ (n = 5) or aCSF vehicle (n = 5) injection into right hippocampus. Repeated measures ANOVA revealed no statistically significance in path length ($p = 0.078$) between the two groups over all of the days tested, most likely due to increased variability. Error bars represent SEM.

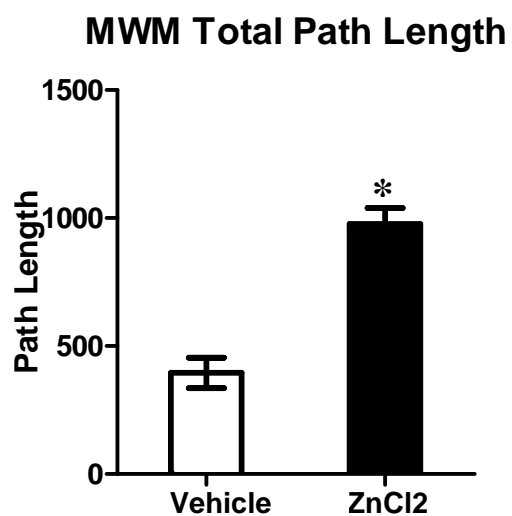


Figure 18B. Total path length values for all 4 trials per day for all 10 days of Morris water maze testing.

Student's t-test revealed a statistically significant difference in the distance traveled to reach platform (path length) overall between the two groups ($p < 0.001$). Error bars represent SEM, $n = 5$ animals per group.

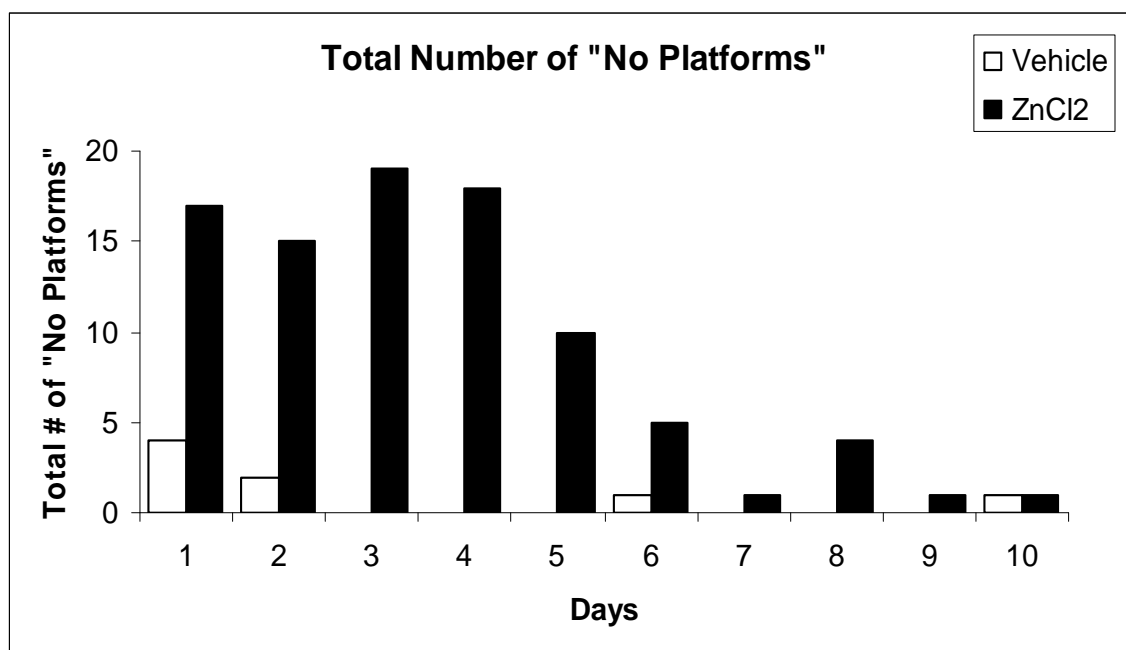


Figure 19. Total number of *no platform* measurements: Morris water maze testing at days 1-10 post-injection.

Each bar represents the total number of failures (no platforms) of 4 trials per rat per day.

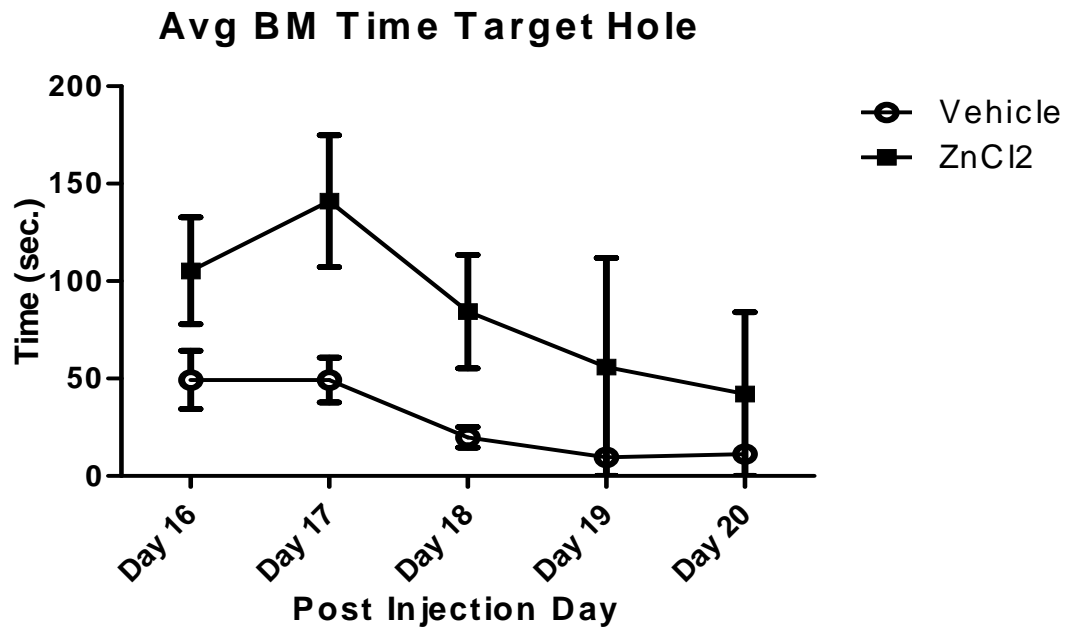


Figure 20A. Time to target hole: Barnes Maze performance at days 16-20 post-injection.

Each point on the graph represents the average of 2 trials per day for all 5 rats in either vehicle or ZnCl₂ injected rats. Repeated measures ANOVA revealed no statistically significant differences between the two treatments over times tested when looking at time to reach target hole. Error bars represent SEM.

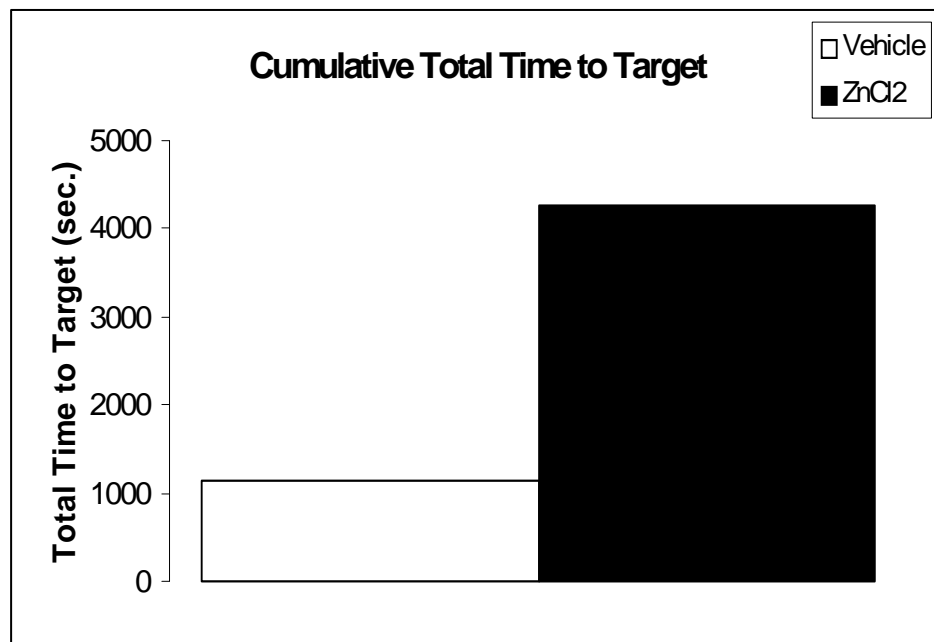


Figure 20B. Cumulative time to target hole in Barnes maze behavior test at days 16-20 post-injection.

Total time to target hole over all 5 days of testing.

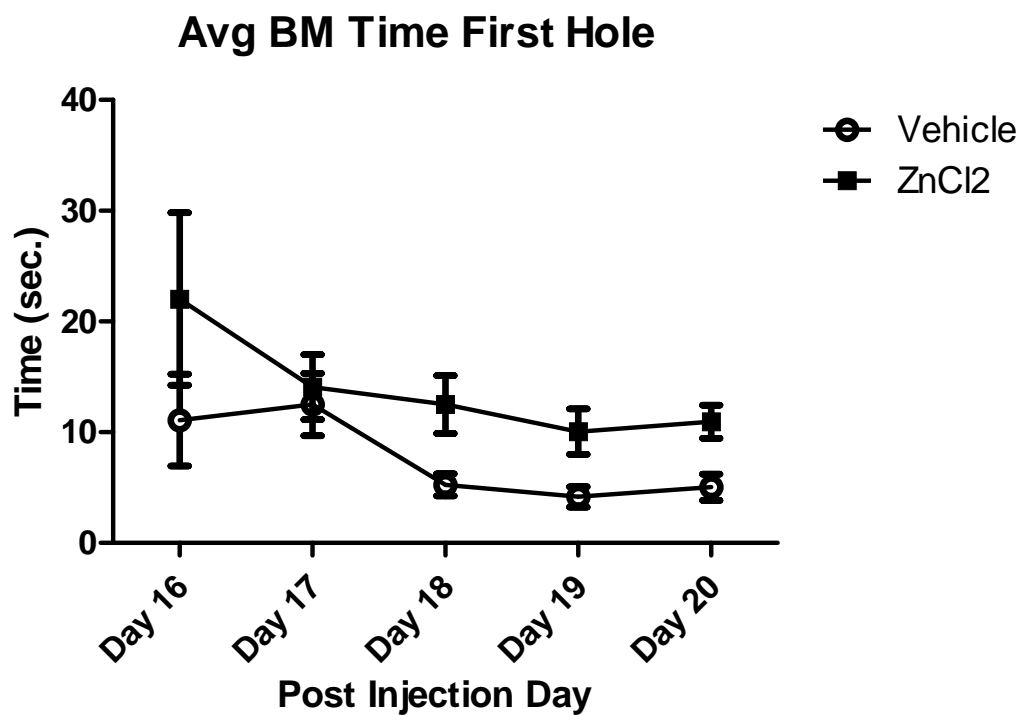


Figure 21A. Time to first hole: Barnes maze locomotor behavior at days 16-20 post-injection.

Each point on the graph represents the average of 2 trials per day for all 5 rats in either vehicle or ZnCl₂ injected rats. Repeated measures ANOVA revealed no statistically significant differences between the two treatments over times tested when looking at time to reach target hole. Error bars represent SEM.

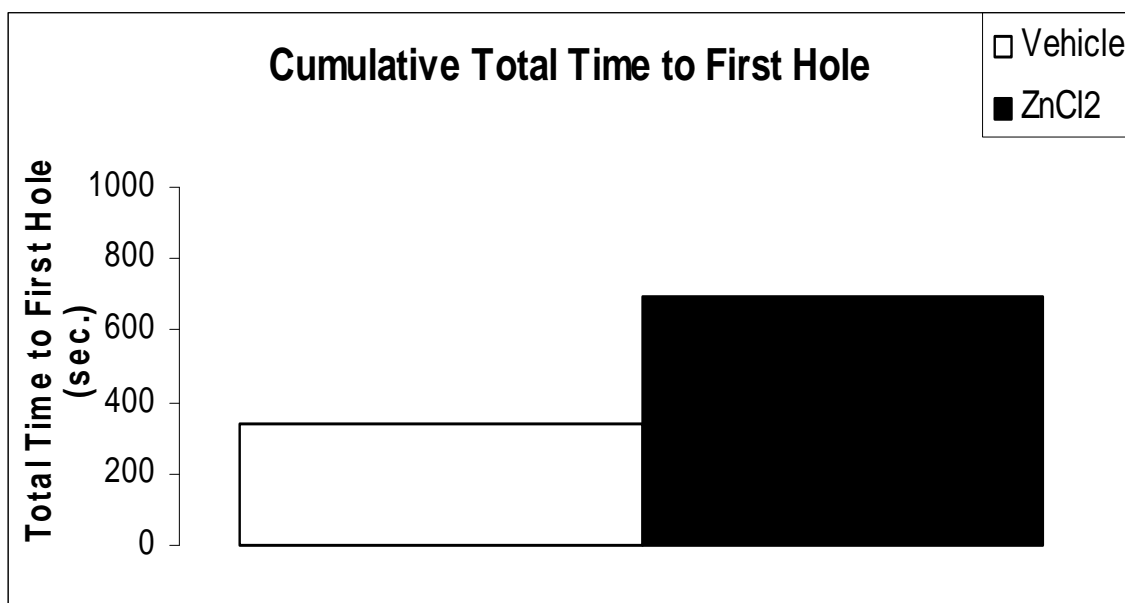


Figure 21B. Cumulative time to first hole in Barnes maze behavior test at days 16-20 post-injection.

Total time to first hole over all 5 days of testing.

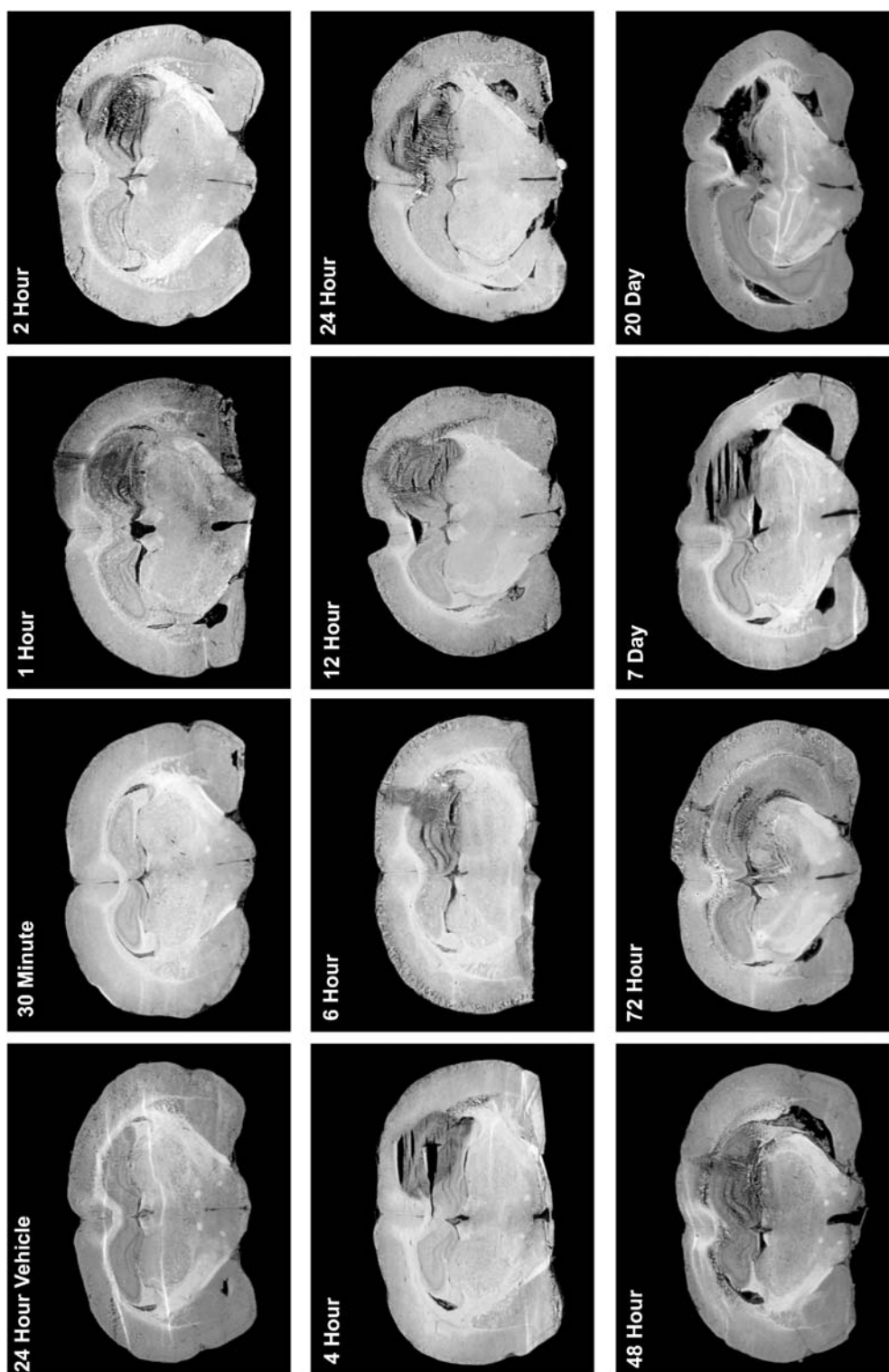


Figure 22. Survival time course of ZnCl₂ injection injury.

Brain section stained with cresyl violet following 30 minutes, 1, 2, 4, 6, 12, 24, 48, 72 hours, or 7 or 20 days survival following 125 µM ZnCl₂ or vehicle injection. Slides were placed on a photoscanner and scanned at 1200 dpi resolution and converted to black and white images using PhotoShop software.

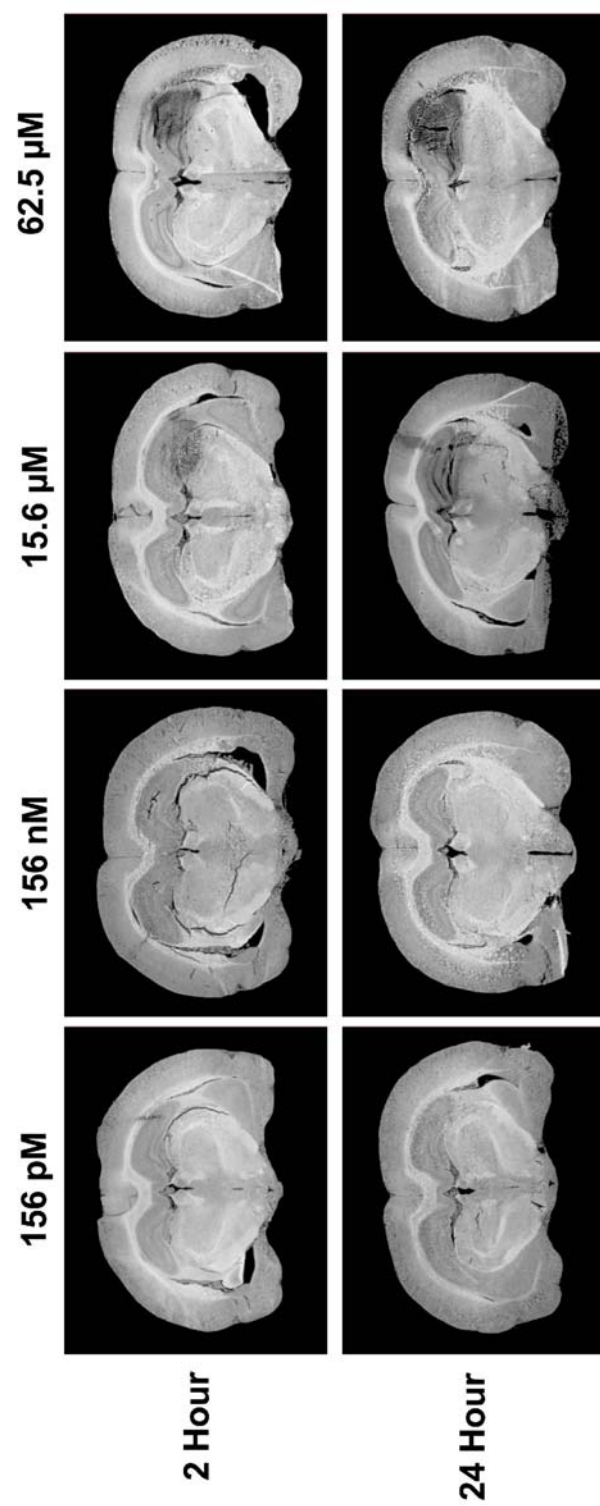


Figure 23. Dose response of ZnCl₂ injection injury.

Brain section stained with cresyl violet following either 2 or 24 hour survival following 156 pM, 156 nM, 15.6 µM or 62.5 µM ZnCl₂ injection. Slides were placed on a photoscanner and scanned at 1200 dpi resolution and converted to black and white images using PhotoShop software.

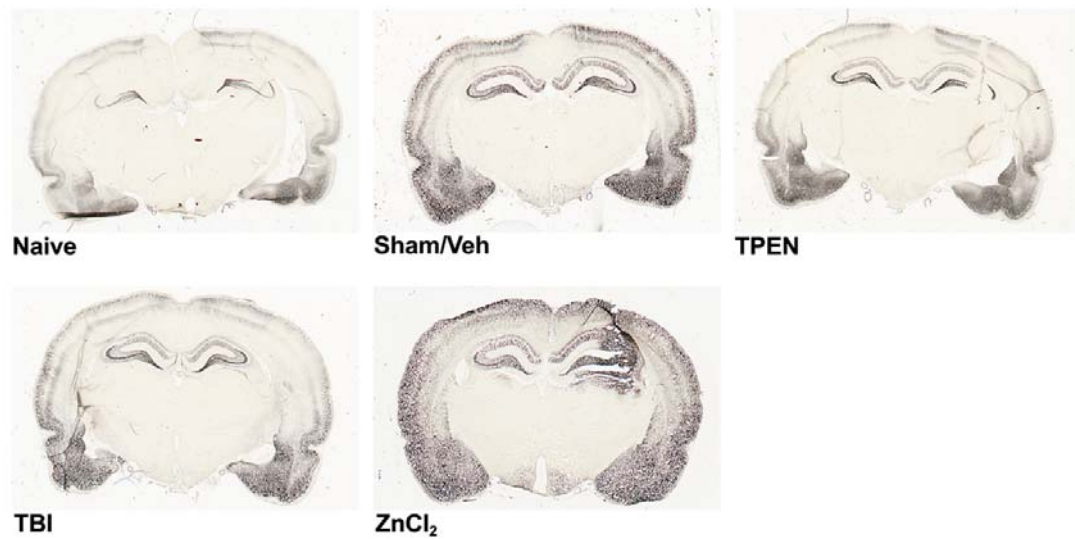


Figure 24. Zn^{2+} detection in brain sections using silver autometallography.

Zn^{2+} detection in brain sections using silver autometallography from rats that received either TBI or sham injury, TPEN or ZnCl_2 injection or naïve (without surgery, injury or injection). Slides were placed on a photoscanner and scanned at 1200 dpi resolution.

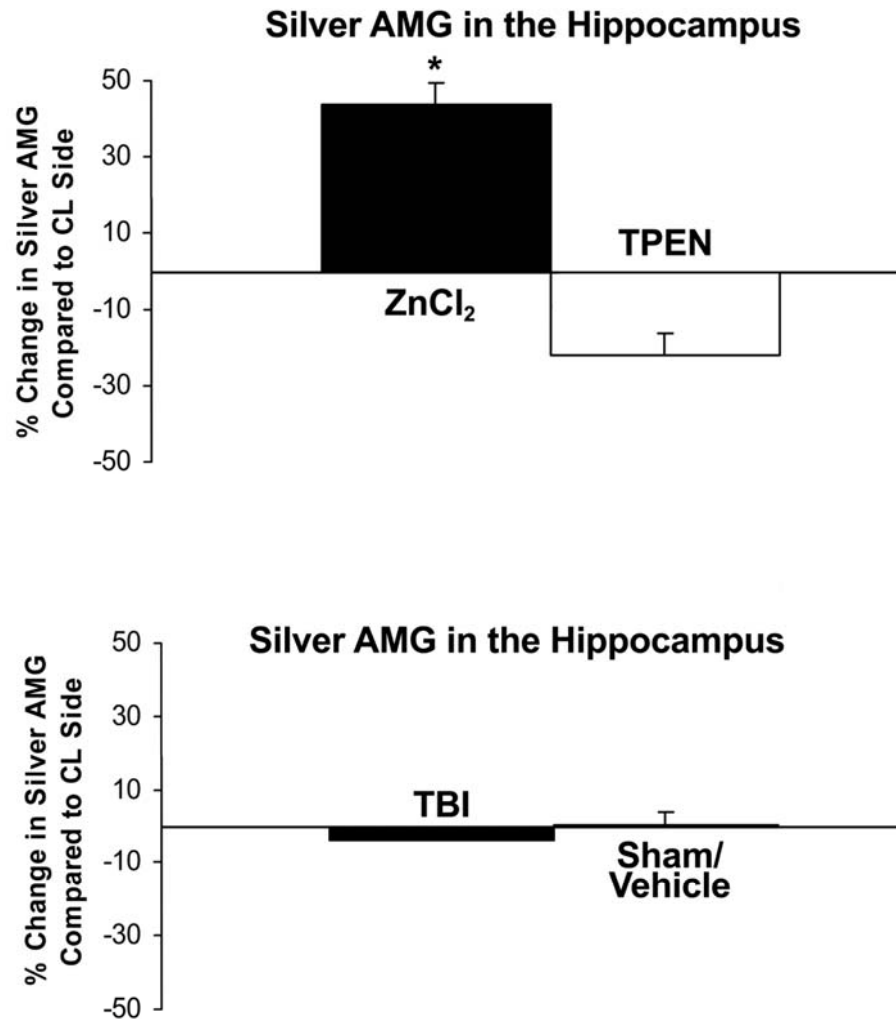


Figure 25. Densitometry measurements of hippocampal Zn^{2+} using silver autometallography.

Hippocampal regions of interest on the ipsilateral sides were compared to the contralateral sides and the percent change was recorded for each section and then an average per group is represented by the bars on the graphs. Error bars represent SEM. Hippocampal Zn^{2+} in the ZnCl_2 group was statistically different from TPEN injection rats ($p < 0.001$). No significant differences existed between the TBI and Sham groups in the hippocampus

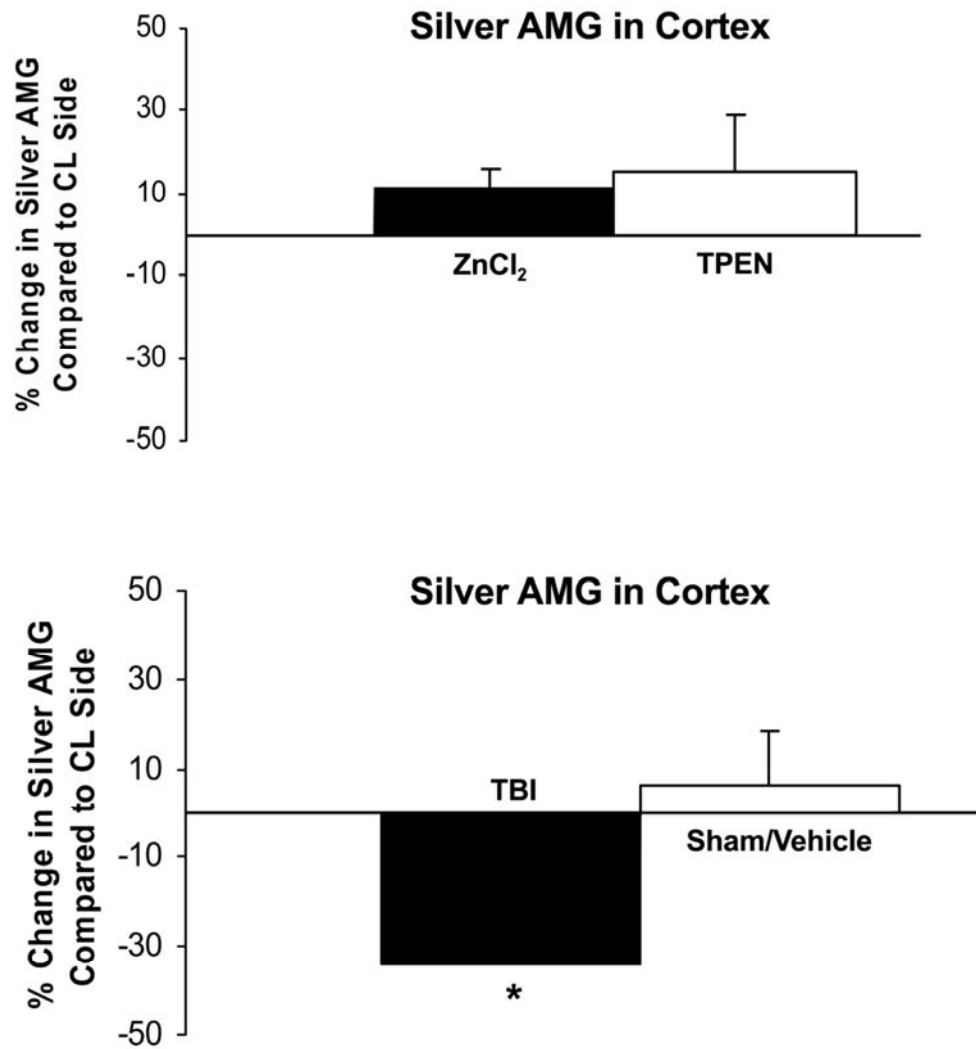


Figure 26. Densitometry measurements of Zn²⁺ in the cortex using silver autometallography.

Regions of interest in the cortex on the ipsilateral sides were compared to the contralateral sides and the percent change was recorded for each section and then an average per group is represented by the bars on the graphs. Error bars represent SEM. Cortical Zn²⁺ in the TBI group was statistically different from sham rats ($p < 0.001$). No significant differences existed between the ZnCl₂ and TPEN injection groups in the cortex.

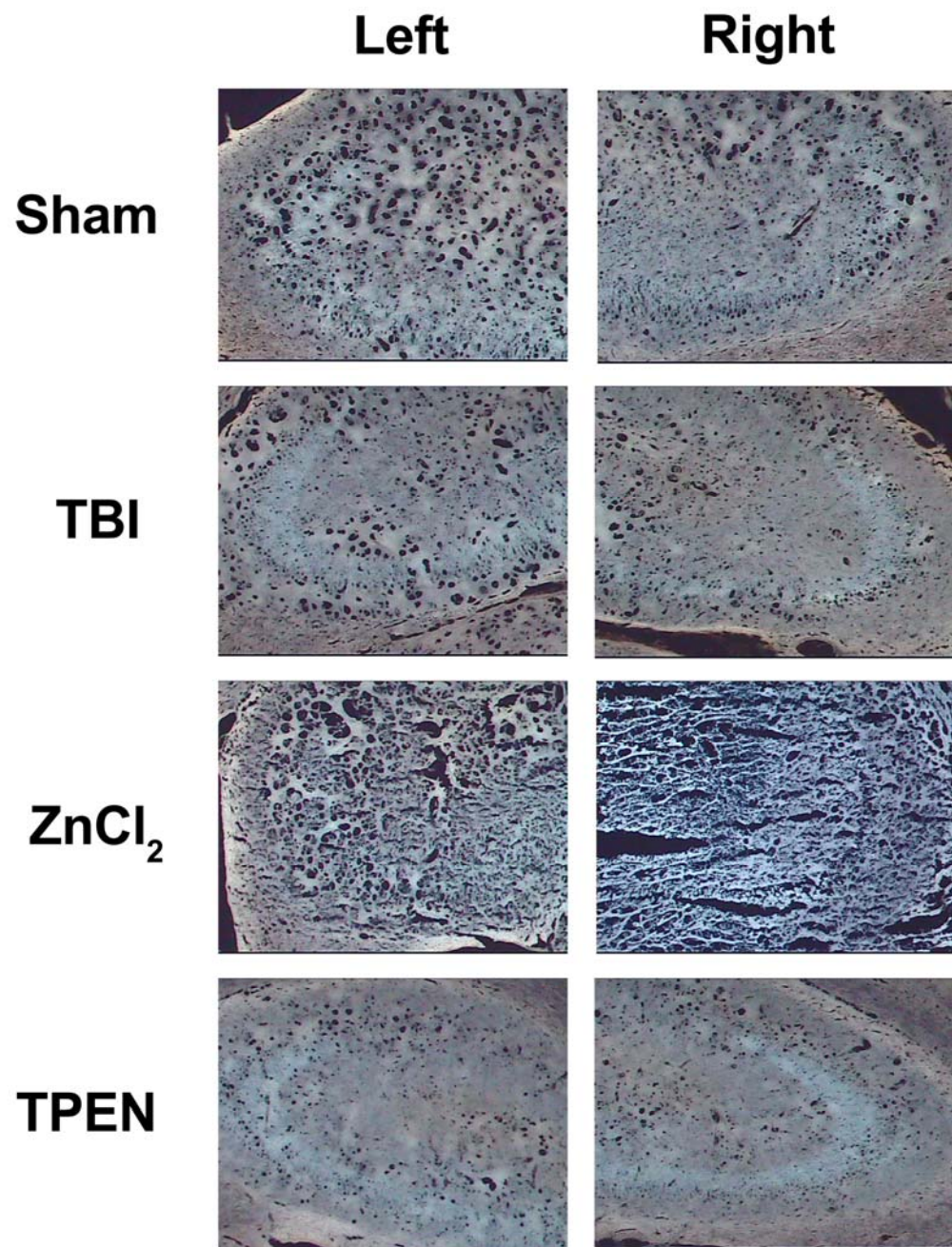


Figure 27. N-(6-methoxy-8-quinoly1)-p-toluenesulfonamide-stained silver AMG sections.

Sections of hippocampus (left and right hemispheres) from rats (sham, traumatic brain injury, ZnCl_2 and TPEN) that were perfused with sodium sulfide (to precipitate loose Zn^{2+} from tissue) followed by glutaraldehyde (fixative). Sections were stained for Zn^{2+} using TSQ in order to confirm most Zn^{2+} was precipitated with sodium sulfide and hence not available to be stained with TSQ.

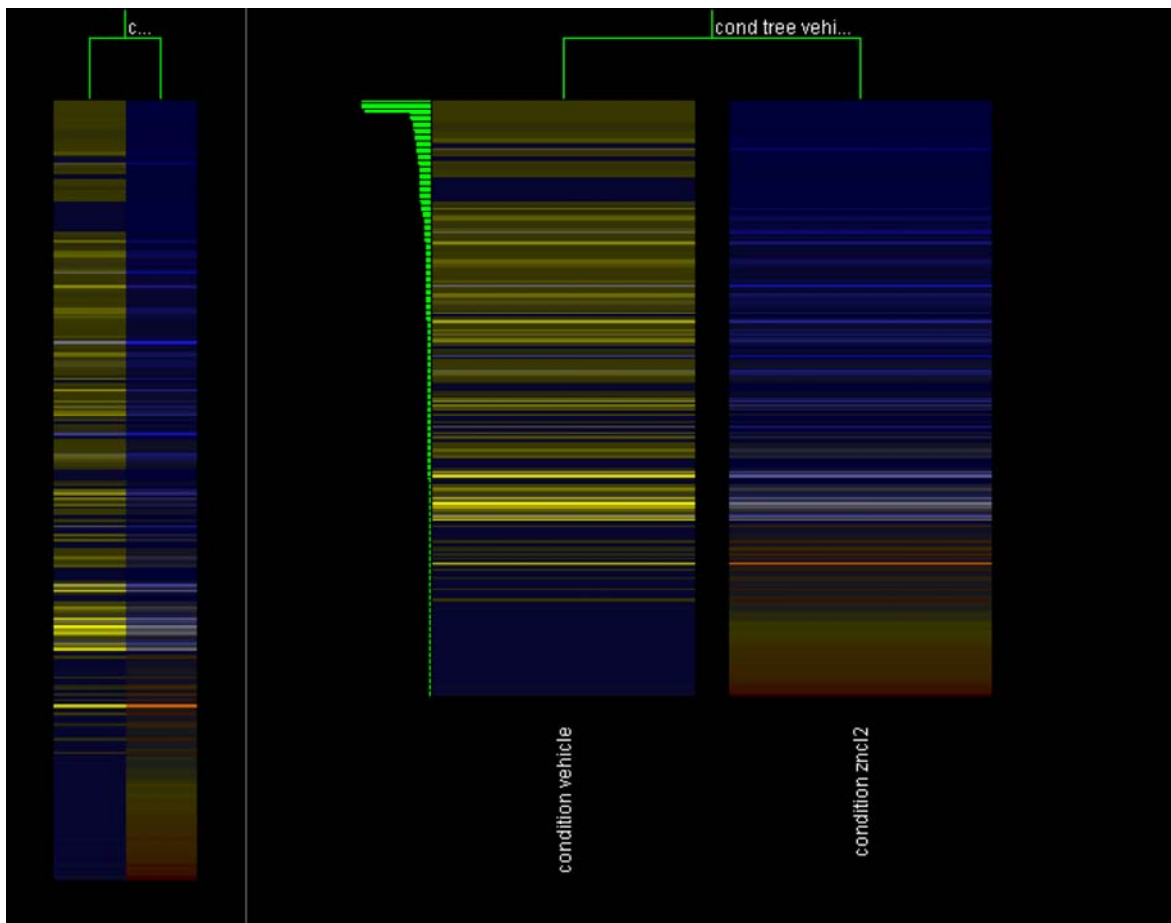


Figure 28. Hippocampal gene expression of vehicle and ZnCl₂ injection rats 24 hours post injection using an Atlas Rat Toxicology 1.2 gene array.

Condition tree includes only genes (279) that exhibited a 2-fold change (or greater) after normalization to housekeeping genes.

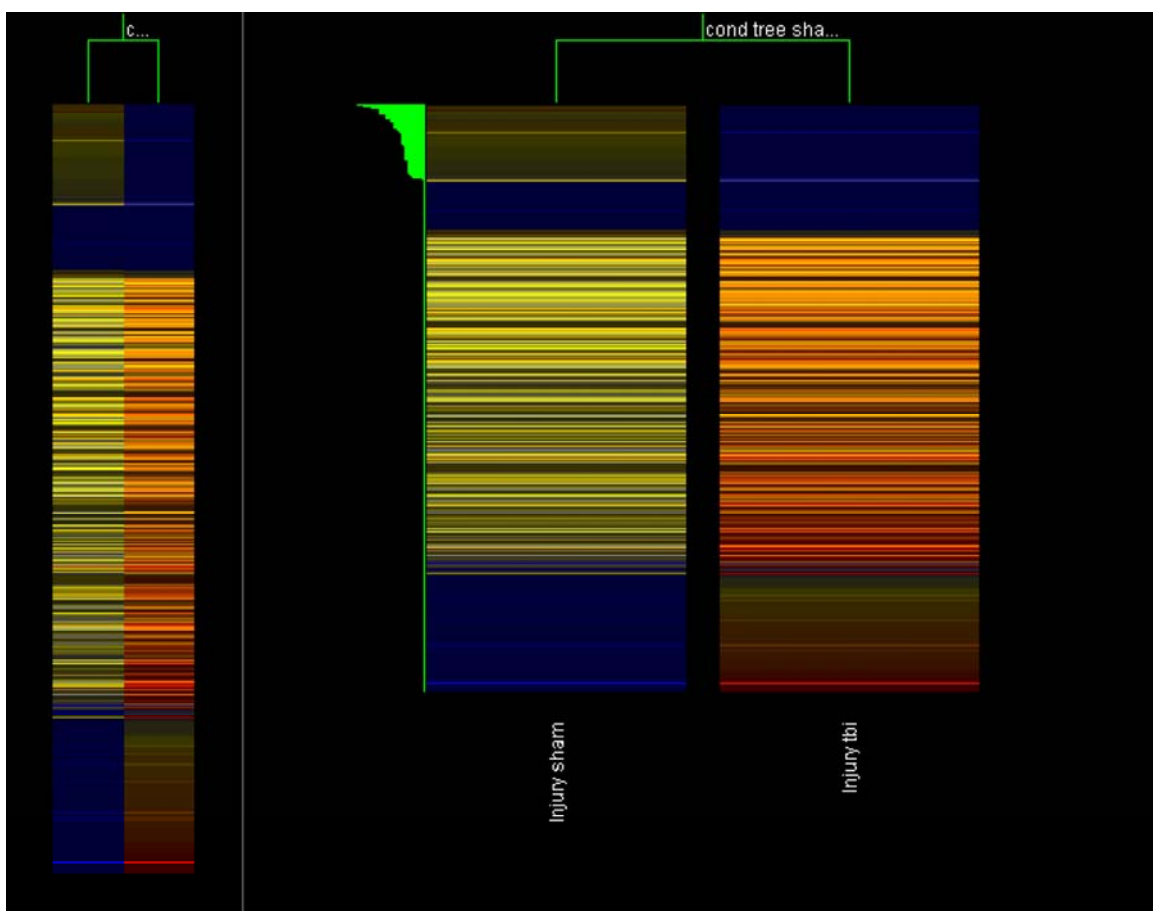


Figure 29. Hippocampal gene expression of sham and TBI rats 24 hours post injury using an Atlas Rat Toxicology 1.2 gene array.

Condition tree includes only genes (428) that exhibited a 2-fold change (or greater) after normalization to housekeeping genes.

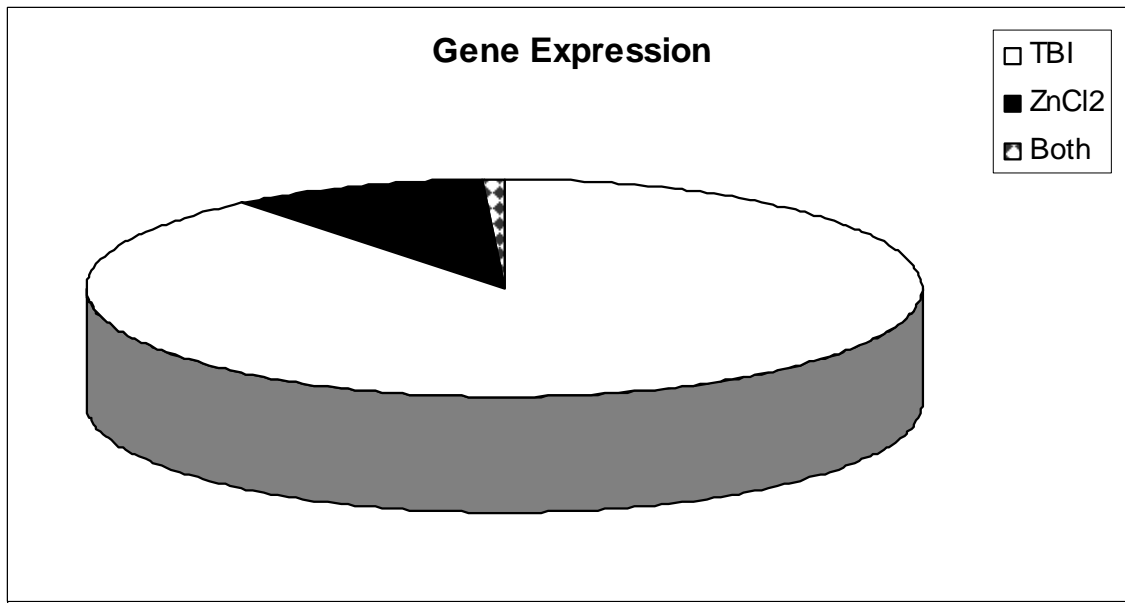


Figure 30. Pie chart of gene expression.

Pie chart of gene expression using pairwise comparison to show genes that were differentially expressed in the hippocampus 24 hours following TBI (126 genes) or ZnCl₂ (15 genes).

Chapter 5: Traumatic Brain Injury Does Not Contribute to Increased Extracellular Zn^{2+}

Vesicular Zn^{2+} may act as a neuromodulator during synaptic transmission at certain glutamatergic nerve terminals (Kay and Toth, 2008). Although evidence exists that suggests this may occur *in vitro* (Assaf and Chung, 1984; Howell et al., 1984; Kettermann and Li, 2008), it has not been shown in an intact brain. While multiple *in vivo* studies have looked at the amount of total zinc found in the extracellular fluid following restraint stress (Itoh et al., 1993), KCl stimulation in the hippocampus (Itoh et al., 1996) and the amygdala (Takeda et al., 1999), cerebral ischemia in gerbils (Yang et al., 2004) and rats (Kitamura et al., 2006a) using middle cerebral artery occlusion (Kitamura et al., 2006b), very few studies have attempted to measure the amount of free Zn^{2+} found in the extracellular fluid (Frederickson et al., 2006). The studies that measured total zinc did so by using flameless atomic absorption spectrophotometry techniques and detected high amounts of extracellular zinc following stimulation. Using a similar method as the Frederickson group to measure free Zn^{2+} , I was able to collect and quantitate the amount of free Zn^{2+} in the microdialysate following either sham or TBI. The animals were prepared using techniques described in the Microdialysis, apo-CA/ABDN and GF-AAS sections of the Methods chapter.

In preparation for the microdialysis (MD) experiments, the *in vitro* recovery rate of the MD probe needed to be determined. For this experiment, I diluted the primary zinc standard (1000 ppm, Sigma) to a concentration of 500 μM (in artificial cerebrospinal fluid

(aCSF) that was chelexed to remove zinc) in a Teflon beaker. The MD probe was then placed into the beaker (kept at 37°C) and the microdialysate from the beaker was collected in a microcentrifuge tube and analyzed for its zinc content, using graphite furnace atomic absorption spectrophotometry (GF-AAS). This value (13.010 µg) was then compared to the amount of zinc in the beaker (67.250 µg) and the recovery rate was determined to be 19%.

I focused on the CA2/CA3 region for my MD experiments, based on previous data collected in our lab suggesting this region is most selectively vulnerable to zinc neurotoxicity following trauma. To verify correct probe placement location, I injected cresyl violet (CV), into the region of interest using a variety of stereotaxic coordinates (Paxinos and Watson, 1986); I found that -3.6 A-P, 3.6 L-R, 3.6 dura gave the best placement into the region of interest (Figure 31). At the end of each MD experiment proposed, I injected CV dye to confirm proper probe placement.

Rats that had undergone either sham (n = 4) or TBI (n = 4) were microdialyzed for a total of 2 hours, collecting samples every 20 minutes. These samples were analyzed for total zinc using GF-AAS in triplicate and then compared to a zinc concentration curve to determine the molar concentration. Extracellular fluid from both sham and TBI rats contained less than 50 nM zinc when analyzed with the normal amount of nitric acid (Figure 32A) and there was no statistically significant difference between the groups at any of the time points tested. We hypothesized that perhaps the zinc was not being fully released from peptides or small proteins, so we added an additional 15 µl of 100% nitric acid to each of the previously analyzed samples and ended up with nearly double the

amount (100 nM zinc, on average) of zinc in each sample (Figure 32B) and still no difference between the sham and TBI groups. We initially believed that this increase was due to possible zinc contamination of the nitric acid that was added to the sample, but there was not a similar increase in the amount of zinc found in the zinc standards which had the same volume of nitric acid added to them. I next decided to look at free ionic Zn^{2+} in the extracellular fluid following sham and TBI.

Fluorimetric techniques are useful for the detection of small concentrations of metal ions. During our first attempt at this, I used FluoZin-3 (FZ3), a zinc indicator dye with high affinity for Zn^{2+} , but there was some controversy about whether or not it would bind to high (mM) concentrations of Ca^{2+} , which may be quite relevant when measuring extracellular fluid. I chelated the Ca^{2+} present in my samples by using oxalates, but was surprised to find that the fluorescence intensity only increased. Suspecting zinc contamination, we tested the oxalate for zinc using GF-AAS and it was found to contain μM levels of zinc.

To quantify the amount of free Zn^{2+} in biological samples without calcium interference, we then used a fluorescence-based biosensor (Fierke and Thompson, 2001; Bozym et al., 2006) using metal-free carbonic anhydrase (apo-CA) that binds to a fluorescent indicator called ABDN which then fluoresces when Zn^{2+} is bound. The microdialysis experiments were repeated using six rats per group and instead of taking 20 minute samples, 60 minute samples were collected. Prior to analysis of these samples, a zinc standard curve was plotted using estimates of free zinc values. All samples were compared to the zinc standard curve (Figure 33) that was fitted using a Hill equation that

produced a sigmoidal curve yielding a minimum reliable detection lower limit of 1 nM Zn^{2+} . There was no statistically significant difference between the sham and the TBI samples collected at any time point and all of the values were below 1 nM. This low value contradicts previous studies that found extracellular Zn^{2+} in the 5-25 nM range in rabbits undergoing ischemia (Frederickson et al., 2006).

At this point we were unsure whether or not Zn^{2+} was being collected and measured with this technique. As a control to show that if Zn^{2+} was present, it could, in fact, be collected and measured in our hands using these techniques, I infused 5 μl of a 500 μM ZnCl_2 solution for 20 minutes while microdialyzing nearby. During the first 20 minute collection, there were mid-nM amounts of Zn^{2+} (data not shown). In the following two 20 minute samples, the amount of Zn^{2+} was below the detection range again, suggesting rapid clearance from the extracellular space.

SUMMARY AND CONCLUSIONS

To summarize, the recovery rate of the microdialysis probes used was 19% for zinc using aCSF *in vitro* kept at 37°C without proteins. The concentration of total zinc that was measured in microdialysate using the GF-AAS techniques was in the range of 30-50 nM, which, assuming 19% recovery, equates to 150-250 nM zinc concentrations. No differences between the sham and TBI groups existed. In a separate set of experiments using apo-CA/ABDN fluorimetric techniques for the measurement of free ionic Zn^{2+} that we adapted for use in microdialysis fluid, the range of Zn^{2+} measured was below the detectable range of 1-2 nM as determined by a zinc standard curve, despite measuring appreciable amounts of Zn^{2+} in our positive (ZnCl_2 injection) control.

In studies (reviewed in Appendix Table 4) where exogenously applied zinc was added to cortical cell cultures for 15 minutes, the ED₅₀ (effective dose, 50%) was 600 μ M Zn²⁺ while the lower concentrations took longer to cause neuronal injury (ED₅₀ 225 μ M Zn²⁺ for 24 hour exposure) (Choi et al., 1988). The minimum concentration of Zn²⁺ injected *in vivo* to cause injury, as demonstrated by my ZnCl₂ injection experiments was shown to be 15.6 μ M. In order for Zn²⁺ release to be toxic *in vivo* following experimental TBI, we would need to show μ M Zn²⁺ present in the extracellular fluid. As shown by my microdialysis data, the concentration of Zn²⁺ found in the extracellular fluid (below 1 nM free Zn²⁺ and below 250 nM total zinc) was orders of magnitude lower than the minimum amount shown to cause injury (24 hour exposure of 100 μ M Zn²⁺ *in vitro* or 24 hour exposure to 15.6 μ M Zn²⁺ *in vivo*). There were also no differences in the amount of ionic or total zinc detected in the microdialysate of rats following sham (where no FJ+ cells are detected) or TBI. This leads us to conclude that extracellular Zn²⁺ released after experimental TBI is not a direct cause of neuronal injury.

The next step in this line of research may be to try to collect extracellular Zn²⁺ in awake, freely moving animals before and after TBI to rule out any effects of the isoflurane on synaptic release of Zn²⁺. Although my experiments could not support the hypothesis that extracellular Zn²⁺ is a direct cause of neurotoxicity following TBI, the concentration of intracellular free Zn²⁺ following TBI has not been determined and may reach neurotoxic levels. The effects of intracellular Zn²⁺ on cell death following TBI should be further explored and may lead not only to a better understanding of TBI pathophysiology but also better therapeutics to improve outcomes after TBI.

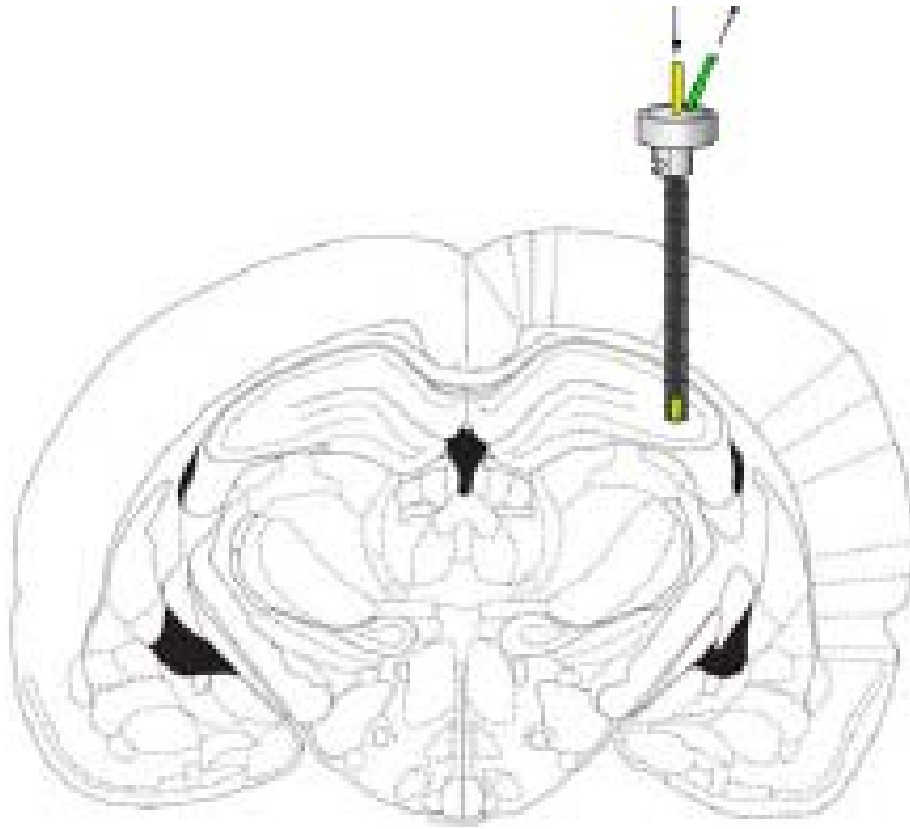


Figure 31. Illustration of microdialysis probe placement.

Adapted from Paxinos and Watson, 1986.

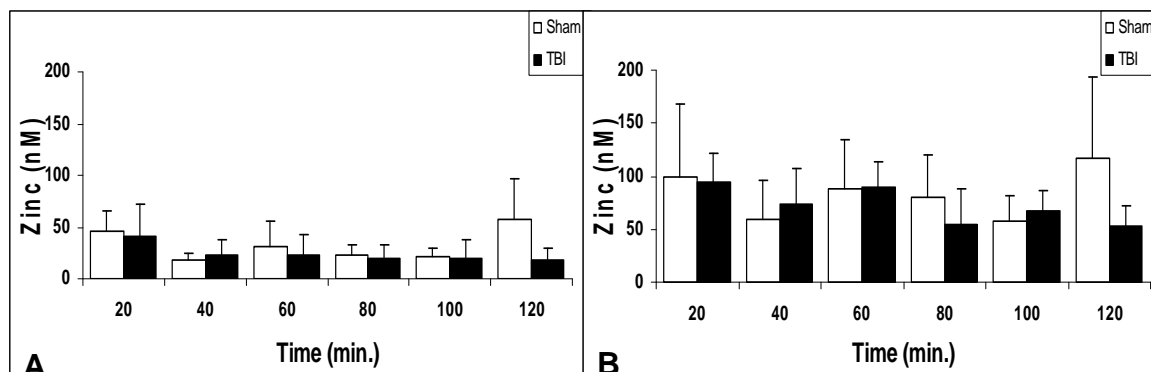


Figure 32. Total zinc measured in microdialysate from rats receiving sham injury or moderate traumatic brain injury, using Graphite Furnace Atomic Absorption Spectrophotometry.

Samples were digested in 0.25 M HNO₃ (A) or 0.25 M HNO₃ + 15 μl 100% v/v HNO₃ (B). Open bars represent sham injured samples while filled bars represent TBI samples. Error bars represent standard deviation, n = 4 per group, individual samples analyzed in triplicate.

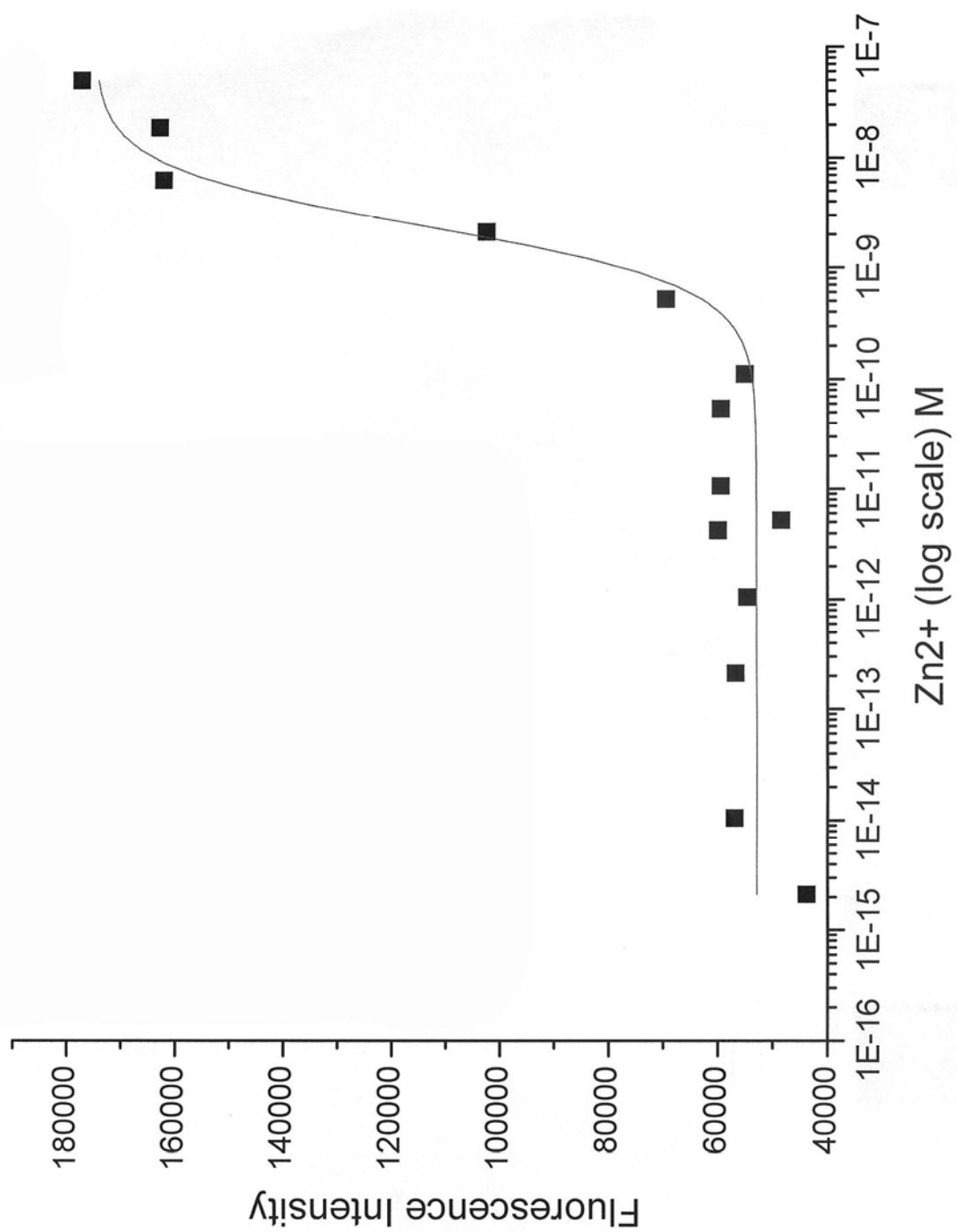


Figure 33. Free Zn^{2+} standard curve that was fit using the Hill equation.

DISCUSSION

Chapter 6: Summary and Conclusions

The overall goal of my research was to examine the role of Zn^{2+} in neuronal cell death following TBI *in vivo*. We hypothesized that Zn^{2+} is an important pathogenic component of TBI and we predicted the following: 1) TBI caused accumulation of intracellular Zn^{2+} , 2) Injections of exogenous Zn^{2+} produced hippocampal damage similar to TBI, and 3) Zn^{2+} levels present in the extracellular fluid following TBI were toxic.

First, TBI appeared to lead to a delayed accumulation of intracellular Zn^{2+} , as evidenced by the *zinc indicator time course comparison* experiments. In these experiments, Zn^{2+} and degenerating (FJ+) stained neurons only appeared after the 2 hour survival time point, suggesting a delayed terminal process which was associated with increased intracellular Zn^{2+} . This intracellular Zn^{2+} found following TBI was partially prevented with pretreatments of either a sodium channel blocker (lamotrigine) or an L-type calcium channel blocker (nicardipine).

Second, injections of exogenous Zn^{2+} , in the form of ZnCl_2 , produced hippocampal damage that was dissimilar to TBI. ZnCl_2 injections appeared to cause massive necrosis at higher doses (over 125 μM) and all toxic concentrations appeared to cause damage at 1 hour post injection, which was much sooner than detectable injured neurons following TBI. Patterns of cortical and hippocampal Zn^{2+} availability in coronal sections of the rat brain as demonstrated by silver AMG point to additional differences between the ZnCl_2 injection model and TBI following 6 hour survival. Significant differences in gene expression between ZnCl_2 and TBI animals have also been shown,

which strengthens the idea that ZnCl_2 injections and TBI produce dissimilar injury to the hippocampal region.

Third, Zn^{2+} levels present in the extracellular fluid following TBI were found to be much lower than the range of extracellular Zn^{2+} that causes toxicity. This was demonstrated by looking at the amount of total and ionic Zn^{2+} present in the microdialysate fluid. Therefore, my research does not support the idea of a translocation hypothesis where Zn^{2+} is released from presynaptic vesicles, transverses the cleft and enters the postsynaptic neuron via calcium channels (most likely glutamate or voltage-gated), which leads to a deadly accumulation of Zn^{2+} intracellularly which then causes the cell to undergo apoptosis. Intracellular Zn^{2+} release after TBI may play a role in neuronal cell death cascades and thus should be further explored.

Lamotrigine significantly reduced both Zn^{2+} accumulation and neuronal injury in hippocampal neurons after TBI. The effects of lamotrigine may be due to inhibition of presynaptic glutamate or to effects on post-synaptic sodium channels. Nicardipine treatment also reduced Zn^{2+} accumulation in CA1 but was less effective than lamotrigine at reducing neuronal injury as assessed by FJ staining. This difference between the two channel blockers may be due to differences in gene expression, specifically upregulation of neuroprotective genes that increase their chances of survival.

Zinc accumulation in injured neurons seems to occur as a pre-terminal, rather than a gradual, event and appears to happen in between 2 and 8 hours post trauma. This may be an effect of the cell releasing large quantities of Zn^{2+} that is normally bound to proteins and may be the result of the cell irreversibly committing itself to die. It is unclear at this time whether the intracellular Zn^{2+} contributes to the cell death process or if the Zn^{2+} is itself the principle cause of death.

Injecting ZnCl_2 ($>15.6 \mu\text{M}$) directly into the hippocampus results in neuronal damage after 1 hour survival. Results that intrahippocampal injections of zinc were associated with significantly impaired MWM performance within the first 10 days after injection suggest that zinc accumulation may contribute to early cognitive deficits after TBI. This is particularly relevant because in human TBI cases, cognitive deficits and learning and memory dysfunction and loss are the most common long-lasting effects suffered. There may have been some compensation from the unaffected hippocampus located in the contralateral hemisphere when rats were tested at later time points (Figure 12).

Zn^{2+} distribution (shown by silver AMG grains) in the rat's brain after sham or TBI or ZnCl_2 or TPEN injections was different when compared to the naïve rat's brain. The lack of Zn^{2+} in the CA1 region of the naïve hippocampus suggests that perhaps it is induced from stress (or isoflurane exposure) to the animal. This could be studied by repeating the same experiment but expose the naïve rats to isoflurane for the same length of time as an animal that underwent surgery. This appearance of CA1 hippocampal Zn^{2+} in the sham rats may be due to MT proteins releasing their Zn^{2+} stores to react with isoflurane (or a downstream effect resulting from isoflurane exposure) to prevent further injury to the cell. This is purely speculative, but it may account for the neuroprotective effect of isoflurane on neuronal cells following TBI.

The differences in silver AMG grains that exist between my data and that of Suh et al., 2000 can be explained by differences in animal preparation, including anesthesia, and that they used a weight-drop model of TBI whereas our lab uses a fluid percussion model of injury. In a cortical stab wound model of brain trauma, Doering et al. could not replicate the Silver AMG patterns shown in Suh et al., 2000 (Doering et al., 2007). In wildtype mice, they saw an increase of Zn^{2+} staining adjacent to the lesion site, but not in

individual soma, whereas the ZnT3 knockout mice displayed silver-enhanced ZnSe crystals in the neuronal somata near the lesion. The authors concluded that vesicular zinc may not contribute to neuronal damage following neurotrauma (Doering et al., 2007).

Differences in gene expression changes between the ZnCl₂ and TBI animals were difficult to ascertain using a mini-array and may best be served by looking at a time course of survival (instead of one survival time point) from 30 minutes to 24 hours and by using a gene array that looks at not only toxicology-related genes but the entire genome. Overall, in terms of gene expression, the two models of injury were distinctly different.

The amount of total zinc that was measured in microdialysate using GF-AAS techniques was in the range of 30-50 nM. No differences between the sham and TBI groups existed. In a separate set of experiments using apo-CA/ABDN fluorimetric techniques for the measurement of free ionic Zn²⁺ that we adapted for use in microdialysis fluid, the range of Zn²⁺ measured was below the detectable range of 1-2 nM as determined by a Zn²⁺ standard curve, despite measuring appreciable amounts of Zn²⁺ in our positive (ZnCl₂ injection) control. In these experiments, I was still unable to detect any differences in extracellular Zn²⁺ between sham and TBI animals.

The next step in this line of research may be to try to collect extracellular Zn²⁺ in awake, freely moving animals before and after TBI to rule out any effects of the isoflurane on synaptic release of Zn²⁺. Although my experiments could not support the hypothesis that extracellular Zn²⁺ is a direct cause of neurotoxicity following TBI, the concentration of intracellular free Zn²⁺ following TBI has not been determined and may reach neurotoxic levels. The effects of intracellular Zn²⁺ on cell death following TBI should be further explored and may lead not only to a better understanding of TBI pathophysiology but also better therapeutics to improve outcomes after TBI.

As the field of Zn^{2+} induced cellular injury is fairly new, there exist many more *unknowns* than *knowns* in the literature. A major question in this field has been whether it is extracellular or intracellular Zn^{2+} that causes neuronal cell death. I have addressed this gap in knowledge with the completion of the microdialysis and ZnCl_2 injection studies (extracellular Zn^{2+}) and channel blocking experiments using lamotrigine and nicardipine (intracellular Zn^{2+}). I have also shown that the intracellular Zn^{2+} present in hippocampal neurons following TBI did not gradually accumulate, but rather increased abruptly at approximately the same time as FJ-positivity developed, suggesting association rather than causation. Those experiments also showed that survival for more than 2 hours was necessary both for Zn^{2+} accumulation (and FJ evidence of neurodegeneration), as assessed with very sensitive dyes. I have also addressed another gap in knowledge by determining the minimum concentration of exogenously applied ZnCl_2 that will cause neuronal injury *in vivo*. This will be useful for those wishing to study Zn^{2+} toxicity in animal models. I have taken a model of ZnCl_2 toxicity and have characterized it by looking at behavioral effects, gene expression changes and histology, including Zn^{2+} distribution in the brain. By addressing these current gaps of knowledge in the field of Zn^{2+} neurotoxicity, I have not only contributed data towards advancing TBI research, but also to the area of Zn^{2+} signaling which can be applied to multiple systems and disease models.

Appendices

Table 1. Primer sequences for gene expression studies.

Gene	Primer Sequence (Forward and Reverse)	Product (bp)	GenBank no.
Caspase 9	5'-GCTTGGTGGTGTCATCCTC-3' (Forward) 5'-CTGAGAGGAGGGACTGCAG-3' (Reverse)	471	NM_031632
Neuronal nitric oxide synthase	5'-CATCAGCTCCTCTCCAGACA-3' (Forward) 5'-CAGCCAGCTGTTCTCTGCAGC-3' (Reverse)	409	U67309
Glutathione peroxidase- 1	5'-GTGGCACAGTCCACCGTGA-3' (Forward) 5'-GGTTGCTAGACTGCTTGGAC-3' (Reverse)	548	NM_030826
Superoxide dismutase 2	5'-GACCTGCCTTACTATGG-3' (Forward) 5'-CAGTGGAAATAAGGCCTGTGG-3' (Reverse)	449	NM_017051
Glyceraldehyde-3-phosphate dehydrogenase	5'-ACCACAGTCCATGCCATCAC-3' (Forward) 5'-TCCACCACCCTGTTGCTGTA-3' (Reverse)	451	NM_017008
Gene	Primer Sequence (T3 T7)	Product (bp)	GenBank no.
Caspase 9	5'- GCCTAATTAAACCCCTCACTAAAGGAGCTGTTCTTCATCCAGGCTGTG-3' (T3) 5'- CTCGGTAATACGACTCACTATAGGGTGGCAAACTTGACACTGGTC-3' (T7)	171	NM_031632
Neuronal nitric oxide synthase	5'- GCCTAATTAAACCCCTCACTAAAGGAGCGTCTCTACCCACACCCGAGACG-3' (T3) 5'- CTCGGTAATACGACTCACTATAGGGGACACCCGAAAGACCAAGCCATG-3' (T7)	268	U67309
Glutathione peroxidase- 1	5'- GCCTAATTAAACCCCTCACTAAAGGAGTATGTCGACCCCGTGGTGGGT-3' (T3) 5'- CTCGGTAATACGACTCACTATAGGGTGTAGGCTGCTTGGACAGCAGG-3' (T7)	313	NM_030826
Superoxide dismutase 2	5'- GCCTAATTAAACCCCTCACTAAAGGAGCAACAGCAAGCAAGCCACCGGA-3' (T3) 5'- CTCGGTAATACGACTCACTATAGGGCGCTTGTAGCCTCCAGCAACTC-3' (T7)	221	NM_017051
Glyceraldehyde-3-phosphate dehydrogenase	5'- GCCTAATTAAACCCCTCACTAAAGGAGCTGCCAAGGCTGTGGGCAAGGT-3' (T3) 5'- CTCGGTAATACGACTCACTATAGGGCTTGATGTCATCATACTTGGCAG-3' (T7)	140	NM_017008

Table 2. ZnCl₂ Injection Gene Expression

Name	Matched Term	Description	Location	Entrez Gene ID for Rat
<u>Enzyme</u>				
UGT2B7	U06273	UDP glucuronosyltransferase 2 family, polypeptide B7	Cytoplasm	83808
NEDD8	AF095740	neural precursor cell expressed, developmentally down-regulated 8	Nucleus	25490
<u>G-protein coupled receptor</u>				
GPR1	S74702	G protein-coupled receptor 1	Plasma Membrane	25457
GRM6	D13963	glutamate receptor, metabotropic 6	Plasma Membrane	24419
<u>Ligand-dependent nuclear receptor</u>				
VDR	J03630, J04147	vitamin D (1,25- dihydroxyvitamin D3) receptor	Nucleus	24873
<u>Miscellaneous</u>				
COL3A1	M21354	collagen, type III, alpha 1 (Ehlers-Danlos syndrome type IV, autosomal dominant)	Extracellular Space	84032
TNFAIP6	AF159103	tumor necrosis factor, alpha-induced protein 6	Extracellular Space	84397
ACPP	M32397	acid phosphatase, prostate	Extracellular Space	56780
MYCN	X63281	v-myc myelocytomatosis viral related oncogene, neuroblastoma derived (avian)	Nucleus	298894
DCC	U68725	deleted in colorectal carcinoma	Plasma Membrane	25311
ITGA7	X65036	integrin, alpha 7	Plasma Membrane	81008
<u>Transporter</u>				
PBSN	M27156	probasin	Extracellular Space	54193
SLC5A1	AB000729, U03120	solute carrier family 5 (sodium/glucose cotransporter), member 1	Plasma Membrane	25552


 Decreased gene expression
 Increased gene expression

Table 3 Traumatic Brain Injury Gene Expression

Name	Matched Term	Description	Location	Entrez Gene ID for Rat
<u>Cytokine</u>				
CXCL10	U17035	chemokine (C-X-C motif) ligand 10	Extracellular Space	245920
<u>Enzyme</u>				
BHMT	AF038870	betaine-homocysteine methyltransferase	Cytoplasm	81508
CAT	M11670	catalase	Cytoplasm	24248
COX8B	X64827	cytochrome c oxidase, subunit VIIIb	Cytoplasm	25250
CYP1A1	X00469	cytochrome P450, family 1, subfamily A, polypeptide 1	Cytoplasm	24296
CYP1B1	U09540	cytochrome P450, family 1, subfamily B, polypeptide 1	Cytoplasm	25426
GSS	L38615	glutathione synthetase	Cytoplasm	25458
GSTM3 (includes EG:2947)	U86635	glutathione S-transferase M3 (brain)	Cytoplasm	64352
HMGCS2	M33648	3-hydroxy-3-methylglutaryl-Coenzyme A synthase 2 (mitochondrial)	Cytoplasm	24450
HSD17B3	AF035156	hydroxysteroid (17-beta) dehydrogenase 3	Cytoplasm	117182
MGST1	J03752	microsomal glutathione S-transferase 1	Cytoplasm	171341
RAB8A	M83675	RAB8A, member RAS oncogene family	Cytoplasm	117103
SPAM1 (includes EG:20690)	X89999	sperm adhesion molecule 1	Plasma Membrane	117037
ASNS	U07201	asparagine synthetase	Unknown	25612
<u>G-protein coupled receptor</u>				
ADRA2B	M32061	adrenergic, alpha-2B-, receptor	Plasma Membrane	24174
ADRB1	D00634	adrenergic, beta-1-, receptor	Plasma Membrane	24925
CRHR1	L24096	corticotropin releasing hormone receptor 1	Plasma Membrane	58959
DRD1	M35077	dopamine receptor D1	Plasma Membrane	24316
EDNRB	X57764	endothelin receptor type B	Plasma Membrane	50672
HTR1B	M89954	5-hydroxytryptamine (serotonin) receptor 1B	Plasma Membrane	25075
HTR2A	M30705	5-hydroxytryptamine (serotonin) receptor 2A	Plasma Membrane	29595

Table 3 Traumatic Brain Injury Gene Expression

Name	Matched Term	Description	Location	Entrez Gene ID for Rat
NPR3	L27339	natriuretic peptide receptor C/guanylate cyclase C (atrionatriuretic peptide receptor C)	Plasma Membrane	25339
PTAFR	U04740	platelet-activating factor receptor	Plasma Membrane	58949
SMO	U84402	smoothened homolog (Drosophila)	Plasma Membrane	25273

Growth factor

BMP7	AF100787	bone morphogenetic protein 7 (osteogenic protein 1)	Extracellular Space	85272
CSPG5	U33553	chondroitin sulfate proteoglycan 5 (neuroglycan C)	Extracellular Space	50568
FGF7	X56551	fibroblast growth factor 7 (keratinocyte growth factor)	Extracellular Space	29348
FIGF	AF014827	c-fos induced growth factor (vascular endothelial growth factor D)	Extracellular Space	360457
IGF2	M13969	insulin-like growth factor 2 (somatomedin A)	Extracellular Space	24483
INHBA	M37482	inhibin, beta A	Extracellular Space	29200
INHBC	AF140031	inhibin, beta C	Extracellular Space	64549
REG3A	M98049	regenerating islet-derived 3 alpha	Extracellular Space	24618
TGFA	M31076	transforming growth factor, alpha	Extracellular Space	24827
TGFB3	U03491	transforming growth factor, beta 3	Extracellular Space	25717
VEGFC	AF010302	vascular endothelial growth factor C	Extracellular Space	114111

Ion channel

CACNB1	X61394	calcium channel, voltage-dependent, beta 1 subunit	Plasma Membrane	50688
CLCN7	Z67744	chloride channel 7	Plasma Membrane	29233
GABRA2 (includes EG:29706)	L08491	gamma-aminobutyric acid A receptor, alpha 2	Plasma Membrane	29706
GABRA3	L08492	gamma-aminobutyric acid (GABA) A receptor, alpha 3	Plasma Membrane	24947
GABRB2	X15467	gamma-aminobutyric acid (GABA) A receptor, beta 2	Plasma Membrane	25451
KCNJ12	X78461	potassium inwardly-rectifying channel, subfamily J, member 12	Plasma Membrane	117052

Table 3 Traumatic Brain Injury Gene Expression

Name	Matched Term	Description	Location	Entrez Gene ID for Rat
<u>Kinase</u>				
PIM1	X63675	pim-1 oncogene	Cytoplasm	24649
CLK3	X94351	CDC-like kinase 3	Nucleus	171305
GAK	D38560	cyclin G associated kinase	Nucleus	81659
ACVR1B	S76466	activin A receptor, type IB	Plasma Membrane	29381
ACVR2B	M87067	activin A receptor, type IIB	Plasma Membrane	25366
CSF1R	X61479	colony stimulating factor 1 receptor, formerly McDonough feline sarcoma viral (v-fms) oncogene homolog	Plasma Membrane	307403
EGFR	M37394	epidermal growth factor receptor (erythroblastic leukemia viral (v-erb-b) oncogene homolog, avian)	Plasma Membrane	24329
ERBB3	U29339	v-erb-b2 erythroblastic leukemia viral oncogene homolog 3 (avian)	Plasma Membrane	29496
FLT1	D28498	fms-related tyrosine kinase 1 (vascular endothelial growth factor/vascular permeability factor receptor)	Plasma Membrane	54251
PDGFRA	M63837	platelet-derived growth factor receptor, alpha polypeptide	Plasma Membrane	25267
TGFR1	L26110	transforming growth factor, beta receptor I (activin A receptor type II-like kinase, 53kDa)	Plasma Membrane	29591
<u>Ligand-dependent nuclear receptor</u>				
NR4A1	U17254	nuclear receptor subfamily 4, group A, member 1	Nucleus	79240
<u>Miscellaneous</u>				
HSPB2	U75899	heat shock 27kDa protein 2	Cytoplasm	161476
NFKBIA	X63594	nuclear factor of kappa light polypeptide gene enhancer in B-cells inhibitor, alpha	Cytoplasm	25493
C4BPA	Z50051	complement component 4 binding protein, alpha	Extracellular Space	24235
COL3A1	M21354	collagen, type III, alpha 1 (Ehlers-Danlos syndrome type IV, autosomal dominant)	Extracellular Space	84032
CST8	AF090692	cystatin 8 (cystatin-related epididymal specific)	Extracellular Space	29679
LAMA3	U61261	laminin, alpha 3	Extracellular Space	307582
LHB	V01542	lutinizing hormone beta polypeptide	Extracellular Space	25329

Table 3 Traumatic Brain Injury Gene Expression

Name	Matched Term	Description	Location	Entrez Gene ID for Rat
MGP	J03026	matrix Gla protein	Extracellular Space	25333
ORM2	J00696	orosomucoid 2	Extracellular Space	24614
PRL7D1	AF139809	prolactin family 7, subfamily d, member 1	Extracellular Space	84377
TIMP3	U27201	TIMP metalloproteinase inhibitor 3 (Sorsby fundus dystrophy, pseudoinflammatory)	Extracellular Space	25358
CCNC	D14013	cyclin C	Nucleus	114839
ANXA4	D38224	annexin A4	Plasma Membrane	79124
CD24	U49062	CD24 molecule	Plasma Membrane	25145
CDH6	D25290	cadherin 6, type 2, K-cadherin (fetal kidney)	Plasma Membrane	25409
ITGA1	X52140	integrin, alpha 1	Plasma Membrane	25118
ITGA7	X65036	integrin, alpha 7	Plasma Membrane	81008
PLP1	M11185	proteolipid protein 1 (Pelizaeus-Merzbacher disease, spastic paraplegia 2, uncomplicated)	Plasma Membrane	24943
SELE	L25527	selectin E (endothelial adhesion molecule 1)	Plasma Membrane	25544
VCAM1	M84488	vascular cell adhesion molecule 1	Plasma Membrane	25361
<u>Peptidase</u>				
MMP10	M65253	matrix metalloproteinase 10 (stromelysin 2)	Extracellular Space	117061
MMP14	X83537	matrix metalloproteinase 14 (membrane-inserted)	Extracellular Space	81707
PLAT	M23697	plasminogen activator, tissue	Extracellular Space	25692
<u>Transcription regulator</u>				
ATF3	M63282	activating transcription factor 3	Nucleus	25389
BTG2	M60921	BTG family, member 2	Nucleus	29619
CDKN2B	S79760	cyclin-dependent kinase inhibitor 2B (p15, inhibits CDK4)	Nucleus	25164
DDIT3	U30186	DNA-damage-inducible transcript 3	Nucleus	29467
EGR4	M65008	early growth response 4	Nucleus	25129
ETS1	L20681	v-ets erythroblastosis virus E26 oncogene homolog 1 (avian)	Nucleus	24356

Table 3 Traumatic Brain Injury Gene Expression

Name	Matched Term	Description	Location	Entrez Gene ID for Rat
FOS	X06769	v-fos FBJ murine osteosarcoma viral oncogene homolog	Nucleus	314322
FOSL2	U18913	FOS-like antigen 2	Nucleus	25446
GTF2B	X65948	general transcription factor IIB	Nucleus	81673
HES1	D13417	hairy and enhancer of split 1, (Drosophila)	Nucleus	29577
HIF1A	Y09507	hypoxia-inducible factor 1, alpha subunit (basic helix-loop-helix transcription factor)	Nucleus	29560
HIVEP1	X54250	human immunodeficiency virus type I enhancer binding protein 1	Nucleus	117140
HMGB2	D84418	high-mobility group box 2	Nucleus	29395
HOXA5	L03556	homeobox A5	Nucleus	79241
IRF1	M34253	interferon regulatory factor 1	Nucleus	24508
JUNB	X54686	jun B proto-oncogene	Nucleus	24517
JUND	D26307	jun D proto-oncogene	Nucleus	24518
MDM2 (includes EG:4193)	Z12020	Mdm2, transformed 3T3 cell double minute 2, p53 binding protein (mouse)	Nucleus	314856
MECP2	M94064	methyl CpG binding protein 2 (Rett syndrome)	Nucleus	29386
MYOG	M24393	myogenin (myogenic factor 4)	Nucleus	29148
NFIA	D78017	nuclear factor I/A	Nucleus	25492
NFKB1	L26267	nuclear factor of kappa light polypeptide gene enhancer in B-cells 1 (p105)	Nucleus	81736
PRDM2	U17837	PR domain containing 2, with ZNF domain	Nucleus	313678
RBBP7	AF090306	retinoblastoma binding protein 7	Nucleus	83712
STAT6	AF055292	signal transducer and activator of transcription 6, interleukin-4 induced	Nucleus	362896
ZFP36	X63369	zinc finger protein 36, C3H type, homolog (mouse)	Nucleus	79426
NOTCH2	M93661	Notch homolog 2 (Drosophila)	Plasma Membrane	29492
<i>Transmembrane receptor</i>				
CHRNA7	X74834	cholinergic receptor, nicotinic, gamma	Plasma Membrane	25753
CNTFR	S54212	ciliary neurotrophic factor receptor	Plasma Membrane	313173
EPOR	D13566	erythropoietin receptor	Plasma Membrane	24336
IL1R1	M95578	interleukin 1 receptor, type I	Plasma Membrane	25663

Table 3 Traumatic Brain Injury Gene Expression

Name	Matched Term	Description	Location	Entrez Gene ID for Rat
IL2RA	M55049	interleukin 2 receptor, alpha	Plasma Membrane	25704
MR1	Y13972	major histocompatibility complex, class I-related	Plasma Membrane	25119
NGFR	X05137	nerve growth factor receptor (TNFR superfamily, member 16)	Plasma Membrane	24596
TNFRSF1A	M63122	tumor necrosis factor receptor superfamily, member 1A	Plasma Membrane	25625

Transporter

FABP9	U07870	fatty acid binding protein 9, testis	Cytoplasm	64822
APOA1	M00001	apolipoprotein A-I	Extracellular Space	25081
APOA2	X03468	apolipoprotein A-II	Extracellular Space	25649
ATP1A2	M14512	ATPase, Na ⁺ /K ⁺ transporting, alpha 2 (+) polypeptide	Plasma Membrane	24212
NNAT	U08290	neuronatin	Plasma Membrane	94270
SLC4A1	J04793	solute carrier family 4, anion exchanger, member 1 (erythrocyte membrane protein band 3, Diego blood group)	Plasma Membrane	24779
SLC7A1	D67087, U70476	solute carrier family 7 (cationic amino acid transporter, y ⁺ system), member 1	Plasma Membrane	25648
TFRC	M58040	transferrin receptor (p90, CD71)	Plasma Membrane	64678



 Decreased gene expression
 Increased gene expression

Table 4 Minimum Concentrations of Zn²⁺ Toxic to Neurons

	15 min	2 hours	24 hours
Zn²⁺ toxic <i>in vitro</i>			
With K⁺ stimulation	400 µM in medium (Cai et al., 2006)		35 µM in medium (Kim et al., 1999)
Without K⁺ stimulation	600 µM in medium (Choi et al., 1988)		100 µM in medium (Choi et al., 1988)
Zn²⁺ toxic <i>in vivo</i>		3µl of 62.5 µM ZnCl ₂ (Hawkins, unpublished)	3µl of 15.6 µM ZnCl ₂ (Hawkins, unpublished)

Reference List

Traumatic Brain Injury in the United States: Emergency Department Visits. Centers for Disease Control and Prevention . 2006. Date Accessed on July 25, 2008.

Brain Injury Association. www.biausa.org . 2008. Date Accessed on June 30, 2008.

Adams JH, Doyle D, Ford I, Gennarelli TA, Graham DI, McLellan DR (1989) Diffuse axonal injury in head injury: definition, diagnosis and grading. *Histopathology* 15:49-59.

Aizenman E, Stout AK, Hartnett KA, Dineley KE, McLaughlin B, Reynolds IJ (2000) Induction of neuronal apoptosis by thiol oxidation: putative role of intracellular zinc release. *J Neurochem* 75:1878-1888.

Alexander MP (1995) Mild traumatic brain injury: pathophysiology, natural history, and clinical management. *Neurology* 45:1253-1260.

Anderson KJ, Fugaccia I, Scheff SW (2003) Fluoro-jade B stains quiescent and reactive astrocytes in the rodent spinal cord. *J Neurotrauma* 20:1223-1231.

Arundine M, Tymianski M (2004) Molecular mechanisms of glutamate-dependent neurodegeneration in ischemia and traumatic brain injury. *Cell Mol Life Sci* 61:657-668.

Ashman TA, Gordon WA, Cantor JB, Hibbard MR (2006) Neurobehavioral consequences of traumatic brain injury. *Mt Sinai J Med* 73:999-1005.

Assaf SY, Chung SH (1984) Release of endogenous Zn^{2+} from brain tissue during activity. *Nature* 308:734-736.

Ayalon L, Borodkin K, Dishon L, Kanety H, Dagan Y (2007) Circadian rhythm sleep disorders following mild traumatic brain injury. *Neurology* 68:1136-1140.

Bacher A, Zornow MH (1997) Lamotrigine inhibits extracellular glutamate accumulation during transient global cerebral ischemia in rabbits. *Anesthesiology* 86:459-463.

Bancila V, Nikonenko I, Dunant Y, Bloc A (2004) Zinc inhibits glutamate release via activation of pre-synaptic K channels and reduces ischaemic damage in rat hippocampus. *J Neurochem* 90:1243-1250.

Bano D, Nicotera P (2007) Ca²⁺ signals and neuronal death in brain ischemia. *Stroke* 38:674-676.

Barnes CA (1979) Memory deficits associated with senescence: a neurophysiological and behavioral study in the rat. *J Comp Physiol Psychol* 93:74-104.

Baron A, Waldmann R, Lazdunski M (2002) ASIC-like, proton-activated currents in rat hippocampal neurons. *J Physiol* 539:485-494.

Baumann CR, Werth E, Stocker R, Ludwig S, Bassetti CL (2007) Sleep-wake disturbances 6 months after traumatic brain injury: a prospective study. *Brain* 130:1873-1883.

Behan LA, Agha A (2007) Endocrine consequences of adult traumatic brain injury. *Horm Res* 68 Suppl 5:18-21.

Berendji D, Kolb-Bachofen V, Meyer KL, Grapenthin O, Weber H, Wahn V, Kroncke KD (1997) Nitric oxide mediates intracytoplasmic and intranuclear zinc release. *FEBS Lett* 405:37-41.

Beyersmann D, Haase H (2001) Functions of zinc in signaling, proliferation and differentiation of mammalian cells. *Biometals* 14:331-341.

Bishop GM, Dringen R, Robinson SR (2007) Zinc stimulates the production of toxic reactive oxygen species (ROS) and inhibits glutathione reductase in astrocytes. *Free Radic Biol Med* 42:1222-1230.

Blasco-Ibanez JM, Poza-Aznar J, Crespo C, Marques-Mari AI, Gracia-Llanes FJ, Martinez-Guijarro FJ (2004) Chelation of synaptic zinc induces overexcitation in the hilar mossy cells of the rat hippocampus. *Neurosci Lett* 355:101-104.

Bozym RA, Thompson RB, Stoddard AK, Fierke CA (2006) Measuring picomolar intracellular exchangeable zinc in PC-12 cells using a ratiometric fluorescence biosensor. *ACS Chem Biol* 1:103-111.

Cai AL, Zipfel GJ, Sheline CT (2006) Zinc neurotoxicity is dependent on intracellular NAD levels and the sirtuin pathway. *Eur J Neurosci* 24:2169-2176.

Chesnut RM, Marshall SB, Piek J, Blunt BA, Klauber MR, Marshall LF (1993) Early and late systemic hypotension as a frequent and fundamental source of cerebral ischemia following severe brain injury in the Traumatic Coma Data Bank. *Acta Neurochir Suppl (Wien)* 59:121-125.

Choi DW, Koh JY (1998) Zinc and brain injury. *Annu Rev Neurosci* 21:347-375.

Choi DW, Yokoyama M, Koh J (1988) Zinc neurotoxicity in cortical cell culture. *Neuroscience* 24:67-79.

Chu XP, Wemmie JA, Wang WZ, Zhu XM, Saugstad JA, Price MP, Simon RP, Xiong ZG (2004) Subunit-dependent high-affinity zinc inhibition of acid-sensing ion channels. *J Neurosci* 24:8678-8689.

Cole TB, Martyanova A, Palmiter RD (2001) Removing zinc from synaptic vesicles does not impair spatial learning, memory, or sensorimotor functions in the mouse. *Brain Res* 891:253-265.

Cole TB, Robbins CA, Wenzel HJ, Schwartzkroin PA, Palmiter RD (2000) Seizures and neuronal damage in mice lacking vesicular zinc. *Epilepsy Res* 39:153-169.

Cole TB, Wenzel HJ, Kafer KE, Schwartzkroin PA, Palmiter RD (1999) Elimination of zinc from synaptic vesicles in the intact mouse brain by disruption of the ZnT3 gene. *Proc Natl Acad Sci U S A* 96:1716-1721.

Colombo JA, Puissant VI (2002) Fluoro Jade stains early and reactive astroglia in the primate cerebral cortex. *J Histochem Cytochem* 50:1135-1137.

Cortez SC, McIntosh TK, Noble LJ (1989) Experimental fluid percussion brain injury: vascular disruption and neuronal and glial alterations. *Brain Res* 482:271-282.

Crumrine RC, Bergstrand K, Cooper AT, Faison WL, Cooper BR (1997) Lamotrigine protects hippocampal CA1 neurons from ischemic damage after cardiac arrest. *Stroke* 28:2230-2236.

Cuajungco MP, Lees GJ (1996) Prevention of zinc neurotoxicity in vivo by N,N,N',N'-tetrakis (2-pyridylmethyl) ethylene-diamine (TPEN). *Neuroreport* 7:1301-1304.

Cuajungco MP, Lees GJ (1998) Nitric oxide generators produce accumulation of chelatable zinc in hippocampal neuronal perikarya. *Brain Res* 799:118-129.

Danscher G, Stoltenberg M, Bruhn M, Sondergaard C, Jensen D (2004) Immersion autometallography: histochemical in situ capturing of zinc ions in catalytic zinc-sulfur nanocrystals. *J Histochem Cytochem* 52:1619-1625.

Dash PK, Kobori N, Moore AN (2004) A molecular description of brain trauma pathophysiology using microarray technology: an overview. *Neurochem Res* 29:1275-1286.

Deshpande LS, Sun DA, Sombati S, Baranova A, Wilson MS, Attkisson E, Hamm RJ, Delorenzo RJ (2008) Alterations in neuronal calcium levels are associated with cognitive deficits after traumatic brain injury. *Neurosci Lett* 441:115-119.

Dietrich WD, Alonso O, Halley M (1994) Early microvascular and neuronal consequences of traumatic brain injury: a light and electron microscopic study in rats. *J Neurotrauma* 11:289-301.

Dineley KE, Votyakova TV, Reynolds IJ (2003) Zinc inhibition of cellular energy production: implications for mitochondria and neurodegeneration. *J Neurochem* 85:563-570.

Dixon CE, Lyeth BG, Povlishock JT, Findling RL, Hamm RJ, Marmarou A, Young HF, Hayes RL (1987) A fluid percussion model of experimental brain injury in the rat. *J Neurosurg* 67:110-119.

Doering P, Danscher G, Larsen A, Bruhn M, Sondergaard C, Stoltenberg M (2007) Changes in the vesicular zinc pattern following traumatic brain injury. *Neuroscience* 150:93-103.

Dominguez MI, Blasco-Ibanez JM, Crespo C, Marques-Mari AI, Martinez-Guijarro FJ (2003) Zinc chelation during non-lesioning overexcitation results in neuronal death in the mouse hippocampus. *Neuroscience* 116:791-806.

Fierke CA, Thompson RB (2001) Fluorescence-based biosensing of zinc using carbonic anhydrase. *Biometals* 14:205-222.

Finkelstein E, Corso P, and Miller T. The incidence and economic burden of injuries in the United States. 2006. New York, NY, Oxford University Press.

Floyd CL, Golden KM, Black RT, Hamm RJ, Lyeth BG (2002) Craniectomy position affects morris water maze performance and hippocampal cell loss after parasagittal fluid percussion. *J Neurotrauma* 19:303-316.

Frederickson CJ, Bush AI (2001) Synaptically released zinc: physiological functions and pathological effects. *Biometals* 14:353-366.

Frederickson CJ, Danscher G (1990) Zinc-containing neurons in hippocampus and related CNS structures. *Prog Brain Res* 83:71-84.

Frederickson CJ, Giblin LJ, Krezel A, McAdoo DJ, Mueller RN, Zeng Y, Balaji RV, Masalha R, Thompson RB, Fierke CA, Sarvey JM, de Valdenebro M, Prough DS, Zornow MH (2006) Concentrations of extracellular free zinc (pZn)_e in the central nervous system during simple anesthetization, ischemia and reperfusion. *Exp Neurol* 198:285-293.

Frederickson CJ, Hernandez MD, McGinty JF (1989) Translocation of zinc may contribute to seizure-induced death of neurons. *Brain Res* 480:317-321.

Frederickson CJ, Klitenick MA, Manton WI, Kirkpatrick JB (1983) Cytoarchitectonic distribution of zinc in the hippocampus of man and the rat. *Brain Res* 273:335-339.

Frederickson CJ, Maret W, Cuajungco MP (2004) Zinc and excitotoxic brain injury: a new model. *Neuroscientist* 10:18-25.

Giza CC, Prins ML, Hovda DA, Herschman HR, Feldman JD (2002) Genes preferentially induced by depolarization after concussive brain injury: effects of age and injury severity. *J Neurotrauma* 19:387-402.

Graham DI, Raghupathi R, Saatman KE, Meaney D, McIntosh TK (2000) Tissue tears in the white matter after lateral fluid percussion brain injury in the rat: relevance to human brain injury. *Acta Neuropathol* 99:117-124.

Haase H, Beyersmann D (2002) Intracellular zinc distribution and transport in C6 rat glioma cells. *Biochem Biophys Res Commun* 296:923-928.

Hall ED (1993) Cerebral ischaemia, free radicals and antioxidant protection. *Biochem Soc Trans* 21:334-339.

Hall ED, Andrus PK, Althaus JS, VonVoigtlander PF (1993) Hydroxyl radical production and lipid peroxidation parallels selective post-ischemic vulnerability in gerbil brain. *J Neurosci Res* 34:107-112.

Hallam TM, Floyd CL, Folkerts MM, Lee LL, Gong QZ, Lyeth BG, Muizelaar JP, Berman RF (2004) Comparison of behavioral deficits and acute neuronal degeneration in rat lateral fluid percussion and weight-drop brain injury models. *J Neurotrauma* 21:521-539.

Hamm RJ (2001) Neurobehavioral assessment of outcome following traumatic brain injury in rats: an evaluation of selected measures. *J Neurotrauma* 18:1207-1216.

Hamm RJ, Temple MD, Pike BR, O'Dell DM, Buck DL, Lyeth BG (1996) Working memory deficits following traumatic brain injury in the rat. *J Neurotrauma* 13:317-323.

Haug FM (1967) Electron microscopical localization of the zinc in hippocampal mossy fibre synapses by a modified sulfide silver procedure. *Histochemie* 8:355-368.

Hayes RL, Stalhammar D, Povlishock JT, Allen AM, Galinat BJ, Becker DP, Stonnington HH (1987) A new model of concussive brain injury in the cat produced by extradural fluid volume loading: II. Physiological and neuropathological observations. *Brain Inj* 1:93-112.

Hellawell DJ, Taylor RT, Pentland B (1999) Cognitive and psychosocial outcome following moderate or severe traumatic brain injury. *Brain Inj* 13:489-504.

Hellmich HL, Capra B, Eidson K, Garcia J, Kennedy D, Uchida T, Parsley M, Cowart J, Dewitt DS, Prough DS (2005a) Dose-dependent neuronal injury after traumatic brain injury. *Brain Res* 1044:144-154.

Hellmich HL, Eidson K, Cowart J, Crookshanks J, Boone DK, Shah S, Uchida T, Dewitt DS, Prough DS (2008) Chelation of neurotoxic zinc levels does not improve neurobehavioral outcome after traumatic brain injury. *Neurosci Lett* 440:155-159.

Hellmich HL, Eidson KA, Capra BA, Garcia JM, Boone DR, Hawkins BE, Uchida T, Dewitt DS, Prough DS (2007) Injured Fluoro-Jade-positive hippocampal neurons contain high levels of zinc after traumatic brain injury. *Brain Res* 1127:119-126.

Hellmich HL, Frederickson CJ, Dewitt DS, Saban R, Parsley MO, Stephenson R, Velasco M, Uchida T, Shimamura M, Prough DS (2004) Protective effects of zinc chelation in traumatic brain injury correlate with upregulation of neuroprotective genes in rat brain. *Neurosci Lett* 355:221-225.

Hellmich HL, Garcia JM, Shimamura M, Shah SA, Avila MA, Uchida T, Parsley MA, Capra BA, Eidson KA, Kennedy DR, Winston JH, Dewitt DS, Prough DS (2005b) Traumatic brain injury and hemorrhagic hypotension suppress neuroprotective gene expression in injured hippocampal neurons. *Anesthesiology* 102:806-814.

Hey JG, Chu XP, Seeds J, Simon RP, Xiong ZG (2007) Extracellular zinc protects against acidosis-induced injury of cells expressing Ca^{2+} -permeable acid-sensing ion channels. *Stroke* 38:670-673.

Hicks R, Soares H, Smith D, McIntosh T (1996) Temporal and spatial characterization of neuronal injury following lateral fluid-percussion brain injury in the rat. *Acta Neuropathol* 91:236-246.

Hicks RR, Smith DH, Lowenstein DH, Saint MR, McIntosh TK (1993) Mild experimental brain injury in the rat induces cognitive deficits associated with regional neuronal loss in the hippocampus. *J Neurotrauma* 10:405-414.

Hovda DA, Becker DP, Katayama Y (1992) Secondary injury and acidosis. *J Neurotrauma* 9 Suppl 1:S47-S60.

Howell GA, Welch MG, Frederickson CJ (1984) Stimulation-induced uptake and release of zinc in hippocampal slices. *Nature* 308:736-738.

Inao S, Marmarou A, Clarke GD, Andersen BJ, Fatouros PP, Young HF (1988) Production and clearance of lactate from brain tissue, cerebrospinal fluid, and serum following experimental brain injury. *J Neurosurg* 69:736-744.

Itoh, T, Saito, T, Watanabe, S, and Saito, K. Endogenous zinc release in the hippocampus of the anesthetized rat brain using microdialysis. *Trace Elem Electrolytes* 13[4], 196-199. 1996.

Itoh T, Saito T, Fujimura M, Watanabe S, Saito K (1993) Restraint stress-induced changes in endogenous zinc release from the rat hippocampus. *Brain Res* 618:318-322.

Jiang D, Sullivan PG, Sensi SL, Steward O, Weiss JH (2001) Zn(2+) induces permeability transition pore opening and release of pro-apoptotic peptides from neuronal mitochondria. *J Biol Chem* 276:47524-47529.

Kawamata T, Katayama Y, Hovda DA, Yoshino A, Becker DP (1995) Lactate accumulation following concussive brain injury: the role of ionic fluxes induced by excitatory amino acids. *Brain Res* 674:196-204.

Kawamura Y, Manita S, Nakamura T, Inoue M, Kudo Y, Miyakawa H (2004) Glutamate release increases during mossy-CA3 LTP but not during Schaffer-CA1 LTP. *Eur J Neurosci* 19:1591-1600.

Kay AR, Toth K (2008) Is zinc a neuromodulator? *Sci Signal* 1:3.

Ketterman JK, Li YV (2008) Presynaptic evidence for zinc release at the mossy fiber synapse of rat hippocampus. *J Neurosci Res* 86:422-434.

Kim YH, Kim EY, Gwag BJ, Sohn S, Koh JY (1999) Zinc-induced cortical neuronal death with features of apoptosis and necrosis: mediation by free radicals. *Neuroscience* 89:175-182.

Kirsch JR, Helfaer MA, Lange DG, Traystman RJ (1992) Evidence for free radical mechanisms of brain injury resulting from ischemia/reperfusion-induced events. *J Neurotrauma* 9 Suppl 1:S157-S163.

Kitamura Y, Iida Y, Abe J, Mifune M, Kasuya F, Ohta M, Igarashi K, Saito Y, Saji H (2006a) In vivo measurement of presynaptic Zn²⁺ release during forebrain ischemia in rats. *Biol Pharm Bull* 29:821-823.

Kitamura Y, Iida Y, Abe J, Ueda M, Mifune M, Kasuya F, Ohta M, Igarashi K, Saito Y, Saji H (2006b) Protective effect of zinc against ischemic neuronal injury in a middle cerebral artery occlusion model. *J Pharmacol Sci* 100:142-148.

Koh JY, Choi DW (1994) Zinc toxicity on cultured cortical neurons: involvement of N-methyl-D-aspartate receptors. *Neuroscience* 60:1049-1057.

Kotapka MJ, Gennarelli TA, Graham DI, Adams JH, Thibault LE, Ross DT, Ford I (1991) Selective vulnerability of hippocampal neurons in acceleration-induced experimental head injury. *J Neurotrauma* 8:247-258.

Kwak S, Weiss JH (2006) Calcium-permeable AMPA channels in neurodegenerative disease and ischemia. *Curr Opin Neurobiol* 16:281-287.

Lang-Rollin IC, Rideout HJ, Noticewala M, Stefanis L (2003) Mechanisms of caspase-independent neuronal death: energy depletion and free radical generation. *J Neurosci* 23:11015-11025.

Lee JM, Zipfel GJ, Choi DW (1999) The changing landscape of ischaemic brain injury mechanisms. *Nature* 399:A7-14.

Lees GJ, Lehmann A, Sandberg M, Hamberger A (1990) The neurotoxicity of zinc in the rat hippocampus. *Neurosci Lett* 120:155-158.

Li Y, Hough CJ, Frederickson CJ, Sarvey JM (2001a) Induction of mossy fiber --> Ca³⁺ long-term potentiation requires translocation of synaptically released Zn²⁺. *J Neurosci* 21:8015-8025.

Li Y, Hough CJ, Suh SW, Sarvey JM, Frederickson CJ (2001b) Rapid translocation of Zn(2+) from presynaptic terminals into postsynaptic hippocampal neurons after physiological stimulation. *J Neurophysiol* 86:2597-2604.

Lim HB, Smith M (2007) Systemic complications after head injury: a clinical review. *Anaesthesia* 62:474-482.

Lowenstein DH, Thomas MJ, Smith DH, McIntosh TK (1992) Selective vulnerability of dentate hilar neurons following traumatic brain injury: a potential mechanistic link between head trauma and disorders of the hippocampus. *J Neurosci* 12:4846-4853.

Marciano PG, Brettschneider J, Manduchi E, Davis JE, Eastman S, Raghupathi R, Saatman KE, Speed TP, Stoeckert CJ, Jr., Eberwine JH, McIntosh TK (2004) Neuron-specific mRNA complexity responses during hippocampal apoptosis after traumatic brain injury. *J Neurosci* 24:2866-2876.

Maret W, Vallee BL (1998) Thiolate ligands in metallothionein confer redox activity on zinc clusters. *Proc Natl Acad Sci U S A* 95:3478-3482.

Marklund N, Bakshi A, Castelbuono DJ, Conte V, McIntosh TK (2006) Evaluation of pharmacological treatment strategies in traumatic brain injury. *Curr Pharm Des* 12:1645-1680.

Marmarou A, Foda MA, van den BW, Campbell J, Kita H, Demetriadou K (1994) A new model of diffuse brain injury in rats. Part I: Pathophysiology and biomechanics. *J Neurosurg* 80:291-300.

Marquez de la Plata CD, Hart T, Hammond FM, Frol AB, Hudak A, Harper CR, O'Neil-Pirozzi TM, Whyte J, Carlile M, Diaz-Arrastia R (2008) Impact of age on long-term recovery from traumatic brain injury. *Arch Phys Med Rehabil* 89:896-903.

Maske H (1955) [Relation between insulin and zinc in the islands of Langerhans, with special reference to blood sugar control and insulin secretion.]. *Experientia* 11:122-128.

McCance RA, Widdowson EM (1942) The absorption and excretion of zinc. *Biochem J* 36:692-696.

McIntosh TK, Saatman KE, Raghupathi R, Graham DI, Smith DH, Lee VM, Trojanowski JQ (1998) The Dorothy Russell Memorial Lecture. The molecular and cellular sequelae of experimental traumatic brain injury: pathogenetic mechanisms. *Neuropathol Appl Neurobiol* 24:251-267.

McIntosh TK, Vink R, Noble L, Yamakami I, Fernyak S, Soares H, Faden AL (1989) Traumatic brain injury in the rat: characterization of a lateral fluid-percussion model. *Neuroscience* 28:233-244.

Morales DM, Marklund N, Lebold D, Thompson HJ, Pitkanen A, Maxwell WL, Longhi L, Laurer H, Maegele M, Neugebauer E, Graham DI, Stocchetti N, McIntosh TK (2005) Experimental models of traumatic brain injury: do we really need to build a better mousetrap? *Neuroscience* 136:971-989.

Morris R (1984) Developments of a water-maze procedure for studying spatial learning in the rat. *J Neurosci Methods* 11:47-60.

Naganska E, Matyja E (2002) The protective effect of ZnCl₂ pretreatment on the development of postanoxic neuronal damage in organotypic rat hippocampal cultures. *Ultrastruct Pathol* 26:383-391.

NIH Consensus Statement. Rehabilitation of persons with traumatic brain injury. 1-41. NIH Consensus Statement. Date Accessed October 26, 1998.

NINDS. (2002) Traumatic Brain Injury: Hope Through Research. NIH Publication No. 02-2478.

Olton DS, Walker JA, Gage FH (1978) Hippocampal connections and spatial discrimination. *Brain Res* 139:295-308.

Outten CE, O'Halloran TV (2001) Femtomolar sensitivity of metalloregulatory proteins controlling zinc homeostasis. *Science* 292:2488-2492.

Parcell DL, Ponsford JL, Redman JR, Rajaratnam SM (2008) Poor sleep quality and changes in objectively recorded sleep after traumatic brain injury: a preliminary study. *Arch Phys Med Rehabil* 89:843-850.

Paxinos G, Watson C (1986) The rat brain in stereotaxic coordinates, second edition. New York, NY, Academic Press.

Perez-Clausell J, Danscher G (1985) Intravesicular localization of zinc in rat telencephalic boutons. A histochemical study. *Brain Res* 337:91-98.

Popovic V (2005) GH deficiency as the most common pituitary defect after TBI: clinical implications. *Pituitary* 8:239-243.

Popovic V, Pekic S, Pavlovic D, Maric N, Jasovic-Gasic M, Djurovic B, Medic SM, Zivkovic V, Stojanovic M, Doknic M, Milic N, Djurovic M, Dieguez C, Casanueva FF (2004) Hypopituitarism as a consequence of traumatic brain injury (TBI) and its possible relation with cognitive disabilities and mental distress. *J Endocrinol Invest* 27:1048-1054.

Povlishock JT (1986) Traumatically induced axonal damage without concomitant change in focally related neuronal somata and dendrites. *Acta Neuropathol* 70:53-59.

Qian J, Noebels JL (2005) Visualization of transmitter release with zinc fluorescence detection at the mouse hippocampal mossy fibre synapse. *J Physiol* 566:747-758.

Raghupathi R (2004) Cell death mechanisms following traumatic brain injury. *Brain Pathol* 14:215-222.

Ranchon C, I, Bonhomme B, Doly M (2007) Pre-treatment of adult rats with high doses of erythropoietin induces caspase-9 but prevents light-induced retinal injury. *Exp Eye Res* 85:782-789.

Rothman MS, Arciniegas DB, Filley CM, Wierman ME (2007) The neuroendocrine effects of traumatic brain injury. *J Neuropsychiatry Clin Neurosci* 19:363-372.

Royo NC, Conte V, Saatman KE, Shimizu S, Belfield CM, Soltesz KM, Davis JE, Fujimoto ST, McIntosh TK (2006) Hippocampal vulnerability following traumatic brain injury: a potential role for neurotrophin-4/5 in pyramidal cell neuroprotection. *Eur J Neurosci* 23:1089-1102.

Saatman KE, Duhaime AC, Bullock R, Maas AI, Valadka A, Manley GT (2008) Classification of traumatic brain injury for targeted therapies. *J Neurotrauma* 25:719-738.

Sato M, Chang E, Igarashi T, Noble LJ (2001) Neuronal injury and loss after traumatic brain injury: time course and regional variability. *Brain Res* 917:45-54.

Schmued LC, Albertson C, Slikker W, Jr. (1997) Fluoro-Jade: a novel fluorochrome for the sensitive and reliable histochemical localization of neuronal degeneration. *Brain Res* 751:37-46.

Scoville WB, Milner B (1957) Loss of recent memory after bilateral hippocampal lesions. *J Neurol Neurosurg Psychiatry* 20:11-21.

Sensi SL, Canzoniero LM, Yu SP, Ying HS, Koh JY, Kerchner GA, Choi DW (1997) Measurement of intracellular free zinc in living cortical neurons: routes of entry. *J Neurosci* 17:9554-9564.

Sensi SL, Ton-That D, Sullivan PG, Jonas EA, Gee KR, Kaczmarek LK, Weiss JH (2003) Modulation of mitochondrial function by endogenous Zn²⁺ pools. *Proc Natl Acad Sci U S A* 100:6157-6162.

Shimamura M, Garcia JM, Prough DS, Dewitt DS, Uchida T, Shah SA, Avila MA, Hellmich HL (2005) Analysis of long-term gene expression in neurons of the hippocampal subfields following traumatic brain injury in rats. *Neuroscience* 131:87-97.

Shimamura M, Garcia JM, Prough DS, Hellmich HL (2004) Laser capture microdissection and analysis of amplified antisense RNA from distinct cell populations of the young and aged rat brain: effect of traumatic brain injury on hippocampal gene expression. *Brain Res Mol Brain Res* 122:47-61.

Smith DH, Chen XH, Pierce JE, Wolf JA, Trojanowski JQ, Graham DI, McIntosh TK (1997) Progressive atrophy and neuron death for one year following brain trauma in the rat. *J Neurotrauma* 14:715-727.

Sosin DM, Snizek JE, Thurman DJ (1996) Incidence of mild and moderate brain injury in the United States, 1991. *Brain Inj* 10:47-54.

Suh SW, Chen JW, Motamedi M, Bell B, Listiak K, Pons NF, Danscher G, Frederickson CJ (2000) Evidence that synaptically-released zinc contributes to neuronal injury after traumatic brain injury. *Brain Res* 852:268-273.

Takeda A (2000) Movement of zinc and its functional significance in the brain. *Brain Res Brain Res Rev* 34:137-148.

Takeda A, Sawashita J, Takefuta S, Ohnuma M, Okada S (1999) Role of zinc released by stimulation in rat amygdala. *J Neurosci Res* 57:405-410.

Takeda A, Takefuta S, Okada S, Oku N (2000) Relationship between brain zinc and transient learning impairment of adult rats fed zinc-deficient diet. *Brain Res* 859:352-357.

Thompson RB, Whetsell WO, Jr., Maliwal BP, Fierke CA, Frederickson CJ (2000) Fluorescence microscopy of stimulated Zn(II) release from organotypic cultures of mammalian hippocampus using a carbonic anhydrase-based biosensor system. *J Neurosci Methods* 96:35-45.

Thurman DJ, Alverson C, Dunn KA, Guerrero J, Sniezek JE (1999) Traumatic brain injury in the United States: A public health perspective. *J Head Trauma Rehabil* 14:602-615.

Vallee BL, Auld DS (1990) Zinc coordination, function, and structure of zinc enzymes and other proteins. *Biochemistry* 29:5647-5659.

Vallee BL, Auld DS (1992) Active zinc binding sites of zinc metalloenzymes. *Matrix Suppl* 1:5-19.

Vallee BL, Auld DS (1993) Cocatalytic zinc motifs in enzyme catalysis. *Proc Natl Acad Sci U S A* 90:2715-2718.

Vallee BL, Coleman JE, Auld DS (1991) Zinc fingers, zinc clusters, and zinc twists in DNA-binding protein domains. *Proc Natl Acad Sci U S A* 88:999-1003.

Vallee BL, Falchuk KH (1993) The biochemical basis of zinc physiology. *Physiol Rev* 73:79-118.

Vanlandingham JW, Fitch CA, Levenson CW (2002) Zinc inhibits the nuclear translocation of the tumor suppressor protein p53 and protects cultured human neurons from copper-induced neurotoxicity. *Neuromolecular Med* 1:171-182.

Vogt K, Mellor J, Tong G, Nicoll R (2000) The actions of synaptically released zinc at hippocampal mossy fiber synapses. *Neuron* 26:187-196.

Wang Z, Li JY, Dahlstrom A, Danscher G (2001) Zinc-enriched GABAergic terminals in mouse spinal cord. *Brain Res* 921:165-172.

Weiss JH, Hartley DM, Koh JY, Choi DW (1993) AMPA receptor activation potentiates zinc neurotoxicity. *Neuron* 10:43-49.

Weiss JH, Sensi SL (2000) Ca^{2+} - Zn^{2+} permeable AMPA or kainate receptors: possible key factors in selective neurodegeneration. *Trends Neurosci* 23:365-371.

Wen Y, Perez EJ, Green PS, Sarkar SN, Simpkins JW (2004) nNOS is involved in estrogen mediated neuroprotection in neuroblastoma cells. *Neuroreport* 15:1515-1518.

Werner C, Engelhard K (2007) Pathophysiology of traumatic brain injury. *Br J Anaesth* 99:4-9.

Xiong ZG, Zhu XM, Chu XP, Minami M, Hey J, Wei WL, MacDonald JF, Wemmie JA, Price MP, Welsh MJ, Simon RP (2004) Neuroprotection in ischemia: blocking calcium-permeable acid-sensing ion channels. *Cell* 118:687-698.

Yang DY, Lee JB, Lin MC, Huang YL, Liu HW, Liang YJ, Cheng FC (2004) The determination of brain magnesium and zinc levels by a dual-probe microdialysis and graphite furnace atomic absorption spectrometry. *J Am Coll Nutr* 23:552S-555S.

Yeiser EC, Vanlandingham JW, Levenson CW (2002) Moderate zinc deficiency increases cell death after brain injury in the rat. *Nutr Neurosci* 5:345-352.

Yermolaieva O, Leonard AS, Schnizler MK, Abboud FM, Welsh MJ (2004) Extracellular acidosis increases neuronal cell calcium by activating acid-sensing ion channel 1a. *Proc Natl Acad Sci U S A* 101:6752-6757.

Yin HZ, Sensi SL, Ogoshi F, Weiss JH (2002) Blockade of Ca^{2+} -permeable AMPA/kainate channels decreases oxygen-glucose deprivation-induced Zn^{2+} accumulation and neuronal loss in hippocampal pyramidal neurons. *J Neurosci* 22:1273-1279.

Young B, Ott L, Kasarskis E, Rapp R, Moles K, Dempsey RJ, Tibbs PA, Kryscio R, McClain C (1996) Zinc supplementation is associated with improved neurologic recovery rate and visceral protein levels of patients with severe closed head injury. *J Neurotrauma* 13:25-34.

Yuan XQ, Prough DS, Smith TL, Dewitt DS (1988) The effects of traumatic brain injury on regional cerebral blood flow in rats. *J Neurotrauma* 5:289-301.

Yuan XQ, Wade CE (1993) Lactated Ringer's solution alleviates brain trauma-precipitated lactic acidosis in hemorrhagic shock. *J Neurotrauma* 10:307-313.

Zhan RZ, Wu C, Fujihara H, Taga K, Qi S, Naito M, Shimoji K (2001) Both caspase-dependent and caspase-independent pathways may be involved in hippocampal CA1 neuronal death because of loss of cytochrome c from mitochondria in a rat forebrain ischemia model. *J Cereb Blood Flow Metab* 21:529-540.

VITA

Bridget Eva Hawkins was born in Garden City, Michigan, on September 22, 1977, the daughter of Donna Jean Williams (now Murdock) and Lawrence John Hawkins. She has one younger sister, Kelly Lyn Hawkins, and one older step-sister, Robin Renee Murdock. Ms. Hawkins entered Schoolcraft College during her senior year in high school and completed an Associates of Applied Science degree in Environmental Technology in 1998 after taking part in AmeriCorps National Civilian Community Corps, a residential community service program in Colorado sponsored by the US Government. She then obtained a Bachelors of Science degree in Biology from High Point University in 2000 before moving to Galveston to become a Research Assistant in Dr. Cheryl Watson's lab at the University of Texas Medical Branch in 2001. A year later, she matriculated into the PhD program at UTMB, entered candidacy in the Neuroscience Graduate Program in 2005 and began working on her dissertation work under the mentorship of Dr. Donald S. Prough. She was awarded a Predoctoral Fellowship from the NIEHS Toxicology Training Grant T32 Program from 2004-2006, during which time she was a co-instructor at Texas A&M University at Galveston and obtained an Advanced Business Management Certificate from University of Houston Clear Lake. Ms. Hawkins also received a National Neurotrauma Society Award and a National Student Research Forum Neuroscience & Cell Biology Award.

Education

B.S. Biology, May 2000, *High Point University, High Point, NC*
A.A.S. Environmental Technology, May 1998, *Schoolcraft College, Livonia, MI*

Publications

- 1) Hellmich HL, Eidson KA, Capra BA, Garcia JM, Boone DR, Hawkins BE, Uchida T, DeWitt DS and Prough DS. Injured Fluoro-jade positive hippocampal neurons contain high levels of zinc after traumatic brain injury. *Brain Research* 2007 Jan 5;1127(1):119-26. Epub 2006 Nov 15.
- 2) Westlund KN and Hawkins BE. Thalamic Neurotransmitters and Neuromodulators. Encyclopedia of Pain, R.F. Schmidt and W.D. Willis, Eds, pp. 2412-2418, ISBN-13: 978-3-540-43957-8, Springer, New York, NY 2007.
- 3) Watson CS, Alyea RA, Hawkins BE, Thomas ML, Cunningham KA and Jakubas AA. Estradiol effects on the dopamine transporter—protein levels, subcellular localization, and function. *Journal of Molecular Signaling* 2006 Dec 5;1:5

- 4) Watson CS, Zivadinovic D, Bulayeva N, Hawkins B, Campbell CH, and Gametchu B. A membrane form of estrogen receptor- β mediates estrogenic nongenomic effects. *The Identities of Membrane Estrogen Receptors*, C.S. Watson, Ed., pp. 11-20, ISBN- 1-4020-7344-5, Kluwer, Boston, MA 2003.

Abstracts

- 1) BE Hawkins, DS DeWitt and DS Prough. Zinc-mediated cell death in the hippocampus following experimental traumatic brain injury. Mission Connect, Houston, TX, December 2008.
- 2) Y Li, BE Hawkins, DS DeWitt and W Maret. Cellular mechanisms in traumatic brain injury: oxidative stress and cytotoxic zinc ion fluctuations. National Student Research Forum, Galveston, TX, April 2008.
- 3) BE Hawkins, JM Garcia, DR Boone, T Uchida, HL Hellmich, DS DeWitt and DS Prough. Age-related differences of gene expression in hippocampal neurons following traumatic brain injury in Fisher 344 rats. Mission Connect, Houston, TX, December 2007.
- 4) DR Boone, JM Garcia, JC Cowart, MA Parsley, BE Hawkins, T Uchida, DS Prough, DS DeWitt and HL Hellmich. Traumatic brain injury dysregulates expression of circadian clock genes in rat hippocampus and suprachiasmatic nucleus. Mission Connect, Houston, TX, December 2007.
- 5) BE Hawkins, JM Garcia, DR Boone, T Uchida, HL Hellmich, DS DeWitt and DS Prough. Age-related differences of gene expression in hippocampal neurons following traumatic brain injury in Fisher 344 rats. Society for Neuroscience, San Diego, CA, November 2007.
- 6) BE Hawkins, DS DeWitt and DS Prough. Hippocampal ZnCl₂ injections affect performance on spatial learning and memory behavioral tests. National Neurotrauma Society Symposium, Kansas City, MO, July 2007 *Published: Journal of Neurotrauma 24(7), June 2007.*
- 7) DR Boone, JM Garcia, JC Cowart, MA Parsley, BE Hawkins, T Uchida, DS Prough, DS DeWitt and HL Hellmich. Traumatic brain injury dysregulates expression of circadian clock genes in rat hippocampus and suprachiasmatic nucleus. National Neurotrauma Society Symposium, Kansas City, MO, July 2007 *Published: Journal of Neurotrauma 24(7), June 2007.*
- 8) SA Shah, MA Parsley, BE Hawkins, HL Hellmich, DS DeWitt and DS Prough. Zinc chelation reduces neuronal degeneration after traumatic brain injury in the rat hippocampus. ASA, Chicago, IL, October 2006.
- 9) BE Hawkins, DS DeWitt and DS Prough. Zinc accumulation and neuronal degeneration following fluid percussion injury: a comparison of zinc indicator dyes. National Neurotrauma Society Symposium, St. Louis, MO, July 2006. *Published: Journal of Neurotrauma 23(6), June 2006.*

- 10) SA Shah, MA Parsley, BE Hawkins, JM Garcia, DR Boone, HL Hellmich, DS DeWitt and DS Prough. Effects of CaEDTA and traumatic brain injury on neuronal degeneration and zinc accumulation in the rat hippocampus. National Neurotrauma Society Symposium, St. Louis, MO, July 2006. *Published: Journal of Neurotrauma 23(6), June 2006.*
- 11) BE Hawkins, MA Parsley, VRS Ramanujam, DS DeWitt and DS Prough. Release of zinc by reactive oxygen species and traumatic brain injury measured using microdialysis and atomic absorption spectrophotometry. National Student Research Forum, Galveston, TX, April 2006.
- 12) BE Hawkins, JC Cowart, BA Capra, KA Eidson, MA Parsley, DS DeWitt, HL Hellmich and DS Prough. Hippocampal neurodegeneration and acute changes in cerebral blood flow following trauma and hemorrhage in young and aged rats. National Student Research Forum, Galveston, TX, April 2006.
- 13) BE Hawkins, MA Parsley, VRS Ramanujam, DS DeWitt and DS Prough. Release of zinc by reactive oxygen species and traumatic brain injury measured using hippocampal microdialysis and graphite furnace atomic absorption spectrophotometry. Society of Toxicology, San Diego, CA, March 2006. *Abstract No. 495. 2006 Itinerary Planner. San Diego, CA: Society of Toxicology.*
- 14) BE Hawkins, JC Cowart, BA Capra, KA Eidson, MA Parsley, DS DeWitt, HL Hellmich and DS Prough. Hippocampal neurodegeneration and acute changes in cerebral blood flow following trauma and hemorrhage in young and aged rats. Forum on Aging, Sealy Center on Aging, UTMB, Galveston, TX, September 2005.
- 15) BE Hawkins, MA Parsley, DS DeWitt, and DS Prough. Zinc accumulation in hippocampal neurons following traumatic brain injury is partially prevented by lamotrigine. National Neurotrauma Society Symposium, Washington, D.C., November 2005. *Published: Journal of Neurotrauma 22(10), October 2005.*
- 16) BE Hawkins, JC Cowart, BA Capra, KA Eidson, MA Parsley, DS DeWitt and DS Prough. Increased Fluoro-Jade-positive neurons and acute changes in cerebral blood flow following trauma and hemorrhage in aged and young rats. National Neurotrauma Society Symposium, Washington, D.C., November 2005. *Published: Journal of Neurotrauma 22(10), October 2005.*
- 17) BE Hawkins, JC Cowart, MA Parsley, DS DeWitt and DS Prough. Acute cerebral physiologic changes after traumatic brain injury in young and aged rats. Forum on Aging, Sealy Center on Aging, UTMB, Galveston, TX, September 2004.
- 18) D Zivadinovic, BE Hawkins, B Gametchu and CS Watson. MAPK activation by 17-beta-estradiol in MCF-7 cells enriched and depleted of membrane estrogen receptor- α . National Women's Health Week Meeting, Galveston, TX, May 2003.
- 19) BE Hawkins, AA Jakubas, T Reed, ML Thomas, KA Cunningham, A Levy and CS Watson. Quantitation and effects of estradiol on dopamine transporter protein and function at the cellular level. National Women's Health Week Meeting, Galveston, TX, May 2003.

- 20) D Zivadinovic, BE Hawkins, B Gametchu and CS Watson. MAPK activation by 17-beta-estradiol in MCF-7 cells enriched and depleted of membrane estrogen receptor- α . Texas Forum on Female Reproduction, Houston, TX, April 2003.
- 21) BE Hawkins, AA Jakubas, T Reed, ML Thomas, KA Cunningham, A Levy and CS Watson. Quantitation of rapid estrogenic effects on dopamine transporter protein and function at the cellular level. Texas Forum on Female Reproduction, Houston, TX, April 2003.
- 22) BE Hawkins, AA Jakubas, T Reed, ML Thomas, KA Cunningham, A Levy and CS Watson. Quantitation of rapid estrogenic effects on dopamine transporter protein and function at the cellular level. National Student Research Forum, Galveston, TX, April 2003.
- 23) CS Watson, D Zivadinovic, B Hawkins and B Gametchu. The membrane form of the estrogen receptor-alpha in MCF-7 cells can be quantitatively measured, correlated to estradiol-induced sensitive growth, and linked to activation of MAP kinases. ERA of Hope Breast Cancer Meeting, Orlando, FL, September 2002.
- 24) D Zivadinovic, BE Hawkins, B Gametchu and CS Watson. MCF-7 breast cancer cell membrane estrogen receptor-quantitative measurement and relationship to estrogen induced growth control. FASEB Summer Conference on Steroid Receptors in the Plasma Membrane, Snow Mass, Co, June 2002.
- 25) D Zivadinovic, BE Hawkins, B Gametchu and CS Watson. The membrane form of the estrogen receptor- α can be quantitatively measured and correlated to very sensitive growth control of MCF-7 cells. Texas Forum on Female Reproduction, Houston, TX, May 2002.

Summary of Dissertation

Traumatic brain injury (TBI) is a leading cause of morbidity and mortality of Americans both in the 15-25 age range and in the elderly population. Hippocampal neuronal damage is a key feature of fluid percussion traumatic brain injury. However, the mechanisms contributing to the susceptibility to neuronal injury in this region are largely unknown. Since free ionic zinc (Zn^{2+}) was shown to be toxic to neurons *in vitro*, I sought to examine the effects of Zn^{2+} on neuronal injury following TBI. To study this problem, I characterized a model of Zn^{2+} -induced injury in an attempt to isolate zinc's effect on cell death, *in vivo*. I also adapted a fluorimetric method to measure the amount of extracellular Zn^{2+} present following TBI, using microdialysis techniques. To date, the measurement of free ionic Zn^{2+} release *in vivo* after trauma has not been shown. I demonstrate that the amount of Zn^{2+} found in the extracellular fluid of TBI rats was below the range that causes neuronal injury and was not different than the amount of Zn^{2+} found in sham operated rats. Results of my experiments do not support the idea that Zn^{2+} is presynaptically released and causes injury to surrounding neurons.

Permanent address: 215 Postoffice Street, Galveston, Texas 77550

This dissertation was typed by Bridget Eva Hawkins.